Aus dem Institut für Kardiogenetik
der Universität zu Lübeck
Kommissarische Leitung: Prof. Dr. med. Malte Spielmann

The Influence of the Hypertension Risk Gene *ZC3HC1* on the Phenotype of Smooth Muscle Cells

Inauguraldissertation

zur Erlangung der Doktorwürde
der Universität zu Lübeck
- Aus der Sektion Medizin -

vorgelegt von
Miriam Otto
aus Ede/ Niederlande

Lübeck 2024

1. Berichterstatter: PD Dr. hum. biol. Zouhair Aherrahrou
Ko-Betreuer: Prof. Dr. med. Karl-Friedrich Klotz
2. Berichterstatter: Prof. Dr. med. Kyoung-Ryul Julian Chun
Tag der mündlichen Prüfung: 27.04.2026
Zum Druck genehmigt. Lübeck, den 28.04.2026
-Promotionskommission der Sektion Medizin-

Contents

Abbreviations

APS	Ammonium Persulfate
BrdU	Bromodeoxyuridine
BSA	Bovine Serum Albumin
CAD	Coronary Artery Disease
cAMP	Cyclic Adenosine Monophosphate
cDNA	Complementary DNA
cdk	Cyclin Dependent Kinase
CNN1	Calponin 1
CO_2	Carbon dioxide
CVDs	Cardiovascular Diseases
DAPI	4',6-diamidino-2-phenylindole
DBP	Diastolic Blood Pressure
DMSO	Dimethyl Sulfoxide
dNTP	Deoxyribose Nucleoside Triphosphate
DNA	Deoxyribonucleic acid
EDTA	Ethylenediaminetetraacetic acid
EGF	Endothelial Growth Factor
ELISA	Enzyme-linked Immunosorbent Assay
FBS	Fetal Bovine Serum
FGF	Fibroblast Growth Factor
FITC	Fluorescein Isothiocyanate
GAPDH	Glyceraldehyde 3-phosphate dehydrogenase
GWAS	Genome Wide Association Studies
ILGF-1	Insulin-like Growth Factor 1
KD	Knockdown
KCl	Potassium Chloride
KO	Knockout

KRB	Krebs-Ringer Buffer
LD	Linkage Disequilibrium
MMP	Matrix Metalloproteinases
NIPA	Nuclear Interaction Partner of ALK (Anaplastic Lymphoma Kinase)
NO	Nitric Oxide
OPN	Osteopontin
PBS	Phosphate buffered saline
PCR	Polymerase Chain Reaction
PDGF	Platelet Derived Growth Factor
PE	Phenylephrine
PFA	Paraformaldehyde
PI	Propidium iodide
PMSF	Phenylmethylsulfonyl Fluoride
PVDF	Polyvinylidene Fluoride
qPCR	Quantitative PCR
RNA	Ribonucleic acid
SDS-PAGE	Sodium Dodecyl Sulfate Polyacrylamide Gel Electrophoresis
SBP	Systolic Blood Pressure
SEM	Standard Error of the Mean
SHR	Spontaneously Hypertensive Rats
siRNA	Small interfering RNA
SM-MHC	Smooth Muscle-Myosin Heavy Chain
SMA	α-Smooth Muscle Actin
SMC	Smooth Muscle Cell
SMTN	Smoothelin
SNP	Single-Nucleotide Polymorphism
TEMED	Tetramethylethylenediamine
Tris	Tris(hydroxymethyl)aminomethane
UV	Ultraviolet
WKY	Wistar Kyoto Rats

List of Figures

List of Tables

1 Introduction

1.1 Cardiovascular Diseases and Hypertension

Cardiovascular Diseases (CVDs) are the leading cause of death worldwide [WHO, 2020]. The most common ones are ischemic heart disease, stroke, and congestive heart failure, which together make up 80% of all CVDs [Gaziano et al., 2006].

Hypertension is a very common disease with a worldwide prevalence of 31.1% in adults [Mills et al., 2016]. According to European Guidelines, hypertension is defined as blood pressure $\geq$ 140/90 mmHg [Williams et al., 2018]. There are two different types of hypertension: Primary, also called essential hypertension, which accounts for about 90% of cases. Secondary hypertension has an underlying cause like obstructive sleep apnoea syndrome or renal artery stenosis. [Herold, 2019]. In this thesis, primary hypertension is meant when talking about hypertension. In 2019, high systolic blood pressure was the leading preventable risk factor associated with 19.2% of all deaths [Murray et al., 2020]. Most deaths associated with hypertension were caused by ischemic heart disease [Mills et al., 2020]. Hypertension generally increases the risk of developing CVDs such as ischemic heart disease or left ventricular hypertrophy [Kannel, 1989].

1.1.1 Pathophysiology of Hypertension

Many interacting mechanisms contribute to the pathophysiology of hypertension. Figure 1.1 shows a summary of these pathophysiological mechanisms. Folkow outlines three major causal and interdependent elements in his paper [Folkow, 1982]. Besides genetic predisposition an environmental factors such as psychoemotional influences and habitual salt intake, he mentions the increased peripheral resistance caused by the adaptation of the heart and the vessels as another important factor . A recently published review [Harrison et al., 2021] mentions genetics, sodium intake and storage, sympathetic activation, microbiome, renal mechanisms, vascular/ endothelial dysfunction, oxidative stress, and innate and adaptive immunity as interacting factors contributing to hypertension.

Blood pressure is defined as the product of cardiac output and peripheral resistance. [Saxena et al., 2018]. Hence, a hallmark of hypertension is an imbalance of these two factors. While the peripheral resistance is mainly determined by the contraction of Smooth Muscle Cells (SMCs) in the walls of the small arterioles, the big vessels play a tangential role [Beevers et al., 2001]. The relations between cardiac output, peripheral resistance, and their causes are shown in figure 1.1.

Contraction of SMCs can be triggered by various mechanisms, some of which overlapping with the mechanisms contributing to hypertension described above. Important to mention here

are the Renin-angiotensin-aldosterone system, the autonomic nervous system, and vasoactive substances like bradykinin, endothelin, or atrial natriuretic peptide (ANP) [Beevers et al., 2001]. Another important cause is the endothelial cell dysfunction with the Nitric Oxide (NO) pathway [Saxena et al., 2018]. As NO is a potent vasodilator, a disturbance in this pathway increases peripheral resistance. Furthermore, abnormalities in adhesion molecules and extracellular matrix can contribute to increased vascular resistance [Intengan and Schiffrin, 2000]. Moreover, increased calcium levels and membrane depolarization also play a role in the pathogenesis of hypertension [Wellman et al., 2001].

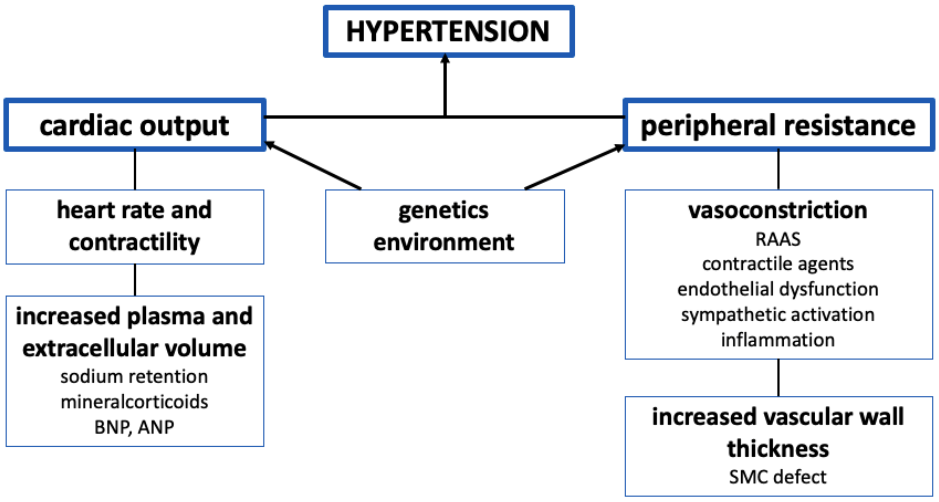

Figure 1.1: Pathophysiological mechanisms of hypertension. As blood pressure is the product of cardiac output and peripheral resistance, disturbance of either of these factors can cause elevated blood pressure. The cardiac output is determined by the heart rate and contractility and an increase in plasma and extracellular volume. The peripheral resistance is determined by the vaso-tonus and the vascular wall thickness, which are both increased in hypertension. Genetics and environmental factors can influence cardiac output and peripheral resistance. Figure based on [Adua, 2022].

1.1.2 Risk Factors for Hypertension

There are several risk factors which lead to hypertension or are associated with it. These include overweight and obesity, smoking, diabetes, alcohol, prehypertension, and albuminuria [Wang et al., 2006]. Another study additionally associates male sex and higher age with hypertension [Singh et al., 2017]. Also, genetics may influence the genesis of elevated blood pressure [Oparil et al., 2003]. Figure 1.2 shows an overview of the main factors contributing to hypertension and its complications.

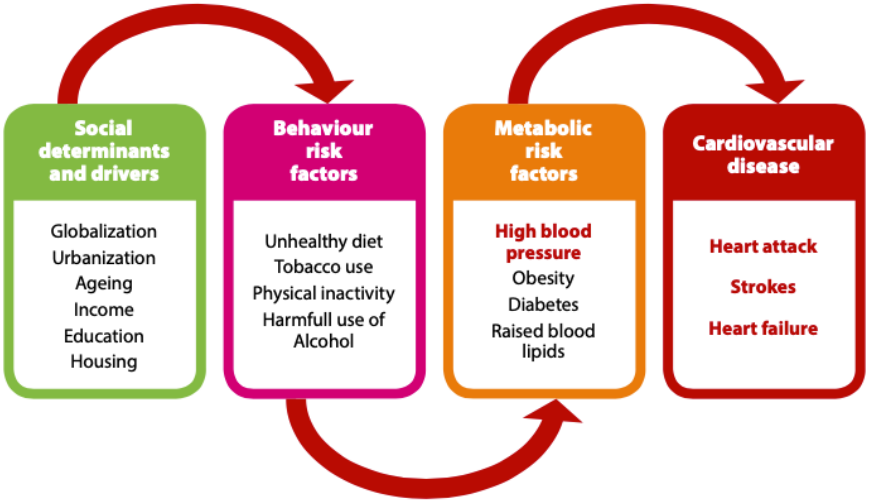

Figure 1.2: Main factors contributing to hypertension and its complications. From *Global status report on noncommunicable diseases* [WHO, 2014]. Social determinants and drivers such as aging or education lead to behavior risk factors like tobacco use or an unhealthy diet. In turn, these behavior risk factors facilitate metabolic risk factors, which include high blood pressure. Finally, the metabolic risk factors may result in cardiovascular diseases like heart attacks or strokes.

1.2 Genetics of Hypertension

Hypertension has a genetic component. More than 60 years ago, researchers already noticed that hypertension runs in families, with the highest correlation found between siblings [Staessen et al., 2003]. The advent of novel methods in genetic research prompted the discovery of monogenic forms of hypertension. At the time of writing, there are 8 monogenic forms of hypertension, that cause for example the Bartter syndrome or the Liddle syndrome. [Lifton et al., 2001]. However, the monogenic forms are rare and do not explain the high prevalence of hypertension in the population. Hence, hypertension is nowadays considered a complex polygenetic disease, which is influenced by host characteristics and environment [Staessen et al., 2003].

1.2.1 Genome Wide Association Studies

Genome Wide Association Studies (GWAS) enable the examination of the genetics of complex polygenetic traits. Their purpose is to detect associations between genetic variants, Single-Nucleotide Polymorphisms (SNPs), and traits in population samples [Visscher et al., 2017]. While linkage analysis focusses on affected families and siblings, GWAS are based on a sample taken from the entire population. Mathematically GWAS are based on the Linkage Disequilibrium (LD), which assumes that an allele associated with a trait should have a higher frequency in affected individuals than in unaffected ones [Risch and Merikangas, 1996].

The first GWAS was conducted in 2005 [Watanabe et al., 2019, Edwards et al., 2005] and up to now, there have been more than 5,700 GWAS conducted for more than 3,300 traits [Uffelmann et al., 2021]. This was only possible with the rapid technological progress, which allowed the identification of a large number of SNPs [Hirschhorn and Daly, 2005], for example with the HapMap Project [Gibbs et al., 2003]. The SNPs are collected in a database (dbSNP: `http://www.ncbi.nlm.nih.gov/SNP`, [Sherry et al., 2001]). SNPs are genetic variants in one base pair position with an allele frequency of 1% or more [Brookes, 1999].

One main purpose of GWAS is a better biological understanding of certain traits that can help to develop new therapies. The output of GWAS, an associated locus, has to be assigned to the corresponding gene to identify the affected pathway. This can sometimes be challenging, as not all variants are located in coding regions. The results of GWAS can also be used for risk prediction of a disease in a target group [Uffelmann et al., 2021].

1.2.2 GWAS in Hypertension

Initially, GWAS sparked hopes that the genetics of hypertension might be decoded and new starting points for therapies might be discovered. The first large studies conducted in 2007 identified risk variants for other complex diseases like coronary artery disease, diabetes, or hypertriglyceridemia, but did not find a locus for hypertension with genome-wide significance [20 et al., 2007, Saxena et al., 2007, Levy et al., 2007].

Hence, identifying loci for hypertension was more challenging than for other complex diseases, but in the following years, more studies were conducted and identified hundreds of loci with an effect on blood pressure [Caulfield et al., 2003, Levy et al., 2009, Newton-Cheh et al., 2009, Wang et al., 2009, Adeyemo et al., 2009, Consortium et al., 2011, Kato et al., 2008, Kato et al., 2011, Warren et al., 2017, Surendran et al., 2020, Kolifarhood et al., 2019].
One can distinguish between variations for Systolic Blood Pressure (SBP), Diastolic Blood Pressure (DBP), or hypertension as a binary trait, where both are elevated [Adeyemo et al., 2009].

The GWAS are addressing complex diseases, including hypertension. However, the majority of the discovered genetic variants have only a small effect. Furthermore, most of the variants are located in non-coding regions, making the identification of the causal gene very challenging [Surendran et al., 2020]. To address this issue, Meta-analysis and post-GWAS studies are currently underway to identify the causal SNP and causal gene [Singh et al., 2023, Rhodes et al., 2019, de Las Fuentes et al., 2021, Padmanabhan and Dominiczak, 2021].

1.3 Phenotype Switch of Vascular Smooth Muscle Cells

Vascular SMCs in mature animals are highly specialized cells whose principal function is contraction. In this way, they regulate the blood vessel tone diameter, blood pressure, and blood flow distribution. SMCs within the adult blood vessel proliferate at an extremely low rate and exhibit very low synthetic activity. They express a unique repertoire of contractile proteins, ion channels, and signaling molecules required for the cell's contractile function. While skeletal or cardiac muscle cells are terminally differentiated, SMCs can still undergo fundamental and reversible phenotype changes depending on environmental stimuli [Owens, 1995, Owens et al., 2004].

It can be distinguished between the differentiated contractile phenotype described above and the hardly differentiated synthetic phenotype. The synthetic phenotype shows higher migration and proliferation and produces a high amount of proteins of the extracellular matrix [Owens, 1995]. It is present in cells that contribute to vessel development, either as new vascularization or as a vessel repair after injury [Shi and Chen, 2014]. Most of the time, the SMCs are in the differentiated contractile phenotype. There are several known markers for this phenotype such as α-Smooth Muscle Actin (SMA), Smooth Muscle-Myosin Heavy Chain (SM-MHC), or calponin [Owens, 1995]. Generally, there are multiple established markers for SMCs, but there is no single marker that can reliably distinguish SMCs from all other cell types [Owens et al., 2004].

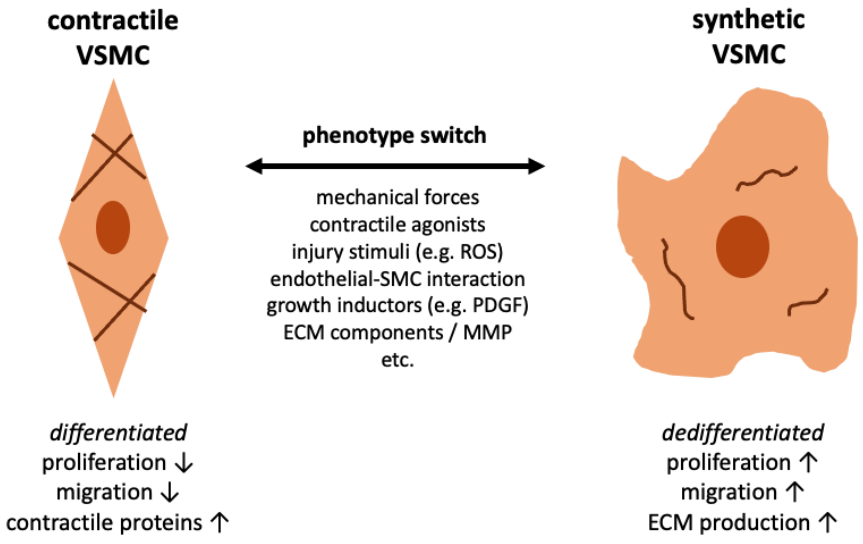

Figure 1.3: Phenotype switch of vascular smooth muscle cells (VSMC). Inducing factors lead in most cases to a switch from contractile to synthetic. ROS: reactive oxygen species, PDGF: platelet-derived growth factor, ECM: extracellular matrix, MMP: matrix metalloproteinase.

There are many elements that can influence the phenotype of SMCs. Environmental cues include mechanical forces, contractile agonists, extracellular matrix components, neuronal factors, reactive oxygen species, and endothelial-SMC interactions [Owens et al., 2004]. For

stimulation with Platelet Derived Growth Factor (PDGF), studies show a suppression in contractile proteins [Holycross et al., 1992, Corjay et al., 1989]. Also influenced by Matrix Metalloproteinases (MMP) and oxidized phospholipids, the SMCs switched their phenotype to a more dedifferentiated one [Wang et al., 2015, Pidkovka et al., 2007]. MicroRNAs and epigenetic factors can also influence the phenotype of SMCs [Davis-Dusenbery et al., 2011, Alexander and Owens, 2012]. A summary of the different characteristics of the phenotypes and inducing factors of the phenotype switch is shown in figure 1.3.

1.3.1 Role of the Phenotype Switch in the Development of Hypertension

The ability of SMCs to change their phenotype plays a big role in the development of hypertension and atherosclerosis. A common characteristic of hypertension is the increase in peripheral resistance as a result of increased SMC contractility [Owens et al., 2004]. This increased contractility can mainly be attributed to the decrease in the lumen diameter of the resistance vessels [Intengan and Schiffrin, 2000,Mulvany et al., 1978] while the presence of the contractile phenotype plays a minor role. The predominant phenotype of SMCs in hypertensive individuals is the synthetic phenotype [Fukuda et al., 1999]. The cells proliferate faster [Chobanian et al., 1987] and produce more extracellular matrix proteins, which contributes to the hypertrophic remodeling of the vessel [Intengan and Schiffrin, 2000], which decreases the lumen diameter. The production of proteases, such as MMP, is also increased [Fukuda et al., 1999], which promotes proinflammatory processes in the arterial wall [Wang et al., 2015, Sun et al., 2017]. Looking at the higher proliferation rate on a molecular level, it is shown, that SMCs from Spontaneously Hypertensive Rats (SHR) have an accelerated entry into the S-phase of the cell cycle compared with normotensive Wistar Kyoto Rats (WKY) [Hadrava et al., 1992] and that they differ in G1 progression as well as in G2 progression [Tanner et al., 2003].

1.4 The Gene *ZC3HC1* and the Encoded Protein NIPA

ZC3HC1, the zinc finger C3H3-type containing 1 gene, lies on chromosome 7 and encodes the protein Nuclear Interaction Partner of ALK (Anaplastic Lymphoma Kinase) (NIPA). NIPA was first discovered in 2003 in the context of lymphoma research [Ouyang et al., 2003], where an antiapoptotic function for the 60kDa protein was shown. Further studies portrayed its function as a human F-box-containing protein, that defines an SCF-type E3 ligase [Bassermann et al., 2005b]. SCF ubiquitin ligases are part of the ubiquitination system to degrade proteins [Hochstrasser, 1996]. The E3 ligase enzyme binds the target substrate and activates the ubiquitin-E2 complex [Cardozo and Pagano, 2004]. The SCF ubiquitin ligases consist of Skp1, a Cullin protein, a RING finger protein, and an F-box protein, which promotes the substrate binding and is differs depending on the SCF complex [Cardozo and Pagano, 2004, Jackson and Eldridge, 2002].

NIPA is only present in the nucleus and nuclear cyclin B1 could be identified as a substrate of SCF^{NIPA} [Bassermann et al., 2005b]. Cyclin B1 is a cell cycle regulating protein. In complex with Cyclin Dependent Kinase (cdk) 1 it promotes the transition from G2-phase to mitosis [Johnson and Walker, 1999, Lim and Kaldis, 2013], where it has the highest activity [Hwang et al., 1995]. During the interphase, it accumulates in the cytoplasm and only enters the nucleus at the beginning of the M phase.

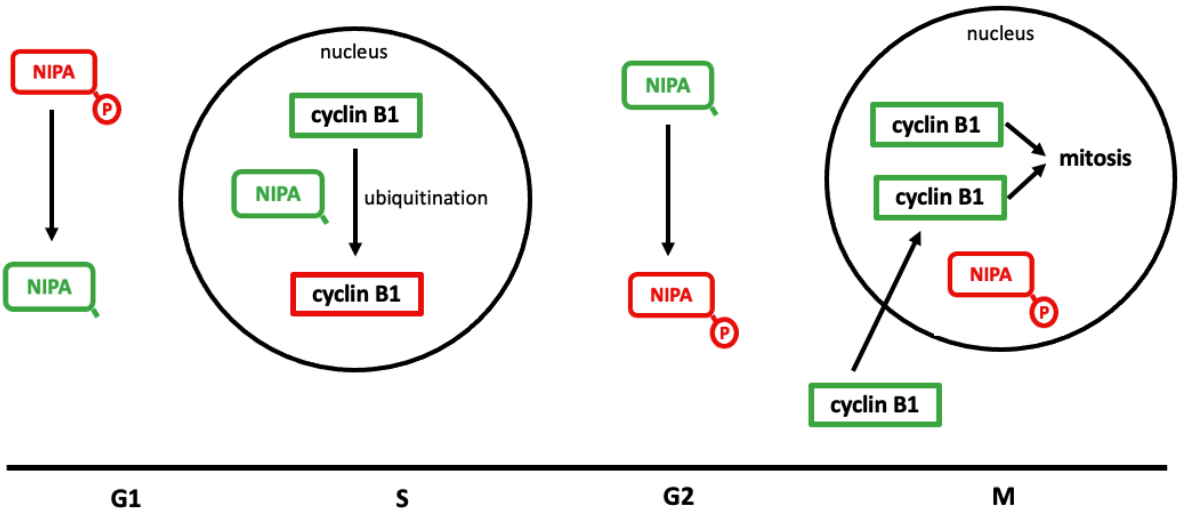

Figure 1.4: Role of NIPA and its interactions with cyclin B1 during the cell cycle. Active proteins are shown in green, and inactive are red. NIPA gets activated at the beginning of the G1 phase and ubiquitinates cyclin B1 during the interphase. In G2, NIPA begins to get phosphorylated. At the beginning of the M phase, cyclin B1 enters the nucleus and accumulates, as NIPA is inactivated, and initiates mitosis.

NIPA has several phosphorylation sites [Ouyang et al., 2003, Bassermann et al., 2007], where Serine 354 seems to be the most important. NIPA phosphorylation determines its activity and alternates during the cell cycle. It is active during the interphase, gets phosphorylated

in the G2-phase and stays inactive until reentry into G1-phase [Bassermann et al., 2005a]. Hence, the function of active NIPA is to ubiquitinate nuclear cyclin B1 during the interphase and influences the mitotic entry in this way [Bassermann et al., 2005a]. Figure 1.4 shows the role of NIPA in the cell cycle and its interaction with cyclin B1.

Inactivation of NIPA in HeLa cells is shown to lead to a nuclear accumulation of cyclin B1 and a consecutive premature mitotic entry [Bassermann et al., 2005b]. Another study shows that lower phosphorylation with higher activity of NIPA leads to an effective decrease in the stability of nuclear cyclin B1, which slows down its nuclear accumulation and concludes in an extended mitosis [Jones et al., 2016]. NIPA-deficient mice are viable, but with lower birth rates, body weight, and fertility problems [Al-Hasani, 2017,Illert et al., 2012]. An accumulation of cyclin B1 can be observed in these mice [Illert et al., 2012].

1.4.1 *ZC3HC1* in GWAS

ZC3HC1 was first associated with Coronary Artery Disease (CAD) in 2011 [Schunkert et al., 2011]. The risk locus 7q32.2 contains the polymorphism rs11556924, which lies within the *ZC3HC1* gene and has genomewide significance as shown in figure 1.5. It is a C $\rightarrow$ T polymorphism, which leads to a change of the amino acid Arginine at position 363 to Histidine [Schunkert et al., 2011]. It was discussed, if the neighbor gene *KLHDC10* would be the gene of interest for this polymorphism [Erbilgin et al., 2013], but Braenne et al. confirmed *ZC3HC1* as the most likely causal gene at this locus [Brænne et al., 2015].

In 2013, the SNP could be associated with increased diastolic blood pressure with the C allele as the risk allele [Consortium et al., 2013]. In 2015, the genotype CC was associated with hypertension for the first time [Kunnas and Nikkari, 2015]. For the protective variant, increased phosphorylation of Ser354 could be shown as well as a reduced proliferation rate in HeLa cells [Linseman et al., 2017]. In contrast to this, another almost simultaneously published study showed higher phosphorylation in the risk variant with an increased mitotic index and cyclin B1 accumulation [Jones et al., 2016]. A Japanese group recently examined three other SNPs within the gene and found the polymorphism rs1464890 to have a strong protective effect for hypertension [Ma et al., 2019].

Regarding CVDs the rs11556924 polymorphism could also be associated with atrial fibrillation [Yamase et al., 2016] and increased intima-media thickness in patients with rheumatoid arthritis [López-Mejías et al., 2013], where in both cases the T allele or the TT genotype could be identified as the risk factor in contrast to the associations presented before.

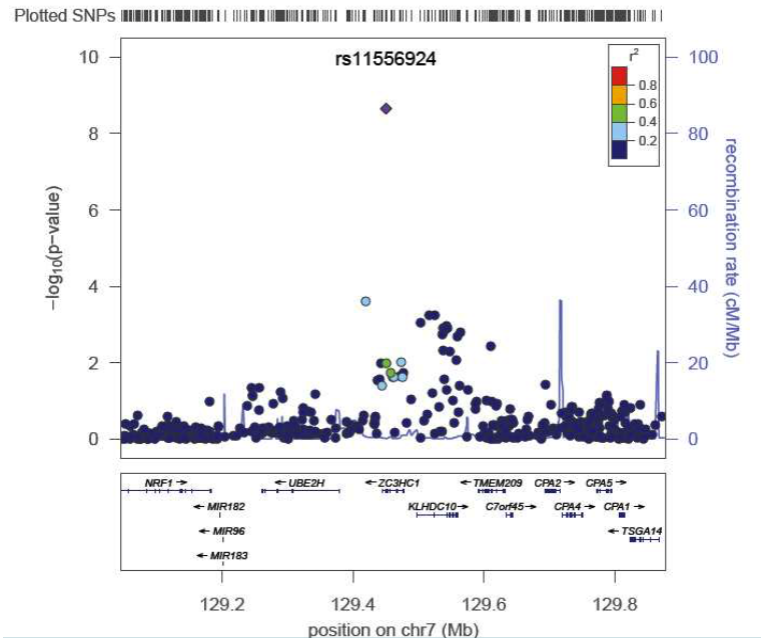

Figure 1.5: Regional association plot of the locus 7q32.2. The position on chromosome 7 and the genes on the x-axis are plotted against the logarithmic p-value (left y-axis) and the recombination rate (right y-axis). The Linkage Disequilibrium (LD) of the other SNPs with the lead SNP r^2 is color-coded. The only genomewide significant SNP is the rs11556924 polymorphism in the gene ZC3HC1. Image from [Schunkert et al., 2011].

1.5 Aims of this Thesis

ZC3HC1 was found to be a risk gene for hypertension and other CVDs. But especially for hypertension, the pathomechanisms are unclear. Hypertension is a complex disease, in which SMCs play a major role. SMCs can switch their phenotype between contractile and synthetic, which contributes to the development of diseases. The main aim of this thesis is to investigate the influence of the risk gene *ZC3HC1* on the phenotype characteristics of human vascular SMCs. Thus, this thesis aims to advance our current understanding of the role of *ZC3HC1* in SMCs and bring new insight into the pathophysiology of hypertension in general.

The work presented in this thesis comprises a number of steps: Firstly, we generate *ZC3HC1* deficient cells using Small interfering RNA (siRNA) knockdown. Then, in a second step, these cells will be examined regarding their phenotype characteristics like migration, proliferation, and contractility. As a third step, the pathomechanisms of *ZC3HC1* will be studied on a molecular level. As NIPA is a cell cycle protein, its influence on cell cycle regulation is also part of this thesis. To validate the *in-vitro* data *ex-vivo*, a complete knockout mouse model is used and vasoconstriction of the aorta is measured.

2 Material and Methods

2.1 Cell Culture Experiments

2.1.1 Material

Table 2.1: General Material for Cell Culture Experiments

Material	Company
Cell culture plates	
6-Well	Sarstedt
12-/ 24-Well	Nunc by ThermoFisher Scientific
48-/ 96-Well	Greiner bio-one
4-Well Chamber Slides	Sarstedt
Reaction tubes (0.2, 0.5, 1.5 and 2.0mL)	Sarstedt
Reaction tubes (15 and 50mL)	Sarstedt
Serological Pipettes (2, 5, 10 and 25mL)	Sarstedt
Micropipettes Research (100-1000μL, 10-100μL, 2-20μL)	Eppendorf
Biosphere Filter Tips (10, 100 and 1000μL)	Sarstedt
T75, T175 Cell Culture Flasks	Sarstedt
Via1-Cassette for NucleoCounter	ChemoMetec
Glass Pasteur Pipettes	Hecht Assistent
Culture-Insert 4 Well for self-insertion	ibidi
Pasteur Pipettes	Labsolute
Inoculation Loop	Sarstedt
Coverslips	Menzel-Glaeser
Flow Cytometry Tube 5mL	pluriSelect
Pre-Separation Filters (20 μm)	Miltenyi Biotec

Table 2.2: Reagents and Buffer for Cell Culture Experiments

Reagent/Buffer	Composition	Company
SMC Medium M231		Gibco
Smooth Muscle Growth Supplement (SMGS)	Containing: FBS 4.9%, Human basic FGF (2ng/mL), Human EGF (0.5ng/mL), Heparin (5mg/mL), Recombinant Human ILGF-1 (2μg/mL), BSA (0.2μg/mL)	Gibco
PBS	without Calcium and Magnesium	Lonza
0.05% Trypsin / 0.02% EDTA	diluted 1 : 10 in PBS	ThermoFisher

Trypsin Neutralizer Solution	containing 0.5% FBS	ThermoFisher
Cell Lysis Solution	from RNA isolation kit	IST Innuscreen
GenMute siRNA Transfection Reagent Kit	GenMute siRNA Transfection Reagent	SignaGen Laboratories
	GenMute 5x Transfection Buffer	
Recombinant Human PDGF-BB	100μg/mL in PBS + 0.1% BSA	PeproTech
Mitomycin C powder	from *Streptomyces caespitosus*	Sigma-Aldrich
Cell Proliferation ELISA, BrdU (colorimetric) kit	BrdU labeling reagent, 1,000x conc.	Roche
	FixDenat	
	Anti-BrdU-POD, stabilized	
	Antibody dilution solution	
	Washing buffer, 10x conc.	
	Substrate Solution	
Ultra Pure Distilled Water	RNase and DNase free	invitrogen
4% PFA solution	in PBS	Morphisto
DAPI	1:10,000 in Aqua dest.	Sigma-Aldrich
Aphidicolin	1mg/mL in DMSO	Sigma-Aldrich
DMSO		Sigma-Aldrich
BrdU labeling reagent from Cell Proliferation kit	1,000x conc.	Roche
Acetone:Methanol	1:1	Carl Roth
BSA	diluted in PBS in different concentrations	Sigma-Aldrich
Triton-X	diluted in PBS in different concentrations	Sigma-Aldrich
Muriatic acid (HCl)	1M	Carl Roth
Sodium Tetraborate Decahydrate Buffer	0.1M, adjust pH to 8.5 and fill up to 1L with Aqua dest.	Sigma-Aldrich
Ethanol	70%	
Muriatic acid (HCl)	2M	Merck
Propidium Iodide	50μg/mL	ThermoFisher
RNase A, DNase and Protease-free	diluted to 0.1μg/mL	ThermoFisher Scientific
FoxP3 Staining Buffer Set	Fixation/Permeabilization Solution 1+2	Miltenyi Biotec
	Permeabilization Buffer	
Rat tail collagen type 1	liquid in 2M acetic acid, diluted to 3mg/mL	Corning
Acetic acid	2M	Sigma-Aldrich
6x DMEM	DMEM powder 6x conc. in Aqua dest. with 6mL/100mL Sodium Pyruvate and 22.2g/L Sodium Bicarbonate	

DMEM powder, high glucose	with 4.6g/L D-Glucose and L-Glutamine without Sodium Pyruvate and Sodium Bicarbonate	ThermoFisher
Sodium Bicarbonate ($NaCO_2$)	powder	Honeywell Fluka
Sodium Pyruvate	solution 100mM	Sigma-Aldrich
Bradykinin Acetate	powder	Sigma-Aldrich
Cytochalasin D	from *Zygosporium masonii*, 5mg/mL in DMSO	Sigma-Aldrich
Cell Permeabilization Solution	3% BSA + 1% Triton-X in PBS / 1% BSA + 0.2% Triton-X in PBS	
Cell Blocking Solution	5% BSA in PBS / 3.5% BSA in PBS	
Fluorescence Mounting Medium		Dako

Table 2.3: Devices and Software for Cell Culture Experiments

Device/Software	Company
CO_2-Incubator Hera cell	Heraeus
NucleoCounter NC-200	ChemoMetec
Centrifuge 5702R	Eppendorf
Varifuge 3.0R	Heraeus
Fluorescence Microscope IX-70	Olympus
Laminar Flow Clean Bench	CleanAir
Shaking Water bath 1083	GFL
Microscope Eclipse TS100	Nikon
Vaccuum Suction System	LabArt
Vortex-Genie 2	Scientific Industries
Duomax 1030	Heidolph
Synergy HT Microplate Reader	BioTek
Fluorescence Microscope BZ9000	Keyence
bizhub C4050	Konica Minolta
FACSCanto	BD Biosciences
Rainin Pipet-X	Mettler Toledo
NucleoView NC-200 V 1.2.0.0	ChemoMetec
Office 365 Excel	Microsoft
GraphPad PRISM 9	GraphPad Software, Inc.
CellSens Software	Olympus
ImageJ 11.16.17	NIH
FlowJo 10	BD BioSciences

Table 2.4: Biological Material for Cell Culture Experiments

Biological Material	Company/ Details
Primary Human Aortic SMCs	Cell Applications Inc. #345-05a Lot 2228 Genotype CC for SNP rs11556924 in ZC3HC1
Immortalized Human Coronary Artery SMCs	Cell Applications Inc. #350-05a Lot 1848, immortalized by inScreen-Ex Genotype CC for SNP rs11556924 in ZC3HC1
ZC3HC1-siRNA # 13.1	2 nmol in 200 μL RNase free water ($c = 10\mu M$), Integrated DNA Technologies 5' - GGUCACAGUGGAAUGUGAUAUGCTC - 3' 3' - ACCCAGUGUCACCUUACACUAUACGAG - 5'
Negative Control Dicer substrate siRNA	2 nmol in 200 μL RNase free water ($c = 10\mu M$, Integrated DNA Technologies #51011403

2.1.2 Cell Cultivation, Splitting and Counting

All the SMCs were cultivated in the incubator (see table 2.3) at 37°C and 5% Carbon dioxide (CO_2). For all of them, the SMC medium with Smooth Muscle Growth Supplement as described in table 2.2 was used. The cells were cultivated in T75 or T175 cell culture flasks until they reached 80-90 % confluency. The primary human aortic SMCs were all passage 6 when they were split to be used for experiments. The immortalized cells were originally from human coronary artery SMCs, which were immortalized. For splitting the cells, they were first washed once with Phosphate buffered saline (PBS). They were then incubated for 3-4 minutes with trypsin/Ethylenediaminetetraacetic acid (EDTA) solution (see table 2.2) and manually detached from the ground of the flask by shaking and taping it. Twice as much trypsin neutralizer solution containing Fetal Bovine Serum (FBS) was added and the cells were transferred to a falcon. About 0.5mL of the cell suspension was kept in a small reaction tube for counting the cells. Counting was done with the NucleoCounter NC-200 as described by the manufacturer. The rest of the cells were centrifuged for 3 minutes at 200xg. The trypsin and trypsin neutralizer solution were removed and the cell pellet was resuspended in SMC medium at the requested dilution and seeded on cell culture plates for experiments as described in the following sections.

2.1.3 Knockdown of *ZC3HC1* Gene Expression in Human Smooth Muscle Cells Using siRNA

Generally, transfection describes the process of introducing foreign genetic material into cells to get genetically modified cells. Cells could be transfected either with Deoxyribonucleic acid (DNA) or Ribonucleic acid (RNA) and the transfected material could be integrated permanently into the genome (stable transfection) or influence the genes just transiently (transient transfection) [Kim and Eberwine, 2010]. There are different methods to introduce the genetic material into the cell. The possibilities for DNA transfer could be read for example in [Recillas-Targa, 2006]. Here a transfection with RNA was used. It is a transient transfection, as the RNA is not integrated into the genome and is degraded after some time. Transfection with siRNA can be done with physical or chemical-based methods such as microinjection or liposomal reagents, respectively [Brazas and Hagstrom, 2005]. A schematic presentation of the processes in the cell cytoplasm is shown in figure 2.1. This method was used to achieve the knockdown of *ZC3HC1* in human smooth muscle cells.

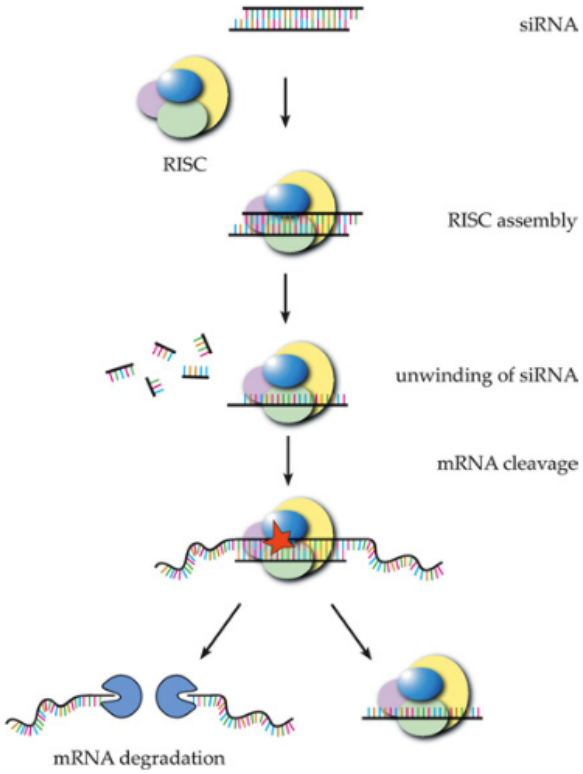

Figure 2.1: RNA interference with siRNA transfection. The siRNA induces the formation of the RNA-induced silencing complex (RISC), which incorporates and unwinds it. The antisense strand binds to the target mRNA and this is degraded by the RISC. Image modified from [Cejka et al., 2006].

Primary or immortalized human SMCs were seeded at $0.4 * 10^5$ cells per cm^2 on a cell culture plate in an SMC cell culture medium. After 24 hours at 37°C and 5% CO_2, the cells were transfected with 5nM *ZC3HC1*-siRNA or negative control siRNA. Therefore the GenMute siRNA Transfection Reagent kit was used as described by the manufacturer. GenMute reagent, the transfection buffer, and the siRNA were mixed as shown in table 2.5, incubated for 15 minutes at room temperature, and then carefully added to the medium. The final concentration of siRNA was 5nM. Cells were incubated with the transfection cocktail overnight. Then transfection medium was removed and the cells were incubated further 48 hours with the SMC medium. Cells were now detached and stored at −80°C for Quantitative PCR (qPCR) and Western Blot.

For some experiments, the primary aortic SMCs were stimulated with PDGF. They were incubated with the transfection reagent for 24 hours before the medium was changed and PDGF at a final concentration of 100 ng/mL was added. Cells were incubated for another 24 hours. Cell lysis solution was then added to the cells and they were stored for RNA isolation and qPCR.

Cell Culture Plate	96-Well	48-Well	24-Well	12-Well	6-Well
Surface per Well	0.32 cm^2	1.0 cm^2	1.8 cm^2	3.5 cm^2	9.6 cm^2
Transfection Buffer 5x [μL]	6.4	25	45	90	240
siRNA 10μmol/L [μL]	0.04	0.14	0.25	0.48	1.32
GenMute [μL]	0.13	0.5	0.9	1.8	4.8
SMC Medium [μL]	64	250	450	900	2400
Total Volume per Well [μL]	70.4	275	495	990	2640

Table 2.5: Volumes of Reagents for the Transfection Cocktail with GenMute siRNA Transfection Reagent Kit for 1 Well of a 96-, 48-, 24-, 12- or 6-Well Plate. Other well sizes can be calculated by the surface. Volume is sufficient for 1 well for 1 gene. The transfection buffer, GenMute, and siRNA were mixed and incubated for 15 minutes at room temperature before adding to the cells. The final concentration of the siRNA was 5nM.

2.1.4 Migration assay

A wound healing assay as illustrated in Figure 2.2 was performed to determine the role of *ZC3HC1* knockdown in migration of primary human aortic SMCs. For that, cells were seeded on 6-well cell culture plates at $5 * 10^5$ cells per well. They were immediately transfected as described in section 2.1.3 and incubated overnight with the transfection medium. The next day, the transfection medium was removed and the cells were incubated for 24 hours with SMC medium. The 4-well inserts were placed in 12-well plates with sterile forceps. The cells were detached with Trypsin, counted, and diluted to $7 * 10^5$ cells/mL. Each small well was filled with 100μL cell suspension either of cells with *ZC3HC1* knockdown or without. A few cells were stored at $-80\circ$C for knockdown confirmation with qPCR. Cells were then again incubated overnight. Two hours before the inserts were removed, mitomycin in a final concentration of 10μg/mL was added to the cells as described in [Di et al., 2015]. Mitomycin inhibits proliferation here to separate migration from proliferation. After incubation for two hours, the inserts were removed carefully and the cells were washed once with PBS. Fresh medium without mitomycin was added to the cells. Pictures of the gap were taken at 0, 12, 24, and 48 hours after removing the inserts with the Olympus microscope. Migration was determined by measuring the confluency in the gap with the Confluency Checker software. The assay was performed in four replicates.

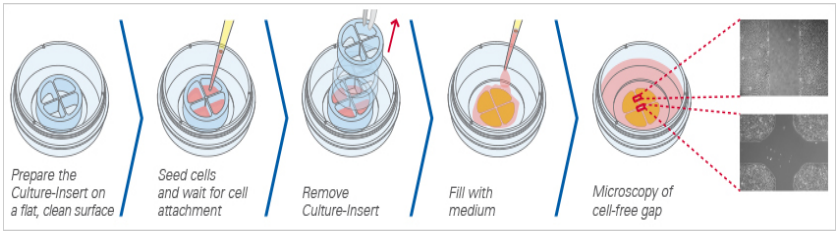

Figure 2.2: Principle of the Wound Healing Migration assay. From `https://www.ibidi.com/culture-inserts/29-25-culture-inserts-4-well-for-self-insertion.html/#34-pcs_box-25_in_1_case`, accessed 19. October 2022

2.1.5 Proliferation assays

Furthermore, the influence of *ZC3HC1* knockdown in SMCs on proliferation was determined with different proliferation assays. At first, an Enzyme-linked Immunosorbent Assay (ELISA) with cells that incorporated Bromodeoxyuridine (BrdU) was done. Then cells were counted once after staining with 4',6-diamidino-2-phenylindole (DAPI) and once with a cell counting device and software. All of the assays were done with primary human aortic SMCs and at least three replicates of each assay were done. In every assay, a few cells were stored at $-80°$C for knockdown confirmation with qPCR.

The first one was an ELISA with BrdU performed with the "Cell Proliferation ELISA, BrdU (colorimetric) "kit from Roche. The steps of the assay were done according to the protocol of the manufacturer. Transfected cells with or without ZC3HC1 knockdown were 24 hours

after transfection seeded on 96-well cell culture plates at 7000 cells per well. After 24 hours the cells were incubated with a BrdU labelling solution. The cells were again incubated for 24 hours and as BrdU is an analog of the nucleoside thymidine, it was incorporated in the replicating DNA of the cells when they were proliferating. After the incorporation of BrdU, the cells were denatured and an anti-BrdU solution was added. The cells were incubated with the antibody for 90 minutes at room temperature, before removing the antibody solution and washing the cells three times with the kit's washing buffer. For measuring, the substrate solution was added to the cells and incubated for another 30 minutes. The color development could now be measured photometric with an ELISA reader at 370nm. The values were normalized to the blank measurement.

To confirm the results, transfected SMCs were seeded on a 12-well plate at $0.25 * 10^5$ cells per well in 0.5mL SMC medium. Proliferation was determined after 4, 24, 48, 72 and 96 hours. At these points of time cells were fixed and stained with DAPI, which is fluorescent and binds strongly to adenine-thymine-rich regions in DNA. For this, the medium was removed and the cells were washed once with PBS. To fix the cells, they were incubated at room temperature with 4% Paraformaldehyde (PFA) for 5 minutes. To make them permeable for the DAPI, they were incubated for 10 minutes with 0.1% Triton-X in PBS and washed once after that. Then DAPI staining solution was applied for 15 minutes to stain the cells and they were washed again once with PBS. The stained cells were viewed with a Keyence fluorescence microscope. They were counted with an in-house macro for ImageJ described in [Al-Hasani, 2017]. 10 pictures per well were taken and counted. The average was multiplied by 3.06 to extrapolate the area of the whole well.

As the DAPI staining assay had its limitations (see section 3.3.2), results were confirmed by counting the cells with the cell counter. The transfected cells with and without *ZC3HC1* knockdown were again seeded at $0.25 * 10^5$ cells per well on a 12-well plate. The points of time to determine proliferation were again at 4, 24, 48, 72, and 96 hours after seeding the cells on the plate. SMC medium was removed and the cells were incubated in the incubator with 0.3mL trypsin per well for 3-5 minutes to detach the cells. Trypsin Neutralizing Solution was added and the cells were transferred to a small reaction tube. They were then counted three times with the cell counter and the average of the number of cells was analyzed.

2.1.6 Cell Cycle Synchronization of SMCs

Aphidicolin was used to synchronize the cell cycle of SMCs. It is a well-known inhibitor of DNA polymerase α [Ikegami et al., 1978], so it arrests the cell cycle at the end of the G1 phase before the entry into the S phase [Jackman and O'Connor, 1998] (see also figure 2.3). This is a common approach to study G2 progression [Tanner et al., 2003, Wright et al., 1999], where NIPA has its main activity.
Different assays were performed to first find an appropriate concentration and incubation time for aphidicolin and then to show its efficacy in cells in general and also in transfected

cells. All experiments were performed in triplicates with primary human aortic SMCs.

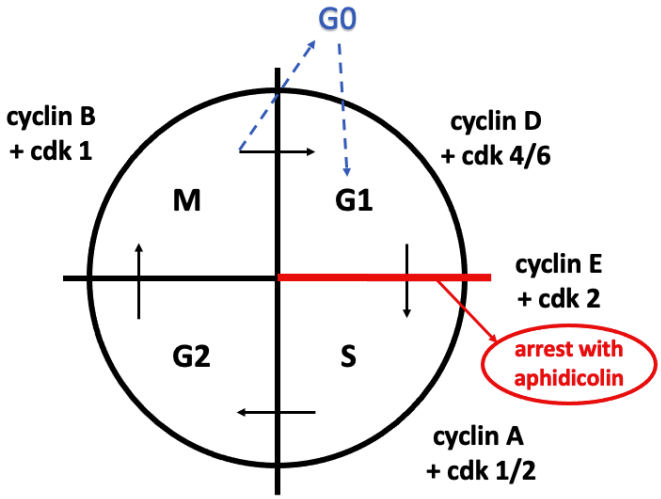

Figure 2.3: Function of cyclins and cyclin dependent kinases (cdks) in the cell cycle according to [Johnson et al., 2017]. Cell cycle arrest with aphidicolin is marked. Cyclin D + cdk4/6 controls the G1 phase, cyclin E + cdk2 controls the transition from G1 to S, cyclin A + cdk 1/2 controls the S phase, and cyclin B + cdk1 controls the M phase.

For the first experiments, cells were seeded at $0.1 * 10^5$ cells per well in SMC medium on 4-well chamber slides. Cells were incubated for several days in the incubator to get the desired density. On day 5 medium was changed and fresh SMC medium was added to the cells. On day 7 aphidicolin with a concentration of 10μg/mL was added to half of the wells and Dimethyl Sulfoxide (DMSO) as a control to the other half of the wells. Cells were incubated with aphidicolin or DMSO for 6, 12, 18, 24, 30, 36, and 48 hours. At these points in time, cell lysis solution was added to the cells and they were stored at $-20°$C for RNA isolation and qPCR with different cell cycle proteins. Cyclin B1, cyclin D1, cyclin E1, and cdk2 were chosen for this analysis. The different concentrations during the cell cycle are shown in figure 2.4.

As the qPCR with cell cycle proteins did not give the desired proof of cell cycle arrest (see section 3.4.2), another method should be established with the next experiment. Furthermore, different concentrations of aphidicolin should be tested. Cells were seeded at $0.3 * 10^5$ cells per well in SMC medium on a 48-well plate. The next day, aphidicolin or DMSO at concentrations of 10, 25, or 50μg/mL was added and one part of the cells was incubated for 24 hours and one part for 48 hours. After this time, cells were treated with 50μM BrdU solution stained following the protocol in section 2.1.7.

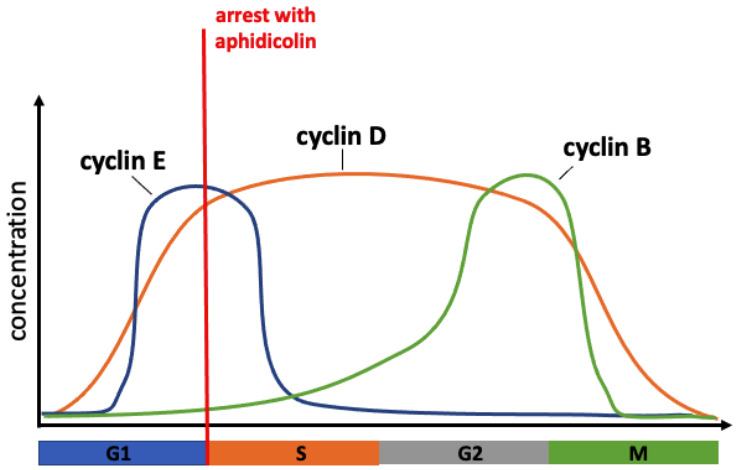

Figure 2.4: Concentration of different cyclins during the cell cycle according to [Johnson et al., 2017]. Cell cycle arrest with aphidicolin is marked. Cyclin E is present during the G1 and S phases, cyclin B accumulates during the G2 phase and degrades in the M phase and cyclin D accumulates in G1, is present during the whole cell cycle, and degrades only in the M phase.

The third experiment was performed with transfected cells. Cells were seeded at $0.25 * 10^5$ cells per well in SMC medium on a 48-well plate. They were transfected with *ZC3HC1* or negative control siRNA as described in section 2.1.3 the next day. After 48 hours aphidicolin or DMSO at 10μg/mL was added to the cells and they were incubated for 24 hours. BrdU was added to one part of the cells and they were treated as described in section 2.1.7 and the other part was treated with cell lysis solution and stored at $-20°$C for RNA isolation and qPCR.

2.1.7 BrdU assay with Immunofluorescence Staining

To assess the cell cycle progression of the cells seeded on a cell culture plate, they were incubated with 50μM BrdU for 24 hours and then stained. For that, the medium was removed and washed once with PBS. To fix them, they were incubated at -20°C with acetone:methanol 1:1 for 30 minutes and then dried for 10 minutes under the fume hood. For permeabilization, cells were incubated for 5 minutes with 3% Bovine Serum Albumin (BSA) in PBS and 1% Triton-X at room temperature and then washed with PBS once. In the next step, the DNA was hydrolyzed by incubating the cells with 1M hydrochloric acid for 30 minutes at room temperature first and then with 0.1M sodium borate buffer for another 30 minutes at room temperature. Cells were then washed with PBS three times. For blocking cells were then incubated with 5% BSA in PBS. BSA binds to unspecific binding sites to prevent the binding of the antibodies to those sites. The primary antibody for BrdU diluted in 5% BSA in PBS was added and incubated overnight at 4°C. The next day, cells were washed with PBS three times. From that point on, steps were performed in the dark to protect the secondary fluorescence antibody. Cells were incubated with the secondary antibody diluted in PBS for

one hour at room temperature and then washed three times with PBS. As a reference cells were also stained with DAPI. DAPI in Aqua dest. was added and cells were incubated for 15 minutes with it. After that, they were washed several times with Aqua dest. and pictures were taken with a fluorescence microscope.

Antibody	Dilution	Company
BrdU Monoclonal Antibody Mouse-IgG	1:200 in 5% BSA in PBS	Invitrogen #B35128
Goat anti-Mouse IgG Cross-Adsorbed Secondary Antibody, Alexa Fluor 488	1:300 in PBS	Invitrogen #A-11001

Table 2.6: Primary and Secondary Antibodies for BrdU Immunofluorescence staining.

2.1.8 Flow Cytometry

The cell cycle arrest of the SMCs with Aphidicolin was also confirmed with flow cytometry based on [Tanner et al., 2003]. For this experiment immortalized human aortic SMCs were used because of the high amount of cells needed. Cells were seeded in T175 and T75 cell culture flasks in SMC medium with about $5 * 10^6$ and $2 * 10^6$, respectively. Aphidicolin or DMSO was added to the SMC medium to a final concentration of 10μg/mL. After 24 hours treatment with Aphidicolin or DMSO medium was changed, so that the Aphidicolin was removed and the cells could proceed in the cell cycle. Cells were harvested 0, 12, and 24 hours after removal of Aphidicolin or DMSO. 12 hours before each time point, BrdU 10μg/mL was added to the medium. As mentioned before, BrdU incorporates into the DNA in the replication phase of the cell and shows in this way the progression of the cell cycle to the S phase.

Cells were prepared for the flow cytometry measurement according to the following protocol: Medium was removed from the flasks and cells were washed with PBS once. Cells were detached with trypsin by incubating for 5 minutes at room temperature and then pipetted into a falcon. They were then centrifuged for 10 minutes with 600xg and the supernatant was discarded. Cells were then washed with PBS followed by centrifugation for 5 minutes at 600xg two times. At the last washing step, cells were counted with the cell counter. In the next steps, cells were fixed, permeabilized, and stained for the flow cytometry measurement.

For fixation, 70% cold ethanol was added to the cells (100 μL / $1 * 10^6$ cells) and they were incubated for 30 minutes at -20°C. They were then centrifuged for 10 minutes with 1000xg and the supernatant was discarded. Cells were washed once with PBS and centrifuged for 5 minutes with 1000xg and the supernatant was discarded. They were resuspended in 2M muriatic acid and incubated for 30 minutes at room temperature. Samples were centrifuged for 5 minutes with 1000xg and the supernatant was discarded. After this step, cells were stored at 4°C in PBS overnight. For Permeabilization, samples were centrifuged for 5 min-

utes with 1000xg and the supernatant was discarded. 0.5% Tween 20 (100μL / $1 * 10^6$ cells) was added to the cells. They were now split up into samples in 1.5mL reaction tubes with a volume of 100μL per reaction tube so that each sample contained $1 * 10^6$ cells.

The samples of interest were all stained with an AlexaFluor 488 anti-BrdU antibody (see table 2.7)and Propidium iodide (PI), which is a red-fluorescent nuclear and chromosome counterstain. It intercalates between the bases in the DNA without sequence preference. As a control, there was an unstained sample, one single stained with the AlexaFluor 488 antibody, and one single stained with PI. The AlexaFluor 488 antibody was directly added to the samples into the permeabilization buffer with 5μL per sample and incubated for 30 minutes at room temperature. Cells were then centrifuged for 5 minutes with 1000xg and the supernatant was discarded. Samples were resuspended in 500μL per reaction tube for the measurement. PI at 50μg/mL was added as necessary. All samples were mixed with RNase at 0.1μg/mL. Samples were then measured at the BD FACS Canto. For analysis of the results, FlowJo software was used.

Antibody	Dilution	Company
BrdU Monoclonal Antibody, FITC	5 μL/test	Invitrogen #11-5071-42

Table 2.7: Antibody for Flow Cytometry.

2.1.9 Gel Contraction Assay

The role of the *ZC3HC1* knockdown in contractility of primary human aortic SMCs was determined with a gel contraction assay as described in [Sakota et al., 2014]. For the gels, ingredients as shown in table 2.8 were mixed in a 24-well cell culture plate until the color was homogeneous. Cells transfected with *ZC3HC1*- and control-siRNA were used. The gels were then polymerized for one hour in the incubator and then 500μL SMC medium per well was added on top of the gels. They were then incubated for 24 hours in the incubator. The medium was then carefully removed and fresh SMC medium was added. One-third of the cells got medium with 10nM bradykinin for stimulating the contraction, one-third got medium with 0.5μM cytochalasin D for inhibiting the contraction, and one-third got SMC medium without any additives. The gels were then released from the well carefully with an inoculation loop so that they could float in the medium. Images of the gels were taken with a scanner at 1, 2, 3, 4, 5, and 24 hours after the release. For quantification of the contraction, the area of the gels was measured manually with ImageJ. Three replicates of the assay were performed.

Ingredients	Volume
6x DMEM	80μL
Rat tail collagen type 1 3mg/mL	400μL
Cell suspension $1 * 10^6$ cells/μL	120μL
Total	600μL

Table 2.8: Composition of One Gel in One Well of a 24-Well Plate for the Gel Contraction Assay. After polymerization, 500μL SMC medium was added on top of the gels. For the cell suspension, primary human aortic SMCs with and without *ZC3HC1* knockdown were used.

2.1.10 Immunofluorescence Staining for Contractile Phenotype Markers with Calponin and Alpha-Smooth-Muscle Actin

SMCs of the vessels have usually a contractile phenotype. They are not terminally differentiated but can undergo a phenotype switch to a synthetic phenotype with a higher migration and proliferation rate. [Owens et al., 2004]. The SMCs express different markers for both of the phenotypes. Calponin and SMA are contractile proteins that are a marker for the contractile phenotype of the cells. The influence of *ZC3HC1* on the phenotype switch of SMCs should be determined with immunofluorescence staining for calponin and SMA. For this, primary human aortic SMCs were seeded on a 4-well chamber slide with $0.3 * 10^5$ cells per well. Three chamber slides with four wells each were seeded. As a knockdown control, 6 wells on a 48-well plate were seeded at $0.35 * 10^5$ cells per well. Cells were incubated for 24 hours and then transfected with *ZC3HC1*-siRNA and negative control siRNA as described in section 2.1.3. After 24 hours the medium was changed and the cells for control of the knockdown were covered with cell lysis solution and stored at -20°C for qPCR analysis. The cells on the chamber slides were incubated for a further 48 hours. The medium of the cells was discarded, they were then washed once with PBS and then stained with steps 1-5. One slide was single-stained with calponin, one slide was single-stained with SMA, and one slide was stained with both. All slides were additionally stained with DAPI.

1. Fixation: Cells were covered with methanol:acetone 1:1 and were incubated for 30 minutes at -20°C. The supernatant was discarded and cells were dried under the fume hood.

2. Permeabilization: Cells were incubated with 0.2% Triton-X and 1% BSA in PBS for 30 minutes at room temperature.

3. Blocking: The slides were incubated with 3.5% BSA in PBS for 30 minutes at room temperature to prevent unspecific binding.

4. Primary Antibody: The slides were incubated with the primary antibodies for calponin and SMA in PBS as shown in table 2.9 overnight on a shaker at 4°C. The next day they were washed 3 times with PBS for 5 minutes.

5. Secondary Antibody: The slides were incubated with the secondary antibodies in PBS as shown in table 2.9 for one hour at room temperature. Calponin was stained red and SMA was stained green fluorescent.

After that, the slides were stained with DAPI. DAPI with Aqua dest. 1:10,000 was added to the slides and they were incubated for 15 minutes light-excluded. They were then washed several times with Aqua dest. As the last step, the chambers were removed and the slides were covered with cover glasses using Dako Fluorescence mounting medium. Slides were cured for 30 minutes light-excluded and then stored light-excluded at 4°C.
The slides were viewed with the Keyence fluorescence microscope and images were taken.

Antibody	Dilution	Company
Monoclonal Anti-Actin, α-Smooth Muscle - FITC, antibody produced in mouse	1:100 in PBS	Sigma-Aldrich #F3777
Monoclonal Anti-Calponin antibody produced in mouse	1:300 in PBS	Sigma-Aldrich #C2687
Goat anti-Mouse IgG Cross-Adsorbed Secondary Antibody, Alexa Fluor 568	1:300 in PBS	Invitrogen #A-11004

Table 2.9: Primary and Secondary Antibodies for Immunofluorescence Staining with Calponin and SMA.

2.2 Moleculobiological Methods

2.2.1 Material

Table 2.10: General Material for Moleculobiological Methods

Material	Company
Reaction tubes (0.2, 0.5, 1.5 and 2.0mL)	Sarstedt
Reaction tubes 0.2mL for PCR	Greiner
Reaction tubes (15 and 50mL)	Sarstedt
Biosphere Filter Tips (10, 100 and 1000μL)	Sarstedt
Mikropipettes Research (100-1000μL, 10-100μL, 2-20μL)	Eppendorf
Pipette Tips	Sarstedt
384-well plate	Biolab
CRYSTAL optical clear qPCR film	Biolab
96-Well ELISA Strip Plate with F-Bottom	Greiner Bio-One
Drying block	Whatman
Chromatography paper (3mm)	Whatman
Immobilon-P PVDF Transfer Membran	Merck Millipore
Mini Protean Short Plates	Bio-Rad
Mini Protean Glass Plates	Bio-Rad
Mini Protean Tetra Cell Casting Stand and Clamps	Bio-Rad
Pasteur Pipettes	Labsolute
Glass Flasks (0.5 and 1 L)	Schott Duran
Tetra Cell Gel Holder Cassette	Bio-One
Tetra Cell Cooling Unit	Bio-One

Table 2.11: Reagents and Buffer for Moleculobiological Methods

Reagent/Buffer	Composition	Company
InnuPrep RNA Mini Kit 2.0	Lysis Solution RL Washing Solution HS and LS (conc.) RNase-free Water Spin Filter D and R Elution and Receiver Tubes	IST Innuscreen
Ethanol	70%	J.T. Baker
Ultra Pure Distilled Water	RNase and DNase free	invitrogen
M-MLV Reverse Transcriptase Kit	Reverse Transcriptase (200U/μL) DTT 100mM	Invitrogen #28025-021

	Reaction buffer (5x)	
dNTP mix 100mM each	mixed to 4mM	Promega
Hexanucleotide Random Primer Mix		Carl Roth
RiboLock RNase Inhibitor		Thermo Scientific
Primers	see Table 2.13	Eurofins Genomics
PowerUp SYBR Green MasterMix		ThermoFisher
Agarose	1.5% in TBE buffer	Biozym
TBE buffer	100mM Tris-Base + 80mM Boric Acid + 1mM EDTA in aqua dest.	Sigma-Aldrich
SYBR-Green I	diluted 1:200 in DMSO	Invitrogen
DMSO		Sigma-Aldrich
RT^2 Profiler PCR Array (96-Well Format and 384-Well [4 x 96] Format)	Human Cell Motility, cAMP/ Calcium Signaling PathwayFinder	Qiagen
Dextran Blue Buffer	99% Formamide	Fluka by Sigma-Aldrich
	1% Dextran Blue	Sigma-Aldrich
	80μL 5x Nucleic Acid Sample Loading Buffer per mL final volume	Bio-Rad Laboratories
Loading Dye	Dextran Blue buffer : SYBR-Green I 2:1	
DNA Ladder plus 100bp	500ng/μL, diluted to 44ng/μL in aqua dest.	Peqlab
Cell Lysis buffer (10x)		Cell Signaling
Complete Protease Inhibitor Cocktail (25x)	stock solution prepared by dissolving one tablet in 2mL aqua dest.	Roche
PMSF		Sigma
RNase-Free DNase Set	diluted with 550μL Aqua dest.	Quiagen
DC Protein Assay	Reagent A, B and S	Bio-Rad
Protein Standard	2mg/mL BSA	Sigma Aldrich
Acrylamid:Bisacrylamid	37.5:1	Carl Roth
Trizma-Base	powder	Sigma-Aldrich
SDS ultra pure	powder	Carl Roth
Separation Gel Buffer	1.5M Tris pH 8.8 + 0.4% SDS	
Stacking Gel Buffer	0.5M Tris pH 6.8 + 0.4% SDS	
TEMED		Sigma-Aldrich
10% APS	in Aqua dest.	Carl Roth
Ethanol		

Electrophoresis Buffer	12.5M Tris-Base + 9.6mM Glycin + 1.75mM SDS, adjust pH to 8.3 and fill up to 1L with Aqua dest.	
Precision Plus Protein Dual Color Standard		Bio-Rad
Blue Loading Buffer (3x)		New England BioLabs
DTT	1.25M in Aqua dest.	New England BioLabs
Sample Loading Buffer	Blue Loading Buffer : 1.25M DTT 10:1	
Glycin	powder	Sigma-Aldrich
Methanol		Carl Roth
Blot Buffer	25mM Tris-Base + 192mM Glycin + 200mL Methanol, add Aqua dest. to 1L	
Tween 20		Merck
TBS	150mM NaCl + 10mM Tris, add Aqua dest. to 1L, adjust pH to 7.3	
TBS-Tween	1L TBS + 500μL Tween 20	
5% Skimmed Milk	2.5g Skimmed Milk Powder in 50mL TBS	Carl Roth
ECL Prime Western Blotting Detection Reagent	Reagent A+B	GE Healthcare

Table 2.12: Devices and Software for Moleculobiological Methods

Device/Software	Company/URL
PCR Cycler	SensoQuest labcycler
Chemidoc XRS documentation	Bio-Rad
Synergy HT Microplate Reader	BioTek
Centrifuge 5415R	Eppendorf
ND-1000	ThermoFisher
Labinco L46 Vortexmixer	LabMakelaar Benelux B.V.
Scale LA120S	Sartorius
Rotanta 460R	Hettich
Magnetic stirrer Big-Squid ocean	IKA
7900 HT Fast Real-Time PCR	Applied Biosystems
Mini Protean Tetra Cell System	Bio-Rad
PowerPac 300	Bio-Rad
Duomax 1030 Shaker	Heidolph
VXR basic Vibrax	IKA
Electrophoresis Chamber	Peqlab
Electrophoresis Power Supply EPS 300	Pharmacia Biotech

Power PAC 300	Bio-Rad
Primer 3 [Untergasser et al., 2012]	`https://bioinfo.ut.ee/primer3-0.4.0`
Ensembl Gene Database	`https://www.ensembl.org`
SDS 2.4.2	Applied Biosystems
Office 365 Excel	Microsoft
GraphPad PRISM 9	GraphPad Software, Inc.
ImageJ 11.16.17	NIH
Qiagen GeneGlobe Data Analysis Center	`https://geneglobe.qiagen.com/us/analyze`

2.2.2 Design of Primers

For some of the genes of interest, primers for qPCR had to be designed. For that, the gene database Ensembl and the online program Primer 3 [Untergasser et al., 2012] were used. The gene was searched at Ensembl and a transcript was chosen, that contains the most genetic information. The primers should be between two exons and SNPs should not be included. Variants with a minor allele frequency of $< 0.01\%$ were not displayed. The chosen exons were then entered at Primer 3 and primers were picked. The product size should be between 100 and 150 base pairs (bp). Primers were synthesized by Eurofins Genomics.

Primers for *CCNB1*, *CCNE1*, *CCND1*, and *CDK2* were self-designed, the rest was already established in-house. Primers were all diluted at a concentration of 100 pmol/μL and for Polymerase Chain Reaction (PCR) mixed with water 1:20 forward and reverse primer. To test the specificity of the primers, a PCR with each primer pair was done and a gel electrophoresis with the samples was run as described in the following sections.

Table 2.13: Primer pairs used for qPCR with cDNA.

Gene	Primer Forward (F: $5' - 3'$) and Reverse (R: $3' - 5'$)	Expected Product Length
GAPDH	F: AGATTTGGTCGTATTGGG R: GGAAGATGGTGATGGGATT	203 bp
ZC3HC1	F: CTGGCCAGACAGCCCATC R: GAAGCTGGAGGTCCAAGTGA	119 bp
CCNB1	F: GCCAGAACCTGAGCCTGTTA R: CAGAGAAAGCCTGACAC	135 bp
CCNE1	F: CCTCTTCTGCAGCCAAAAAT	123 bp

	R: CGCCATATACCGGTCAAAGA	
CCND1	F: AGACCTTCGTTGCCCTCTGT R: AGTTGTTGGGGCTCCTC	120 bp
CDK2	F: CCAAAAGGTGGAAAAGATCG R: ATGGCAGTACTGGGCACAC	135 bp
CNN1	F: GTTGGCCTCAAAAATGTCGT R: AGGCTCCGTGAAGAAGATCA	121 bp
OPN	F: CACTACCATGAGAATTGCAGTGA R: CTGCTTTTCCTCAGAACTTCC	100 bp
SMTN	F: GAGCCTCAGGAGTCTCCAAC R: GGTGGACTCTCGGTTCTGG	207 bp
VIM	F: GGGACCTCTACGAGGAGGAG R: GGCTTCCTCTCTCTGAAGCAT	158 bp
ACTA2	F: TAGAACATGGCATCATCACCA R: AGGGTGGGATGCTCTTCAG	100 bp
TAGLN	F: CACCAGCTTGCTCAGAATCA R: GTCCTTCCTATGGCATGAGC	185 bp
PCSK9	F: GGCTTCCTGGTGAAGATGAG R: TGGGCAAAGACAGAGGAGTC	95 bp
MGP	F: CAAATACCTTCATATCCCCTCA R: TCTGTAGTCATCACAGGCTTCC	113 bp
MAP1LC3B	F: AGCAGCTTCCTGTTCTGGAT R: AGGCCTGATTAGCATTGAGC	111 bp
ACTG2	F: CCCTCAGTCACTGGGAGAAG R: CCAGAGCCATTGTCACACAC	120 bp
LMOD1	F: GCTCAACTTCTGTGAAAAGGAGA R: TCTTGGCATCTGTCTTGGTCT	95 bp

2.2.3 Polymerase Chain Reaction

With the Polymerase Chain Reaction, specified DNA sequences can be amplified. A PCR consists of the following steps, which are considered one PCR cycle and are repeated several times:

1. Denaturation: By heating the sample at 95°C, the double helix denatures in single helices.
2. Annealing: At 55°C primers anneal to their specific complementary sequences. These are at the beginning and at the end of the sequences, which should be amplified.

3. Elongation: At 72°C a DNA polymerase elongates the DNA with free Deoxyribose Nucleoside Triphosphates (dNTPs) until it gets inactivated by the high temperature in Step 1.

For the PCR here, Complementary DNA (cDNA) from section 2.2.6, primers, MasterMix, and water were mixed as in table 2.14.

Ingredients	Volume
cDNA	1.5μL
PowerUp SYBR Green MasterMix	3.75μL
Primers F+R 5 pmol/μL each	1.125μL
Aqua dest.	1.125μL
Total	6.5μL

Table 2.14: Ingredients for a PCR reaction

The samples were placed in the PCR cycler and the steps of the PCR were done as described in table 2.15.

Step	Time	Temperature	
Degradation of dUTPs from RNA	2 min	50°C	
Initial Denaturation and Activation of the Taq Polymerase	10 min	95°C	
Annealing	15 sec	95°C	repeat
Elongation	1 min	60°C	40x

Table 2.15: Steps of the PCR for Testing the Primers. After an initial degradation of the dUTPs that might be still present from the RNA, there is an initial denaturation step. The HotTaq polymerase is activated. Then an annealing and an elongation step are repeated 40 times.

2.2.4 Gel Electrophoresis

To test the specificity of the primers, gel electrophoresis with the samples generated in Section 2.2.3 was done. A 1.5% agarose gel was produced. 7.5μL of the samples were mixed with 3μL of the Loading Dye (see table 2.11) to a total volume of 10.5μL and each was pipetted into one pocket of the gel. One pocket was filled with 7.5μL of a 100bp-ladder with 3μL Loading Dye. Gel electrophoresis was then run with 105V for 45 minutes until the DNA fragments were separated by their size. If the primers work well, there would be only one strong band, which indicates, that the primers amplify only one DNA part.

2.2.5 RNA Isolation out of SMC and Quantification

RNA isolation out of the SMCs was performed with the innuPREP RNA mini kit 2.0 from IST Innuscreen as described by the manufacturer. Lysis buffer was added to the cells and they were homogenized by pipetting up and down. The solution was then transferred into the first silica membrane filter of the kit, which binds the genomic DNA so that the filtrate contained the RNA. After centrifugation at 4°C, Ethanol 70% was added, and the solution was transferred into the second filter of the kit, which binds the RNA. So after centrifugation, the RNA was transferred to the filter. It was now washed two times with the kit's washing solution, dried by centrifuging, and then with 30μL RNase-free water extracted from the filter. Aliquots were taken to measure the concentration and RNA was stored immediately at -80°C.

RNA concentration was measured with a UV photometer. As nucleic acids have a peak at 260nm in their absorption spectrum, the concentration can be assessed there. Additionally, the absorbance at 230nm (absorption of organic substances) and 280nm (absorbance of protein and phenolics)was measured to determine the purity ratios Absorbance(A)$_{260nm}$/A$_{280nm}$, which should be 2.0 for pure RNA and A$_{260nm}$/A$_{230nm}$, which should be in the range of 2.0-2.2. Concentrations of RNA were between 20 and 30 ng/μL and stored at these concentrations.

2.2.6 Reverse Transcription of RNA into cDNA

The isolated RNA of the SMCs was transcribed into cDNA. As there was only a small amount of RNA, a quality test was not done. The transcription was done with the M-MLV Reverse Transcriptase Kit from ThermoFischer as described by the manufacturer. 10μL of the previously isolated RNA were first denatured at 68°C for 5 minutes in the PCR-cycler, then cooled on ice. A MasterMix as shown in Table 2.16 was prepared and added to the RNA samples to a final volume of 20μL and mixed shortly. The samples were then incubated for one hour at 37°C in the PCR-cycler. The primers could bind to the corresponding RNA-sequences and the reverse transcriptase was synthesizing the cDNA strand. Enzymes were then inactivated for 5 minutes at 95°C. The cDNA samples were stored at -20°C until used for qPCR.

Ingredients	Volume
5x First Strand Buffer	4μL
DTT 100mM	2μL
dNTP-Mix 4mM	1μL
Hexanucleotid Primer Mix	1μL
RiboLock	1μL
M-MLV Reverse Transcriptase	1μL
Total	10μL

Table 2.16: MasterMix for reverse transcription of RNA into cDNA

2.2.7 Quantitative PCR

With the real-time qPCR, it is possible to quantify the amount of the amplified DNA. The ingredients listed in table 2.14 were pipetted into a 384-well plate. The plate was covered with a qPCR film and centrifuged. The qPCR was then done using TaqMan. The steps are shown in table 2.17. In contrast to the PCR described in section 2.2.3, the qPCR has an additional dissociation step at the end. which shows the specificity of the used primers. The temperature is gradually increased up to 95°C and the fluorescence signal is measured. The changes in fluorescence signal are plotted against the temperature. An example is shown in figure 2.5. One peak indicates a single product and so a specific primer.

There are specific and unspecific qPCR methods, her the unspecific dye-based qPCR was performed. The SYBR Green, a fluorescent dye which is contained in the Mastermix, binds to double-strand DNA. The fluorescence signal is measured and is proportional to the amount of double-strand DNA. The qPCR was run with the primers shown in table 2.13. An example of the resulting curves is shown in figure 2.5.

Step	Time	Temperature	
Initial Denaturation and Activation of the Taq Polymerase	10 min	95°C	
Annealing	15 sec	95°C	repeat
Elongation	1 min	60°C	40x
Dissociation	each 15 sec	gradually till 95°C	

Table 2.17: Steps of the qPCR. First, there is an initial denaturation and the HotTaq polymerase is activated. Then an annealing and an elongation step are repeated 40 times. The program ends with a dissociation step, where the temperature is gradually increased up to 95°C.

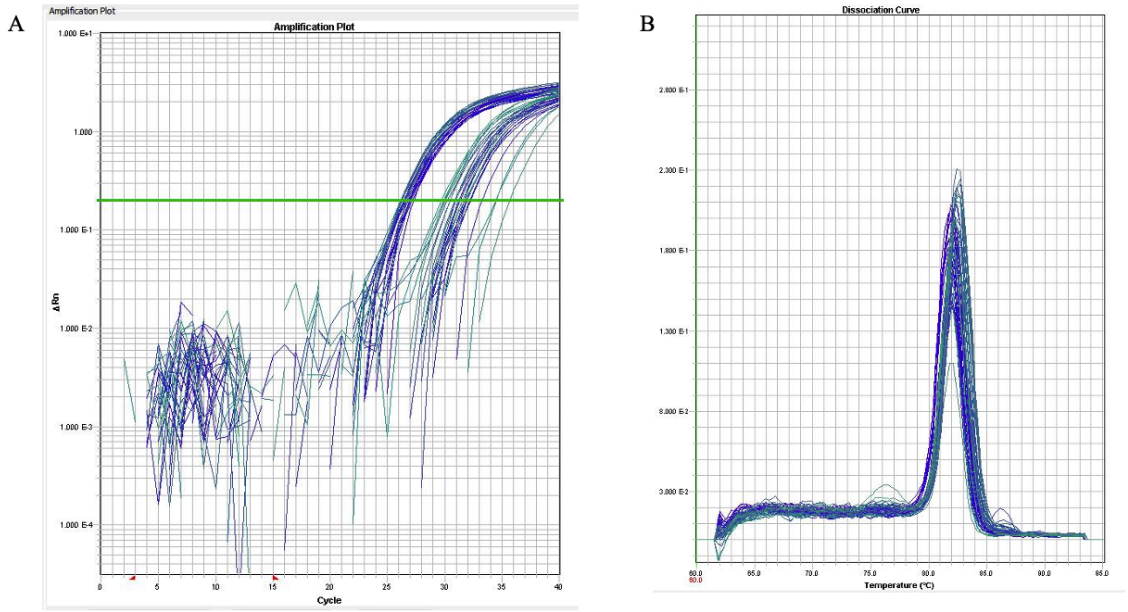

Figure 2.5: A: Amplification plot of a qPCR with the *ZC3HC1* primer. The number of cycles is plotted against ΔRn, which is the fluorescence signal intensity. The green line is the cutoff to determine the C_t value. Here you see two different increases of the signal as the qPCR was done with cDNA from knockout cells and cells without knockout. B: Dissociation curve of a qPCR with the *ZC3HC1* primer. The temperature is plotted against the fluorescence changes. There is only one peak between 80 and 85°C, which indicates a high specificity of the primer.

The qPCR provides a C_t value for each sample. C_t is the number of cycles, that are necessary to reach a certain, previously defined, threshold of fluorescence signal. The smaller C_t is, the more of the certain gene is there in the sample. This could be because of high gene expression or because of higher DNA concentration in the sample. Because of this, it is really important to have the same amount of DNA in each sample. Here, cDNA concentrations of 15-20 ng/μL were used. To make results comparable, C_t values were compared to a housekeeping gene, here *Glyceraldehyde 3-phosphate dehydrogenase (GAPDH)* was used. The mean of three measurements with the same cDNA was calculated for the C_t value. At least three replicates were performed. Data analysis was done with the $\Delta\Delta C_t$ method as described by [Livak and Schmittgen, 2001]. Briefly, there were three steps to calculate the relative gene expression for each sample:

1. Normalization: $\Delta C_t = C_t(\text{gene of interest}) - C_t(GAPDH)$
2. Comparison of cells with *ZC3HC1* knockdown with control cells:
   $\Delta\Delta C_t = \Delta C_t(ZC3HC1 \text{ knockdown}) - \Delta C_t(\text{control})$
3. Relative expression of the gene of interest in the knockdown group compared to the control group: Relative gene expression $= 2^{-\Delta\Delta C_t}$ or $\%KD = (1 - 2^{-\Delta\Delta C_t}) * 100$

For example, when there is no difference between knockdown and control, $\Delta\Delta C_t$ is 0 and $2^{-\Delta\Delta C_t} = 2^0$ is 1, which means the gene expression in the knockdown cells is 100% of the gene expression in the control cells.

2.2.8 RT^2 PCR Profiler Array for Human Cell Motility and Human cAMP/Calcium Signaling PathwayFinder Genes

Two Profiler Arrays for qPCR from Qiagen were performed to identify genes, that are influenced by the *ZC3HC1* knockdown. For the distinction of contractile and synthetic phenotype of SMCs the arrays for cell motility and Cyclic Adenosine Monophosphate (cAMP)/Calcium Signaling PathwayFInder were chosen. Each array contained 84 different genes for analysis as well as genes for positive and negative control. Lists of the genes are shown in section A.1. The arrays were used as described by the manufacturer. Primers on the 96-well plate were diluted with 10μL RNase-free water and pipetted with cDNA and SYBR Green MasterMix on a 384-well plate in the composition as shown in table 2.18. The used cDNA was pooled cDNA from primary human aortic SMCs with or without *ZC3HC1* knockdown from other cell culture experiments. The knockdown was confirmed in all cDNA used. qPCR was run with the 7900 HT Fast Real-Time PCR from Applied Biosystems as described in section 2.2.7. Analysis of the results was done with the Qiagen GeneGlobe Data Analysis Center as described in the protocol.

Ingredients	Volume
cDNA	15ng in 1.75μL
PowerUp SYBR Green MasterMix	3.75μL
Diluted primers	2μL
Total	7.5μL

Table 2.18: Ingredients for the PCR reaction with the Profiler Array

2.2.9 Protein isolation

For the Western Blot (see section 2.2.10), proteins were first isolated out of the cells. During the whole protein isolation, samples were kept on ice all the time. Cells were available as pellets in 1.5mL Eppendorf tubes. A Protein Isolation Buffer was mixed with a cell lysis buffer, a protease inhibitor cocktail, Phenylmethylsulfonyl Fluoride (PMSF), which is another proteinase inhibitor, DNase, and water as shown in table 2.19 and 50μL of the buffer was added to the cell pellets. Samples were homogenized, centrifuged for 1 minute at 4°C with 1000xg, and incubated for one hour at 4°C.

Ingredients	Volume
Cell Lysis Buffer	100μL
Roche Cocktail 25x	100μL
PMSF	10μL
DNase I	15μL
RNase/DNase-free water	790μL
Total	1000μL

Table 2.19: Composition of the Protein Isolation Buffer for a total volume of 1000μL.

Afterward, 5μL of sample or protein standard was pipetted on a 96-well plate for measuring the concentration. This was done in duplicates with the DC Protein Assay by Bio-Rad as described by the manufacturer. To the sample or standard 25μL of a Reagent A: Reagent S 50:1 mix was added. Then 200μL of Reagent B per well for the color development was added and the plate was incubated for 15 minutes at room temperature in the dark. Samples were then measured in the plate reader at 750nm and the mean of the measured protein concentrations was taken for further experiments.

2.2.10 SDS-PAGE and Western Blot

For protein analysis, proteins prepared in section 2.2.9 were first separated with Sodium Dodecyl Sulfate Polyacrylamide Gel Electrophoresis (SDS-PAGE) and then immunoblotted. For the SDS-PAGE, proteins were mixed 1:2 with the Loading buffer (see table 2.2). They were then incubated for 5 minutes at 95°C for denaturation and then immediately put on ice. Here approximately 10μg protein was used.

Gels for SDS-PAGE consist of two parts, a stacking gel with 5% acrylamide and a separation gel with 10% acrylamide. The complete composition of the gels is shown in table 2.20. For preparing the gels, two glass plates with a space of 1mm were cleaned with ethanol and then pressed together in the casting frame. It was tested with water if the plates were leakproof. Then the mixes for the gels were prepared as shown in table 2.20 with TEMED and APS added just before use. The separation gel was filled in between the glass plates in the casting frame and covered with ethanol. A rest for polymerization control was left over. After polymerization ethanol was removed and the edge of the gel was dried carefully with a drying block. After that, the stacking gel was pipetted carefully on top of the separation gel with a comb for the sample pockets. When the stacking gel as well was polymerized, the glass plates were chucked into the electrophoresis module, and electrophoresis buffer was added. The combs were removed, the pockets rinsed with buffer and the samples were pipetted into the pockets including a protein marker on each gel. SDS-PAGE was run for 90-120 minutes at 100V until the samples reached the bottom of the gel.

Ingredients	stacking gel (5%)	separation gel (10%)
Stacking gel buffer	750μL	
Separation gel buffer		2500μL
Acryamid/ Bisacrylamid	500μL	3325μL
Aqua dest.	1750μL	4174μL
TEMED	5μL	10μL
10% APS	30μL	60μL
Total	3035μL	10,069μL

Table 2.20: Composition of SDS-PAGE gels. Volume is sufficient for two 1mm thick gels and a rest for control of polymerization. TEMED and APS should be added right before use.

The separated proteins were then blotted to a Polyvinylidene Fluoride (PVDF)-membrane followed by immunostaining with specific antibodies. For the blotting, the PVDF membrane was washed in methanol and chromatography paper, and sponges for the blot cassette were soaked in blot buffer. The blot cassette was prepared as a sandwich with sponge, chromatography paper, PVDF-membrane, gel, chromatography paper, and again sponge in this order. The whole sandwich was washed over with blot buffer while preparing. The cassette was then put in the blotting chamber and the proteins were transferred at 120V for 60 minutes on ice.

For the immunostaining, the membrane was removed from the blot cassette and incubated on a shaker in 5% skimmed milk to block the proteins for unspecific binding of the antibodies. The primary antibodies for NIPA, Cyclin B1, and GAPDH (see table 2.21) were prepared in 5% skimmed milk. To see NIPA or Cyclin B1 and the house-keeping gene GAPDH on the same membrane, the membranes were cut between the 37 and 50 kDa band as indicated by the marker, as the size of GAPDH is 37kDa, for NIPA 55kDa and for Cyclin B1 62kDa. The membranes were incubated with their appropriate primary antibodies in 5% skimmed milk on a shaker at 4°C overnight. The primary antibodies were removed and the membranes were washed three times with TBS/Tween for 15 minutes. The secondary antibodies were prepared in 5% skimmed milk (see table 2.21) and each membrane was incubated with the appropriate secondary antibody on a shaker for one hour at room temperature. Membranes were then washed again three times for 15 minutes with TBS/Tween on a shaker. After that, ECL Plus Detection Reagent was added to the membranes and they were incubated for 5 minutes at room temperature in the dark. Images were taken with the ChemiDoc XRS and bands were quantified with ImageJ software.

Antibody	Dilution	Company
Rabbit polyclonal anti-NIPA (phospho S354)	1:1000	ab63557, abcam
Recombinant rabbit monoclonal Anti-Cyclin B1 antibody	1:1000	ab181593, abcam
Rabbit polyclonal anti-GAPDH	1:2000	ab9485, abcam
Goat anti-rabbit IgG, HRP-linked	1:2000	#7074, Cell Signaling
Anti-mouse IgG, HRP-linked Antibody	1:2000	#7076, Cell Signaling

Table 2.21: Primary and Secondary Antibodies for Western Blot. All antibodies were diluted in 5% Skimmed Milk.

2.3 Myography

2.3.1 Material

Table 2.22: General Material for Myography

Material	Company
Reaction tubes (15 and 50mL)	Sarstedt
Glass flasks (0.5 and 1L)	Schott Duran
Disposable Scalpel No. 22	Feather
Dumont Tweezers extra fine straight	neolab
Dumont Tweezers No. 7 curved	neolab
Spring Scissors 3mm Cutting Edge	Vannas
Petri dish	Thermo Scientific
Serological Pipette 10mL	Sarstedt
Micropipettes Research (100-1000μL, 10-100μL, 2-20μL)	Eppendorf
Pipette Tips	Sarstedt

Table 2.23: Reagents and Buffer for Myography

Reagent/Buffer	Composition	Company
Sodium chloride (NaCl)	2M in Aqua dest.	Sigma-Aldrich
Potassium chloride (KCl)	2M in Aqua dest.	Sigma-Aldrich
Magnesium chloride ($MgCl_2$)	1M in Aqua dest.	Sigma-Aldrich
Potassium hydrogen phosphate (KH_2PO_4)	1M in Aqua dest.	Sigma-Aldrich
Calcium chloride ($CaCl_2$)	1M in Aqua dest.	Sigma-Aldrich
Sodium hydrogen carbonate ($NaHCO_3$)	powder	Gibco
Glucose	powder	Sigma-Aldrich
Phenylephrine	10^{-5}M, 10^{-4}M, 10^{-3}M, 10^{-2}M, 10^{-1}M, 1M, 2.5M in Aqua dest.	Sigma-Aldrich
Acetic Acid		Sigma-Aldrich
Ultra Pure Distilled Water	RNase and DNase free	invitrogen

Table 2.24: Devices and Software for Myography

Device/Software	Company
Wire Myograph System - 520A	Danish Myo Technology A/S
Scale LA120S	Sartorius
Magnetic stirrer Big-Squid ocean	IKA
Stemi 305 microscope	Carl Zeiss
LabChart v8.1.14	ADInstruments
Office 365 Excel	Microsoft
GraphPad PRISM 9	GraphPad Software, Inc.

Mice

zc3hc1 knockout mice, born in 2019, male and female. They were killed at the age of about 1 year and the aorta was extracted for the experiment.

All animal experiments were performed in accordance with the German Animal Studies Committee of Schleswig-Holstein (request 4.5_2015-03-05) and under international guidelines.

2.3.2 Protocol

With the myography of the aorta from *zc3hc1*-knockout mice, the influence of *zc3hc1* on the contractility of SMCs should be determined. The experiment was performed as described in [Gachkar, 2018] and [Gachkar et al., 2017]. The *zc3hc1* knockout mice are described above. The myograph is a device, where you can mount a small vessel and measure the force that it can develop with contraction. The number of biological replicates was $n = 3$ for male mice and $n = 4$ for female mice.

Preparation

Before the myography could start, the Krebs-Ringer Buffer (KRB) was prepared as shown in table 2.25. The myograph from DMT has two chambers, a near and a far chamber, to measure two pieces of vessel at the same time. Here just one chamber per measurement was used. Before starting, the jaws of the chamber were moved close together. The aorta was extracted and dissected in cold KRB in a petri dish. The adventitia was carefully removed. It was important here to touch and stress the aorta as little as possible to keep the contractility. The chamber was filled with 10mL KRB. For mounting, 2cm pieces of stainless steel wire with 40μm were cut and one piece was threaded through the lumen of a 2mm-piece of the vessel. The wire was then secured at the fixing screws on one side of the chamber. A second piece of wire was threaded through the lumen of the aorta and secured at the fixing screws on the other side of the chamber. The chamber was closed and the temperature was adjusted

to 37.5∘C. Carbogen gas was bubbled into the chamber to adjust a pH of 7.4. The vessel was now heated and equilibrated for 30 minutes.

	Ingredients	Volume/ Weight	Final Concentration in the Myograph Chamber
Base Buffer	NaCl 2M	61.5 mL	123 mM
	KCl 2M	2.35 mL	4.7 mM
	$MgCl_2$ 1M	1.2 mL	1.2 mM
	KH_2PO_4 1M	1.68 mL	1.2 mM
Add before Use	$CaCl_2$ 1M (cold)	2.5 mL	20 mM
	Solid $NaHCO_3$	1.68 g	5.5 mM
	Solid Glucose	1.008 g	2.5 mM

Table 2.25: Composition of the Krebs-Ringer Buffer and Final Concentration of the Ingredients in the Myograph Chamber. Ingredients are sufficient for 1 liter buffer. $CaCl_2$ should be stored at 4°C. $CaCl_2$, $NaHCO_3$, and Glucose should be added right before use.

Normalization

Before the measurement, the optimal diameter for active tension was determined with the normalization. The old buffer was removed and the chamber was filled with new 10mL of KRB. For the test of the contractility and the normalization Potassium Chloride (KCl) was used. A viable vessel contracts quickly when using KCl and dilates quickly when removing it. The curve showing the force was recorded constantly during the whole normalization and an example is shown in figure 2.6. The following steps were repeated until the force reached a maximum:

1. 400μL of 2M KCl were added to the buffer in the chamber and the force was read out after 3 minutes. The difference to the force written down before was calculated.

2. Washing: The buffer was removed and 10mL of new buffer was pipetted into the chamber. It was waited for 3-5 minutes until the force got back to where it started before the use of KCl.

3. Stretching: The diameter was increased by 150μm and the new distance was written down. The start point before the first use of KCl was defined as 0μm.

The normalization ended when the maximum force development was reached. So when in step 1 the force was lower than before, the distance was adjusted back to the value belonging to the maximum force. New buffer was added and the aorta was left equilibrating for one hour.

Figure 2.6: Example for Normalization before a Myograph Measurement. The blue curve is the force in mN, the green curve is the temperature in °C and on the x-axis is the time in minutes. The steps performed are written on the x-axis (wash, stretch, KCl). The values for the force development with KCl can be read out.

Measurement and Analysis

The measurement was done isometrically, which means, that the distance between the jaws of the chamber was not changed. It remained the distance with the maximum force development from the normalization. Before the measurement could start, the buffer was renewed and steps 1 and 2 of the normalization were performed again three times. The maximum force difference here is used for the normalization in the analysis of the data. The curve showing the force was recorded constantly during the whole measurement. As an inductor of contractility Phenylephrine (PE) was used, a selective α_1 -adrenergic receptor agonist which promotes constriction of vessels. PE was added additively to the chamber as shown in table 2.26. It was waited for about 3 minutes until the force curve reached a plateau, and then the next dose of PE was applied. After reaching the plateau after the last dose, the measurement was finished and the recording stopped.

After the measurement, the buffer was removed and the myograph was cleaned with acetic acid. It was incubated for 5 minutes in the device, then removed and rinsed several times with water.

The data during the measurement was recorded with LabChart software. For each dose the response in Newton right before the application of the next dose was read out. The values were normalized with Microsoft Excel to the KCl response at the beginning of the measurement. A dose-response curve with a non-linear fit using the least square method with the three variables (top, bottom, EC_{50}) was done with GraphPad Prism.

Step	PE Dose	Concentration in the Chamber
1	10μL of PE 10^{-5}M	$1 * 10^{-8}$M
2	20μL of PE 10^{-5}M	$3 * 10^{-8}$M
3	7μL of PE 10^{-4}M	$1 * 10^{-7}$M
4	20μL of PE 10^{-4}M	$3 * 10^{-7}$M
5	7μL of PE 10^{-3}M	$1 * 10^{-6}$M
6	20μL of PE 10^{-3}M	$3 * 10^{-6}$M
7	7μL of PE 10^{-2}M	$1 * 10^{-5}$M
8	20μL of PE 10^{-2}M	$3 * 10^{-5}$M
9	7μL of PE 10^{-1}M	$1 * 10^{-4}$M
10	20μL of PE 10^{-1}M	$3 * 10^{-4}$M
11	7μL of PE 1M	$1 * 10^{-3}$M
12	20μL of PE 1M	$3 * 10^{-3}$M
13	28μL of PE 2.5M	$1 * 10^{-2}$M

Table 2.26: Steps of the Measurement with applied Doses of PE and resulting Concentration in the Myograph Chamber. Concentrations range from $1 * 10^{-8}$M to a final concentration of $1 * 10^{-2}$M and PE was increased cumulative.

2.4 Statistical Methods

For the whole thesis, the following symbols and definitions are used for different levels of significance:

- Not Significant (ns): $p \geq 0.05$
- Significant (*): $p < 0.05$
- Very Significant (**): $p < 0.01$
- Highly Significant (***): $p < 0.001$

2.4.1 *t*-Test and Two-Way ANOVA

In most of the experiments described in the first two sections (cell culture and moleculobiological experiments), there is a comparison between two independent groups, knockdown and control. There are always at least three technical replicates, from which the mean was calculated. The means of the three or more biological replicates were the values, that are included in the calculation of the test statistics. There are not enough values to make a statement about the distribution of these. For these experiments, a two-sided *t*-test was calculated. The *p*-values are given in the following sections.

For experiments with time as a third variable, a two-way ANOVA test was performed using GraphPad Prism. There were *p*-values given for interaction, time, and the third variable (for example knockdown yes/no). There were also single comparisons carried out for each time point. The results are presented in the following sections.

2.4.2 Dose-Response Curve

The myography had a different experimental setup, so a different statistical analysis was needed. It was done according to [Gachkar, 2018] using GraphPad Prsim. The contraction values were normalized to the KCl response for the y-axis and the concentrations of the stimulating agent were logarithmised for the x-axis. A nonlinear fit using least squares was used to approach a curve to the data. There are different variables you can use to compare dose-response curves. The top value, the bottom value, or the EC_{50}, which is the half maximal effective concentration, could be compared. Here the $LogEC_{50}$ is chosen, as the curves have the best fit to the data in this area. The *p*-values were given by the software.

3 Results

3.1 *ZC3HC1* Knockdown in Smooth Muscle Cells

The successful knockdown of *ZC3HC1* transcription in primary human aortic SMCs and the consecutive lower levels of NIPA in these cells are the basis for most of the other experiments. The knockdown was confirmed with qPCR and Western Blot.

3.1.1 Knockdown Confirmation with qPCR

A knockdown confirmation with qPCR was done with cells from every experiment in triplicates. Results of the qPCR are shown here for the primary human aortic SMCs, the immortalized SMCs, and the SMCs stimulated with PDGF at 48 hours after transfection. In all cell types, a highly significant knockdown of the *ZC3HC1* transcription could be reached as shown in figure 3.1. The relative expression was reduced to 2.1 % in the immortalized SMCs. For the primary human aortic SMCs, the knockdown was tested at several time points after the transfection. The results are shown in figure 3.2. It could be seen, that the knockdown was successful at all time points and lasted at least up to 120 hours with only a slight increase in the expression of *ZC3HC1* over time. The best knockdown could be reached 48 hours after transfection, where the remaining gene expression was only 3.9 % compared to the cells transfected with the control siRNA.

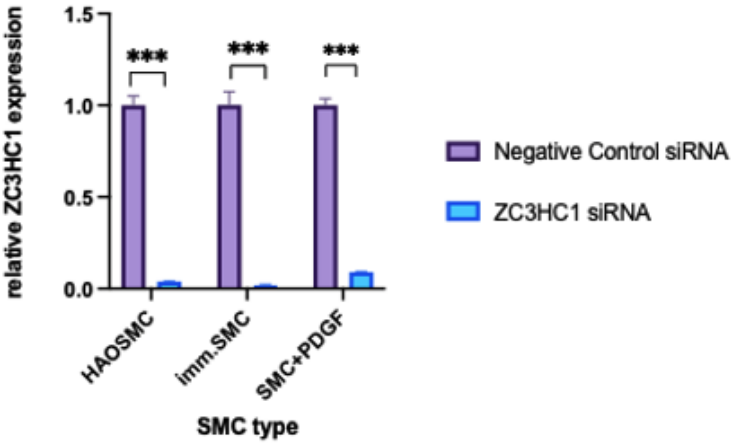

Figure 3.1: Relative Gene Expression of *ZC3HC1* in different SMCs 48 hours after transfection with siRNA. The knockdown is highly significant in all cell types with $p = 5 * 10^{-6}$ for HAOSMC, $p = 2 * 10^{-5}$ for the imm. SMC and $p = 2 * 10^{-6}$ for the SMCs stimulated with PDGF.

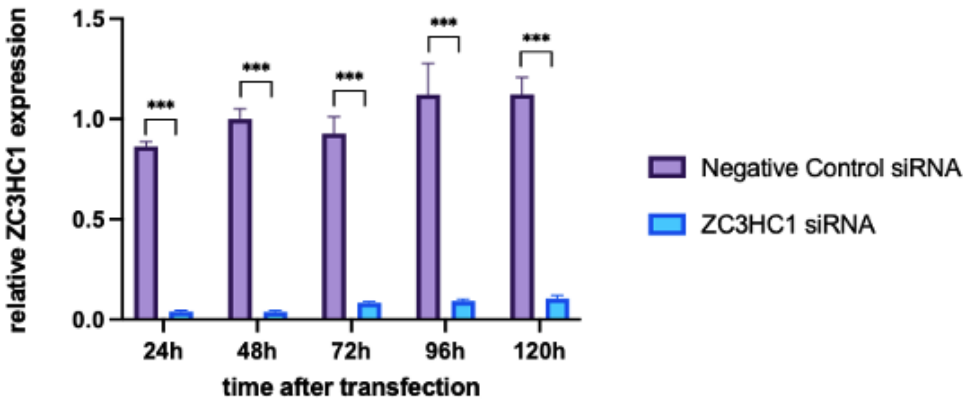

Figure 3.2: Relative Gene Expression of *ZC3HC1* in Human Aortic SMCs at Different Points of Time after Transfection with siRNA. The knockdown was highly significant at every time point with $p = 6 * 10^{-7}$ at 24h, $p = 5 * 10^{-6}$ at 48h, $p = 6 * 10^{-5}$ at 72h, $p = 0.0003$ at 96h and $p = 3 * 10^{-5}$ at 120h.

ZC3HC1 Primer Specificity

The specificity of the *ZC3HC1* primers was tested with gel electrophoresis before running the qPCR. As there was only one strong band on the gel as shown in figure 3.3, it could be assumed, that the primers have a high specificity.

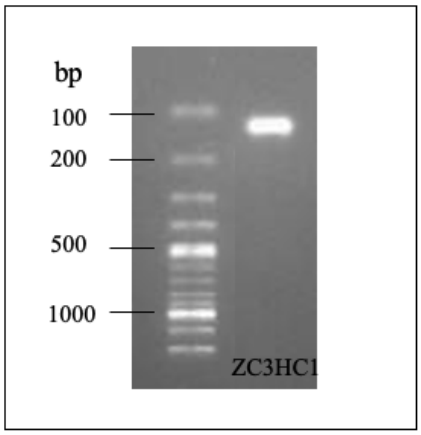

Figure 3.3: Results of the gel electrophoresis with the primer for *ZC3HC1*. As there is only one strong band between 100 and 200 bp (expected product size 119 bp, see table 2.13), a high specificity of the primer could be shown.

3.1.2 Evidence of Low NIPA-Levels in SMCs with *ZC3HC1* Knockdown

The protein levels of NIPA were analyzed with a Western Blot (see also section 2.2.10). The results are shown in figure 3.4. Cells transfected with the ZC3HC1 siRNA showed significantly lower levels of NIPA ($p = 0.0046$) than the cells transfected with the control siRNA.

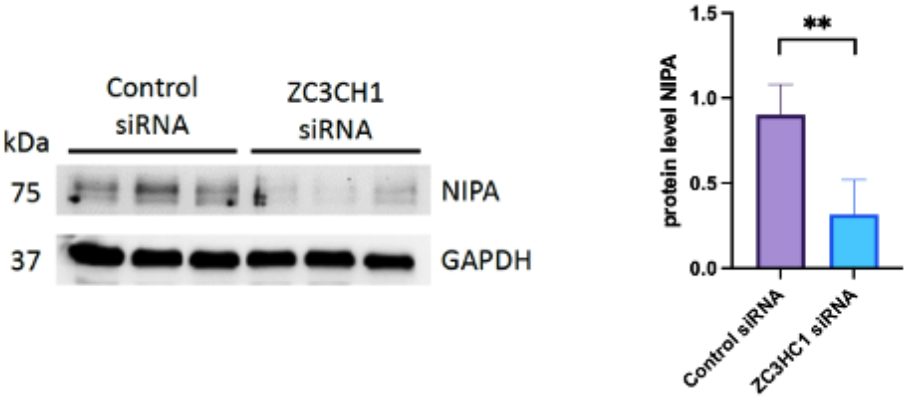

Figure 3.4: Results of the analysis of NIPA levels with Western Blot. A significant ($p = 0.0046$) lower level of NIPA in the knockdown cells can be seen compared to the control cells. On the left, the membranes of the Western Blot with the bands for NIPA and GAPDH are shown for one n with three technical replicates. On the right, you can see the quantification of the bands ($n = 4$).

3.2 The Influence of *ZC3HC1* on the Phenotype of SMCs

SMCs can have a contractile and a synthetic phenotype. In this section, the influence of *ZC3HC1* knockdown on the switch between these phenotypes was examined. The results are presented in the following sections. Looking at the gene expression of markers for contractile phenotype, a downregulation for some of them in knockdown cells could be observed, which would indicate less contractile phenotype in these cells. This could be confirmed by testing the *in-vitro* contractility with a gel contraction assay, where the knockdown cells showed less contractility. Also, the myography of aortas of *zc3hc1* mice and wild type showed less contractility in the knockdown mice.

3.2.1 Gene Expression of Markers for Contractile and Synthetic Phenotype

The expression of markers for contractile and synthetic phenotype was examined in SMCs stimulated with PDGF and SMCs, that were not stimulated.
The expression of *Calponin 1 (CNN1)*and *Smoothelin (SMTN)* as markers for contractile phenotype and of *Osteopontin (OPN)* as markers for synthetic phenotype was determined in SMCs with *ZC3HC1* knockdown and control cells, which were not stimulated with PDGF. The results are shown in figure 3.5. For OPN, a significant downregulation in cells with *ZC3HC1* knockdown at every point in time could be shown. *CNN1* was decreasing in knockdown cells over time with the maximum decrease after 96 hours. *SMTN* showed no significant difference in expression.

In the SMCs stimulated with PDGF, the expression of the genes for contractile proteins, *SMTN, CNN1, VIM, ACTA2, TAGLN, PCSK9, MGP, MAP1LC3B, ACTG2* and *LMOD1*, was examined. The results are shown in figure 3.6. For *LMOD1, MAP1LC3B, TAGLN, MGP*, and *ACTG2* a significant downregulation in the knockdown cells was observed.

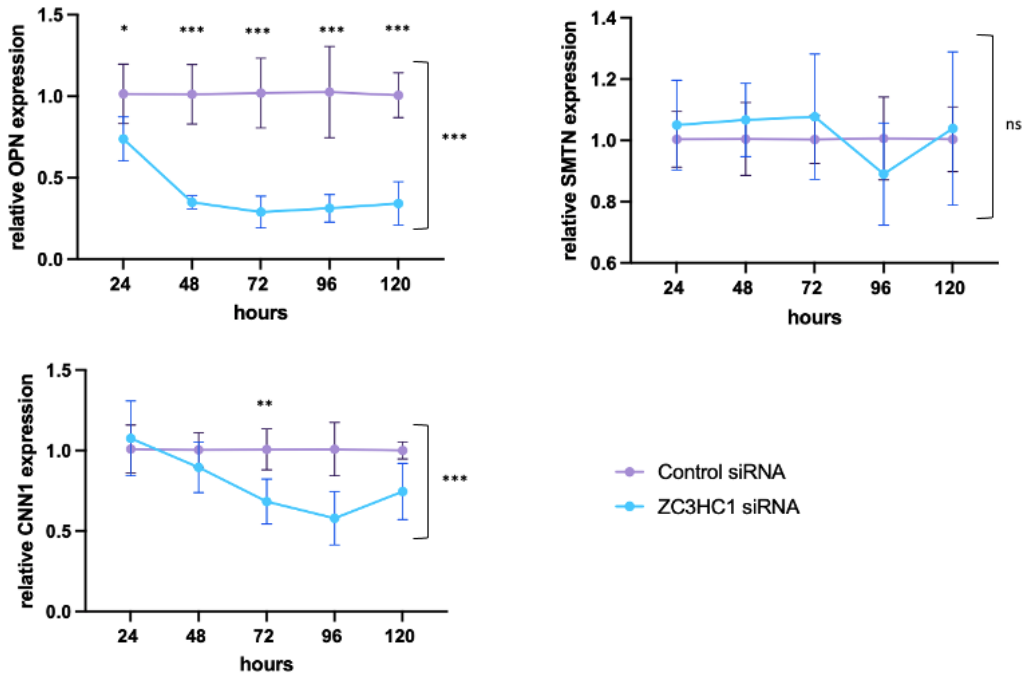

Figure 3.5: Expression of *OPN*, *CNN1*, and *SMTN* over time in SMCs not stimulated with PDGF. Replicates: 24h $n = 9$, 48h $n = 3$, 72h $n = 9$, 96h $n = 3$, 120h $n = 3$. Data was analysed with a two-way ANOVA test with GraphPad Prism. *OPN* (top left): Decrease of expression in knockdown cells with high statistical significance for interaction ($p = 0.0015$), time ($p = 0.0018$), and knockdown (displayed, $p < 0.0001$, explains 58.06% of variation) and high significance for differences at all single time points. *SMTN* (top right): no significance for interaction, time, or knockdown. Also no significance at the single time points. *CNN1* (bottom): Decrease of expression in knockdown cells with significance for interaction ($p = 0.0035$, explains 19% of variation), time ($p = 0.0032$, explains 19% of variation), and knockdown (displayed, $p = 0.0001$, explains 18% of variation). In single comparisons significant at 72h ($p = 0.0046$).

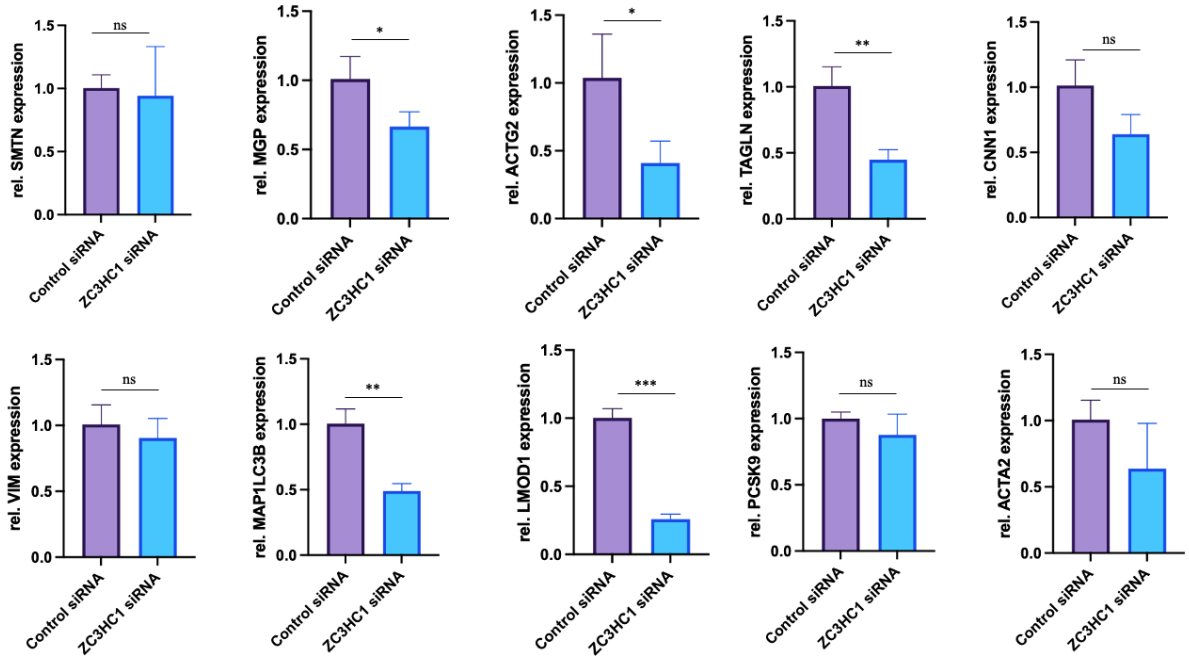

Figure 3.6: Expression of different contractile marker genes in SMCs stimulated with PDGF transfected with *ZC3HC1* and control siRNA. The mean and standard deviation of 3 replicates are shown. You see a downregulation in all of the genes with different significance. The downregulation of *LMOD1* was highly significant, of *MAP1LC3B* and *TAGLN* very significant, of *MGP* and *ACTG2* significant, and of *SMTN, CNN1, VIM, PCSK9*, and *ACTA2* not significant.

Influence of *ZC3HC1* on Genes in the cAMP/ Calcium Signaling Pathway

Several genes (see figure A.2) from the cAMP/ calcium signaling pathway were examined regarding the influence of *ZC3HC1* knockdown on their regulation. The data was analyzed with Qiagen GeneGlobe Data Analysis Center on January 23, 2019, and the results are shown as a scatter plot in figure 3.7. The fold regulation threshold was set to 2 and the *ZC3HC1* knockdown was confirmed in all cDNA used. The genes *EGR1, NR4A2, PTGS2*, and *TACR1* were slightly upregulated with a fold regulation of 2.12 to 2.93. *TACR1* has a relatively low expression in both, knockdown and control cells so this fold-change could have higher variations and should be considered possibly not valid.

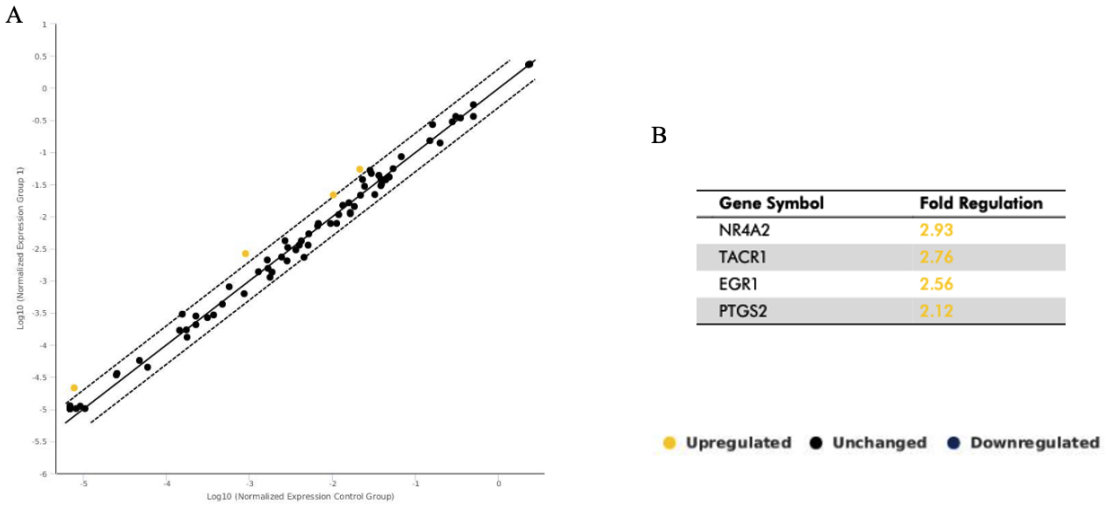

Figure 3.7: Results of the RT^2 Profiler Array for genes in the cAMP/ calcium signaling pathway run with cDNA with *ZC3HC1* knockdown. A: Scatter Plot. Comparison of normalized expression of every gene of the array between knockdown and control. The central line indicates unchanged gene expression. The dotted lines indicate the selected fold regulation threshold of 2. Four data points show an upregulation. B: Table of the upregulated genes with fold regulation.

3.2.2 Analysis of the Phenotype of *ZC3HC1* Knockdown Cells

Primary human aortic SMCs transfected with *ZC3HC1* and control siRNA were stained for α-Smooth-Muscle Actin and Calponin. The images are shown in figure 3.8. They can be considered exemplary as there were not enough images taken to quantify the results.

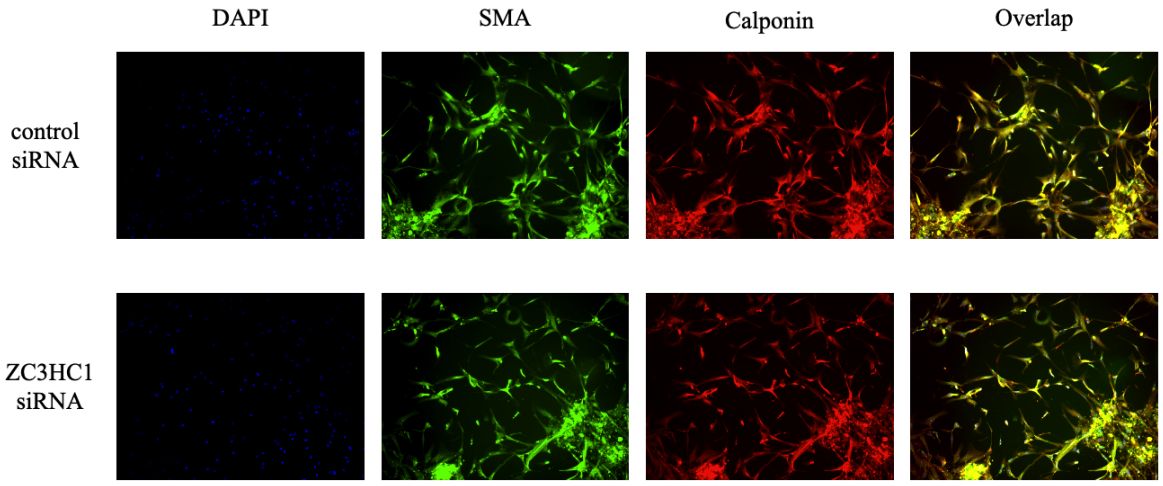

Figure 3.8: Primary human aortic SMCs transfected with *ZC3HC1* (top) and control (bottom) siRNA stained with DAPI (left) and antibodies for SMA (middle left) and Calponin (middle right). An overlap of the stainings is shown on the right. There were not enough images taken to evaluate the results.

3.2.3 Contractility of SMCs *In-Vitro*

The in-vitro contractility of SMCs was determined with a gel contraction assay. Areas of the gels were measured with ImageJ manually as shown in figure 3.9 and normalized to the area of an empty well. The results are shown in figure 3.10. It could be shown, that the gels containing the cells with *ZC3HC1* knockdown contract significantly slower and less when not stimulated or stimulated with bradykinin. With the inhibitor cytochalasin D, no contraction and no difference between knockdown and control cells could be observed.

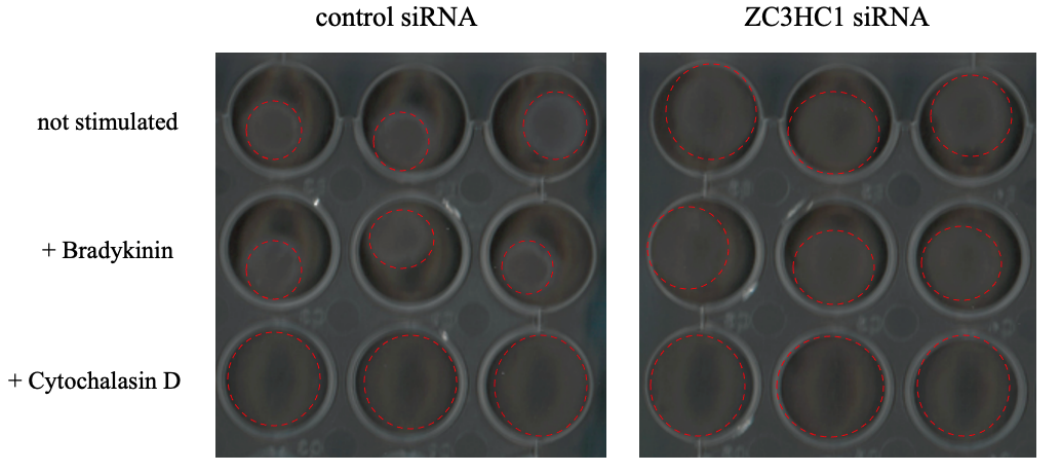

Figure 3.9: Gels from Gel Contraction Assay after 24 hours. On the left the gels with cells transfected with control siRNA and on the right gels with cells with *ZC3HC1* knockdown. Top: unstimulated gels, middle: gels stimulated with bradykinin, bottom: gels inhibited with cytochalasin D. You see, that the gels with knockdown cells have contracted less.

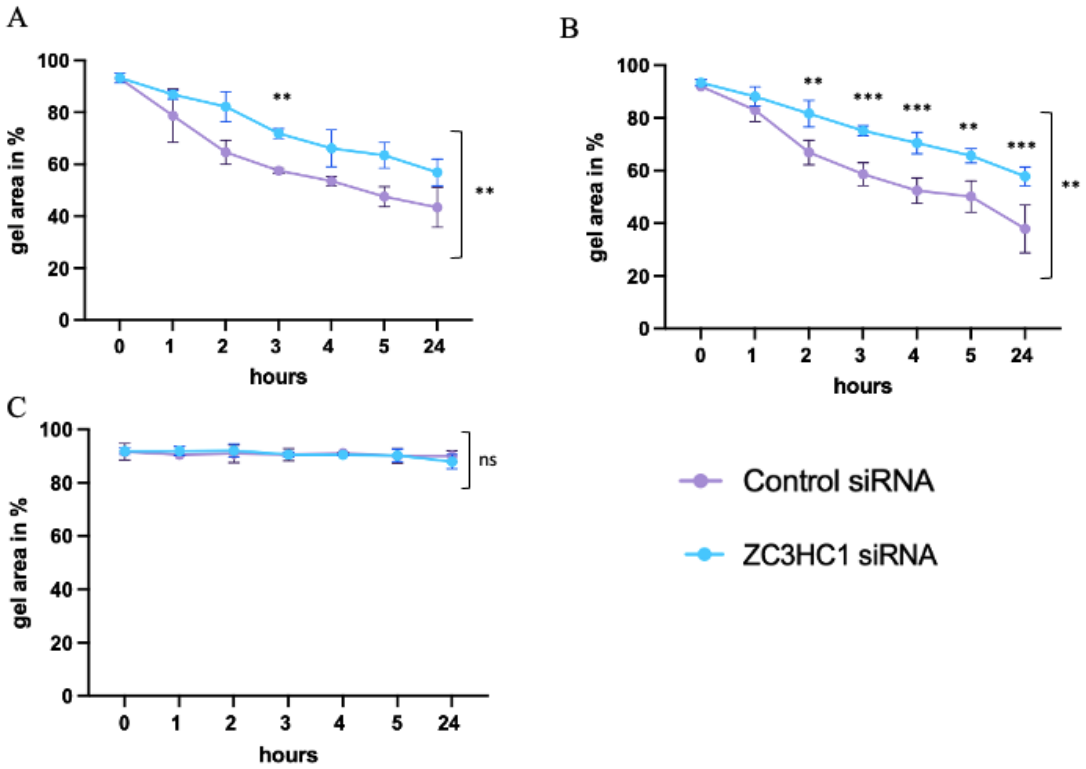

Figure 3.10: Results of the gel contraction assay with SMCs transfected with control siRNA and *ZC3HC1* siRNA over time. The time is plotted against the normalized area of the gel. Data was analyzed with a two-way ANOVA for repeated measurements with GraphPad Prism. Significance was tested for time, knockdown (displayed), interaction (time x knockdown), and the single gels. Single comparisons were made for each time point (displayed when significant). Values are shown as mean ± SEM. A: Not stimulated gels with less contraction in knockdown gels. Significance for interaction ($p = 0.038$), time ($p < 0.0001$), knockdown ($p = 0.0079$), and in between the gels ($p = 0.035$) although in single comparisons only significance after 3 hours. B: Gels stimulated with bradykinin. with less contraction in knockdown gels. Significance for interaction ($p = 0.016$), time ($p < 0.0001$), knockdown ($p = 0.005$), and in between the gels ($p = 0.011$). In single comparisons significance after 2, 3, 4, 5, and 24 hours. C: Gels inhibited with cytochalasin D. No difference between knockdown and control cells.

3.2.4 Contractility of Vessels of *zc3hc1*-Knockout Mice

The contractility of aortas of *zc3hc1*-Knockout (KO) mice was determined with myography. At some measurements, there was no plateau detected after stimulation with KCl before the measurement. These mice were excluded from the analysis. Mice, where the force was less than 1mN when stimulating with KCl were excluded as well. It had to be assumed, that the vessels lost their contractility while preparing for the myography. In total 13 mice were excluded because of these two reasons.

The results are shown as dose-response curves in figure 3.11 for male mice ($n = 3$) and in figure 3.12 for female mice ($n = 4$). The logarithmic concentrations of PE are plotted against the relative force compared to the response to KCl in %. In both groups the knock-out mice showed significant less contraction when stimulated with PE (male $p < 0.0001$ and female $p = 0.0034$). More details to the statistical analysis can be found in section 2.4.

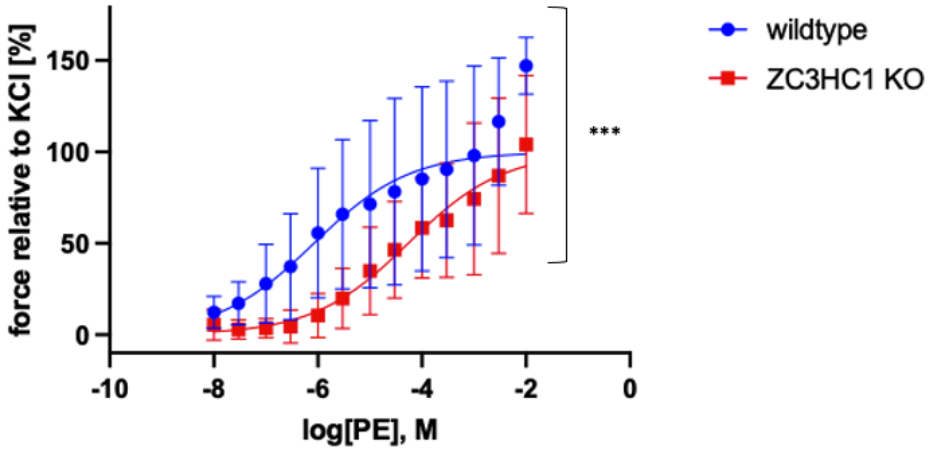

Figure 3.11: Dose-response curve for myography of aortas of male *zc3hc1*-KO mice and wild type ($n = 3$ each). The logarithmic PE doses are plotted against the force relative to the response to KCl in %. The forces are shown as mean ± SEM. A non-linear fit with least squares was used for the curves. A high significance for the difference between knockout and control was shown ($p < 0.0001$ for comparison of LogEC_{50}).

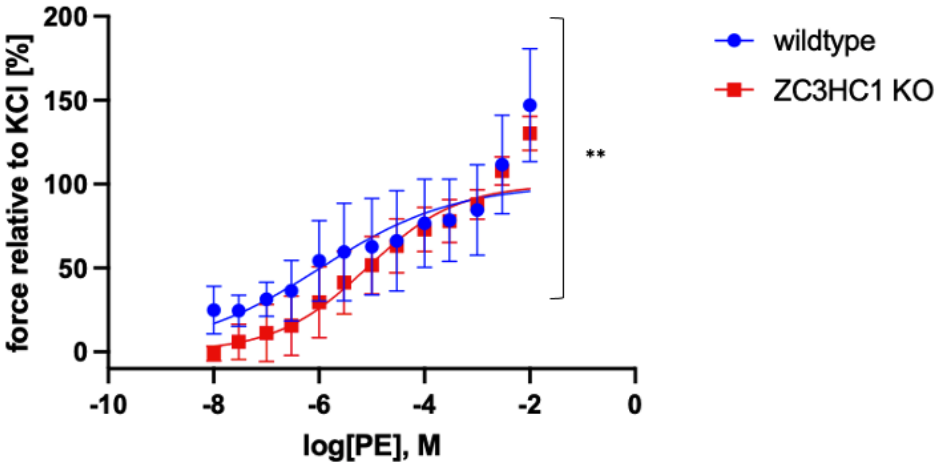

Figure 3.12: Dose-response curve for myography of aortas of female *zc3hc1*-KO mice and wild type ($n = 4$ each). The logarithmic PE doses are plotted against the force relative to the response to KCl in %. The forces are shown as mean ± SEM. A non-linear fit with least squares was used for the curves. A significance for the difference between knockout and control was shown ($p = 0.0034$ for comparison of LogEC_{50}.)

3.3 The Effect of *ZC3HC1* Knockdown on Migration and Proliferation of SMCs

3.3.1 Migration

The influence of *ZC3HC1* knockdown was determined with a wound healing assay with native unstimulated SMCs with *ZC3HC1* and control siRNA transfection as described in the previous sections. The results are shown in figure 3.13. No difference in migration could be observed.

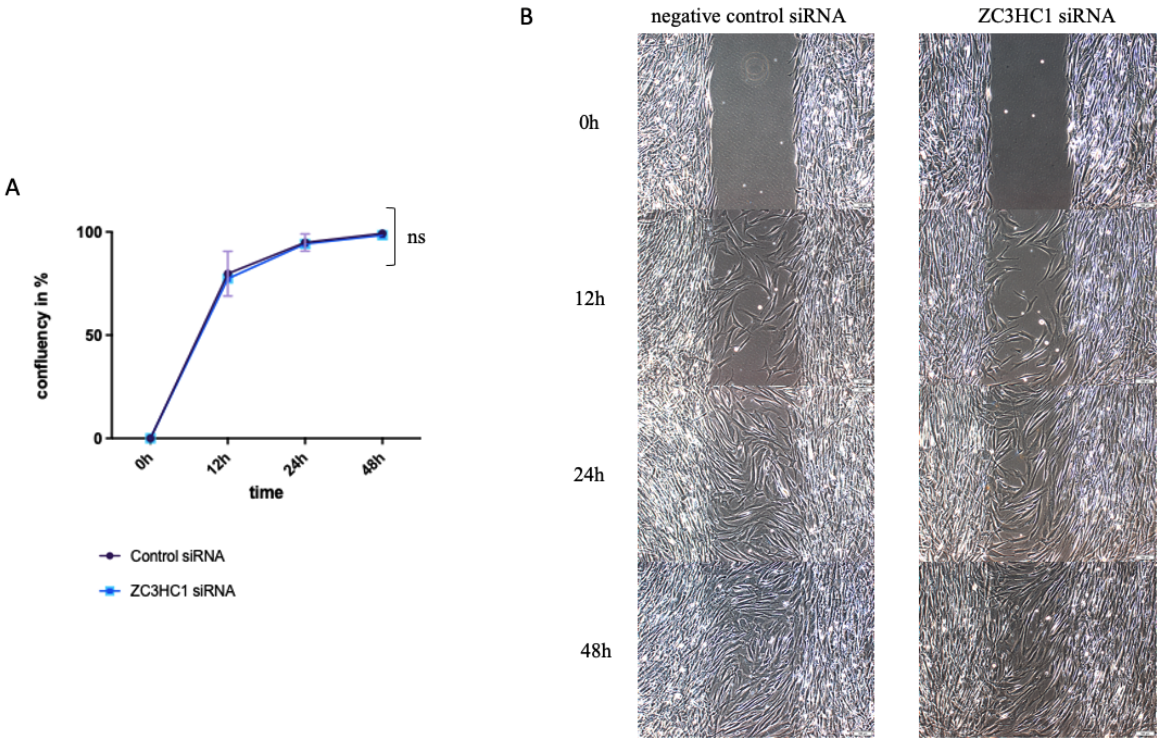

Figure 3.13: Results of the migration wound healing assay. A: Confluency in the gap over time. At time point 12 hours, cells without knockdown had slightly more confluency, but not significant. Data was analyzed with a two-way ANOVA test for repeated measurement with GraphPad Prism. Significance for interaction, time ($p < 0.0001$), knockdown (ns, displayed), and per well was tested. Comparisons between knockdown and controls were performed for each time point with no significant results. B: Examples of migrating cells transfected with control and *ZC3HC1* siRNA at time points 0, 12, 24, and 48 hours.

The Influence of *ZC3HC1* on Cell Motility Genes

A lot of genes (see figure A.1) for cell motility were examined regarding the influence of *ZC3HC1* knockdown on their regulation. The data was analyzed with Qiagen GeneGlobe Data Analysis Center on April 01, 2019, and the results are shown as a scatter plot and a volcano plot in figure 3.14. The fold regulation threshold was set to 2. None of the genes showed a significant up- or downregulation with *ZC3HC1* knockdown. The knockdown was confirmed for all cDNA used.

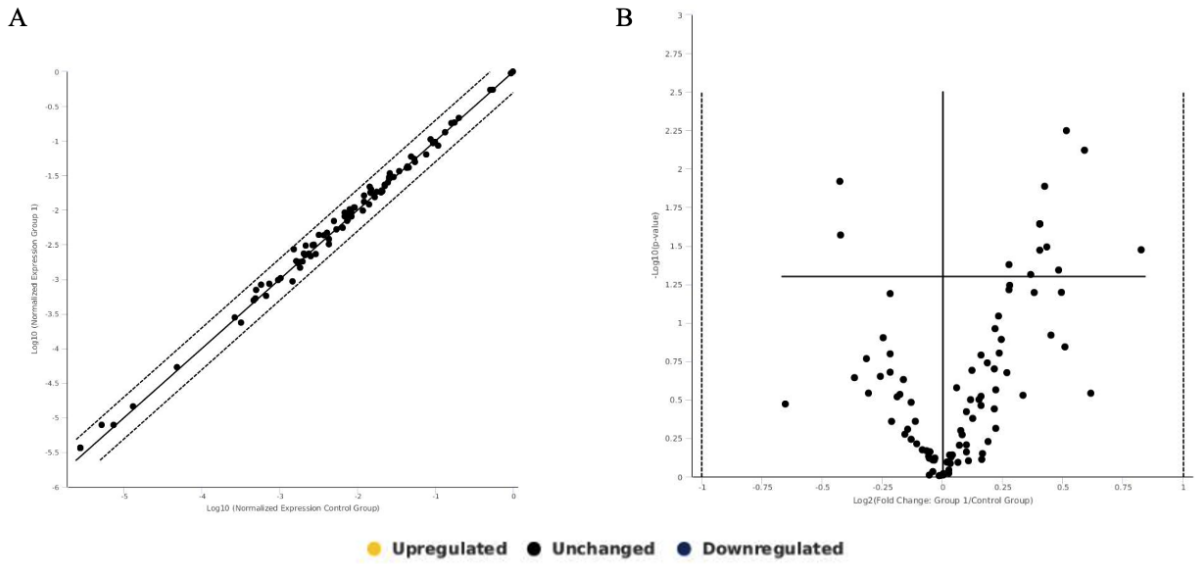

Figure 3.14: Results of the RT^2 Profiler Array for cell motility genes run with cDNA with *ZC3HC1* knockdown. A: Scatter Plot. Comparison of normalized expression of every gene of the array between knockdown and control. The central line indicates unchanged gene expression. The dotted lines indicate the selected fold regulation threshold of 2. All data points are beyond the threshold and show no change in regulation. B: Volcano Plot with fold regulation change on the x-axis and p-value on the y-axis. The dotted lines show the fold regulation change of -1 and 1 so all data points are beyond the chosen threshold of 2.

3.3.2 Proliferation

The influence of *ZC3HC1* knockdown on the proliferation of SMCs was investigated with different experiments with native unstimulated SMCs with *ZC3HC1* and control siRNA transfection. The results are shown in figure 3.15, 3.16, and 3.17. Overall, no significant difference in proliferation could be shown. Depending on the experiment, the knockdown or control cells seem to proliferate faster, respectively. All data showed a high variability.

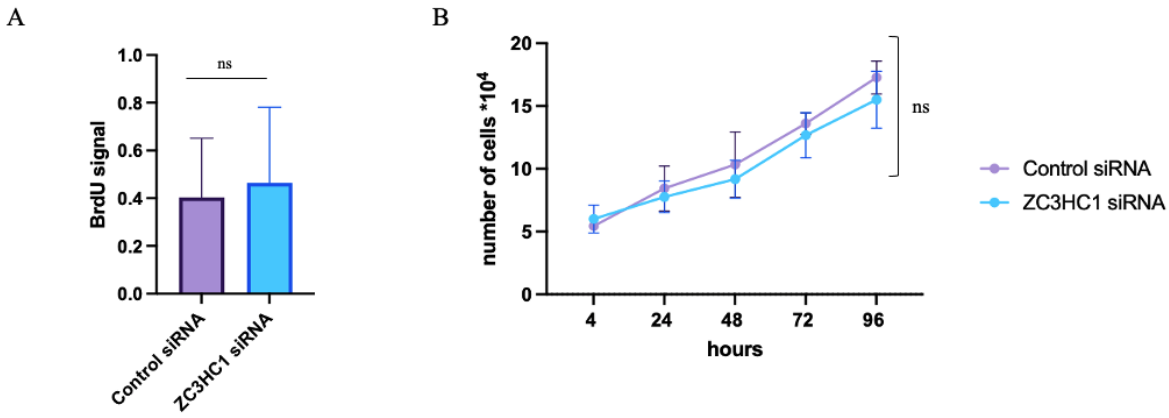

Figure 3.15: Proliferation of SMCs transfected with *ZC3HC1* siRNA and control siRNA. A: Results of the ELISA BrdU assay. Proliferation was measured after 24 hours. The transfected cells proliferated slightly faster, but not significantly. You see a high variability in the raw data. B: Proliferation of SMCs over 96 hours determined by counting the cells with the cell counter. Data was analyzed with a two-way ANOVA test with GraphPad Prism. Significance for interaction, time ($p < 0.0001$), and knockdown (ns, displayed) was tested. Comparisons between knockdown and controls were performed for each time point with no significant results.

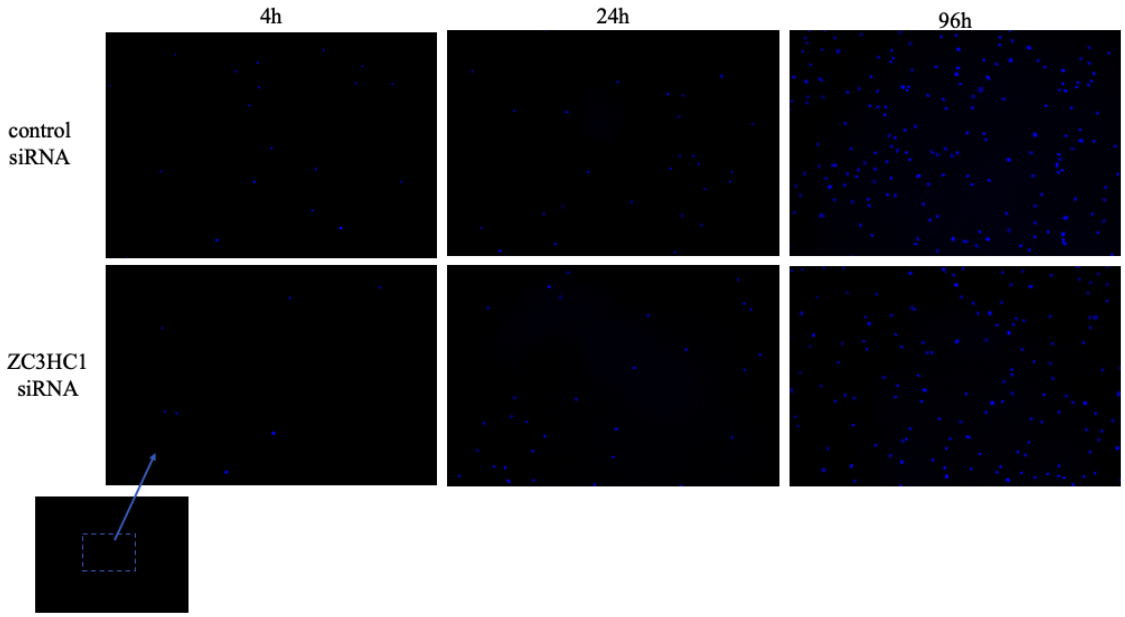

Figure 3.16: Images of DAPI-stained SMCs taken with a fluorescence microscope to examine proliferation. Images were taken 4, 24, 48, 72, and 96 hours after seeding the cells. For better clarity, only three time points and only parts of the images are shown. An increase in cell number could be observed in knockdown and control cells, but without significant difference (see figure 3.17).

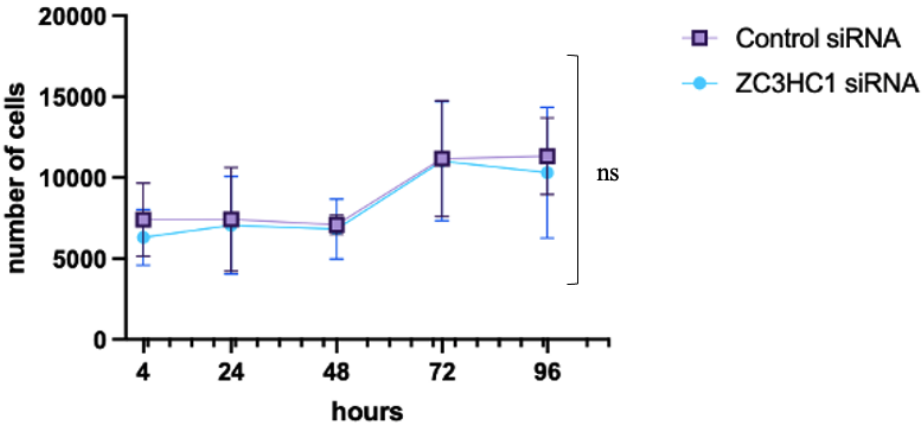

Figure 3.17: Proliferation of SMCs transfected with *ZC3HC1* siRNA and control siRNA over 96 hours. Cells were stained with DAPI (see figure 3.16)and counted with an in-house Image J script described in [Al-Hasani, 2017]. The knockdown cells tend to proliferate slower, but not significant. The data shows a high variability. Data was analyzed with a two-way ANOVA test with GraphPad Prism. Significance for interaction, time ($p = 0.025$), and knockdown (ns, displayed) was tested. Comparisons between knockdown and controls were performed for each time point with no significant results

3.4 The Influence of *ZC3HC1* in the Cell Cycle

As NIPA is a cell cycle protein, the influence of *ZC3HC1* knockdown on the cell cycle should be determined. Cyclin B1 was a protein of special interest here, as it is the main interaction partner of NIPA. The cell cycle was successfully arrested with aphidicolin in transfected and non-transfected SMCs. A protocol for flow cytometry was established to confirm the cell cycle arrest and to investigate the further progression.

3.4.1 Expression of Cyclin B1 under knockdown of NIPA

The expression of cyclin B1 under NIPA knockdown was assessed with qPCR and Western Blot and the results are shown in figure 3.18. In the qPCR analysis, a significant ($p = 0.04$) decrease in expression of cyclin B1 in cells with *ZC3HC1* knockdown could be seen. In the protein analysis, a significant ($p = 0.004$) increase of cyclin B1 on protein level could be shown.

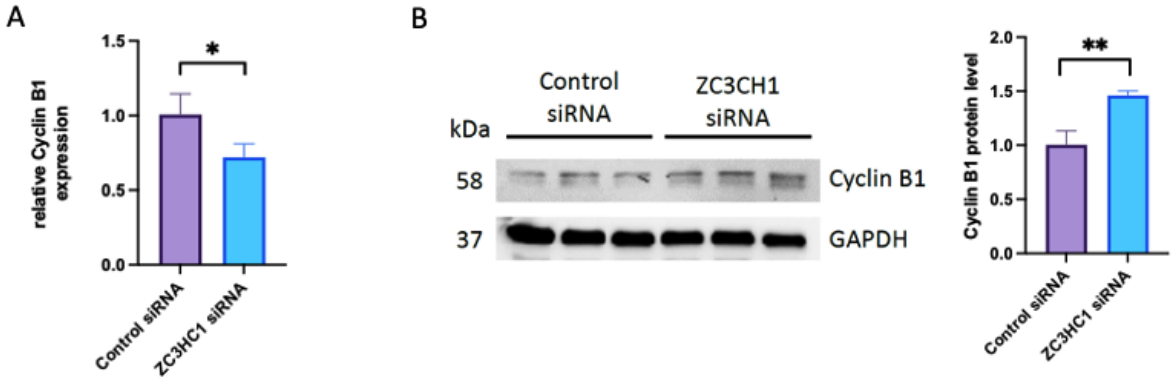

Figure 3.18: Influence of *ZC3HC1* knockdown on Cyclin B1. A: Significant ($p = 0.04$) decrease of relative Cyclin B1 expression at RNA level. B: Western Blot protein analysis of Cyclin B1 in cells with and without *ZC3HC1* knockdown. A significant ($p = 0.004$) increase in protein levels was seen in cells with *ZC3HC1* knockdown.

3.4.2 Cell Cycle Synchronization with Aphidicolin

To get the cells arrested at the end of the G1 phase of the cell cycle, aphidicolin was used [Jackman and O'Connor, 1998]. It was first applied to non-transfected cells. The expression of different cell cycle proteins should show the cell cycle arrest, but a difference could only be seen for cyclin B1. The confirmation of the cell cycle arrest was then assessed by measuring the BrdU incorporation in non-transfected and transfected cells, where it could be shown successfully. Here, also different concentrations of aphidicolin were tried. For a more detailed analysis of the cell cycle, it was analyzed with flow cytometry. The staining could

be established and a successful cell cycle arrest in non-transfected immortalized SMCs with aphidicolin was reached.

Expression of Different Cell Cycle Proteins in Non-Transfected SMCs

After treatment with aphidicolin, the expression of different cell cycle proteins in non-transfected cells with different incubation times of aphidicolin was determined. The results are shown in figure 3.19. For cyclin B1 a significant (6h: $p = 0.023$, 24h: $p = 0.006$, 48h: $p = 0.038$) decrease in cells treated with aphidicolin could be shown. You can also see a general decrease of cyclin B1 over time in both cells. For the other cell cycle proteins, cyclin E1, cyclin D1, and cdk2, no significant difference between control cells and cells treated with aphidicolin could be shown. The qPCR was also run with Cdc25C, a phosphatase that is involved in the dephosphorylation of cyclin B. However, the results were undetermined, which indicates a very low expression and the results are not presented here.

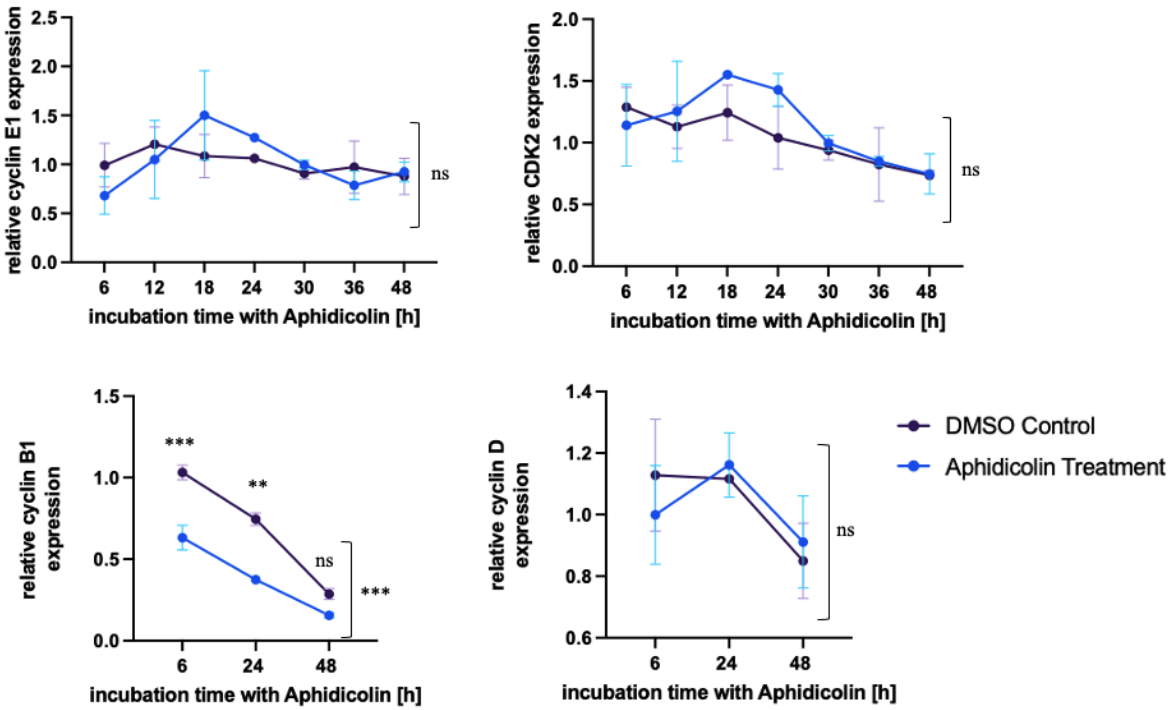

Figure 3.19: Expression of different cell cycle proteins measured with qPCR after different incubation times with aphidicolin. Data was analyzed by performing a two-way ANOVA test with GraphPad Prism. Significance was tested for treatment (aphidicolin or DMSO, displayed), incubation time, and interaction. Only expression of cyclin B1 (bottom right) showed significant results for interaction ($p = 0.0077$), incubation time ($p < 0.0001$, explains 70% of the variation), and also for treatment ($p < 0.0001$). In the single comparisons, significance was observed after 6 and 24 hours of incubation with aphidicolin. The other proteins showed no significant change in expression.

Confirmation of Cell Cycle Arrest with Different Concentrations of Aphidicolin in Non-Transfected SMCs

With a BrdU assay different concentrations of aphidicolin were tested with non-transfected SMCs. The cell cycle arrest should be confirmed. The results are shown in figure 3.20. With all tested concentrations of aphidicolin, there was less incorporation of BrdU, which shows a successful cell cycle arrest. As all concentrations worked, the lowest concentration of 10μg/mL aphidicolin was chosen for further experiments.

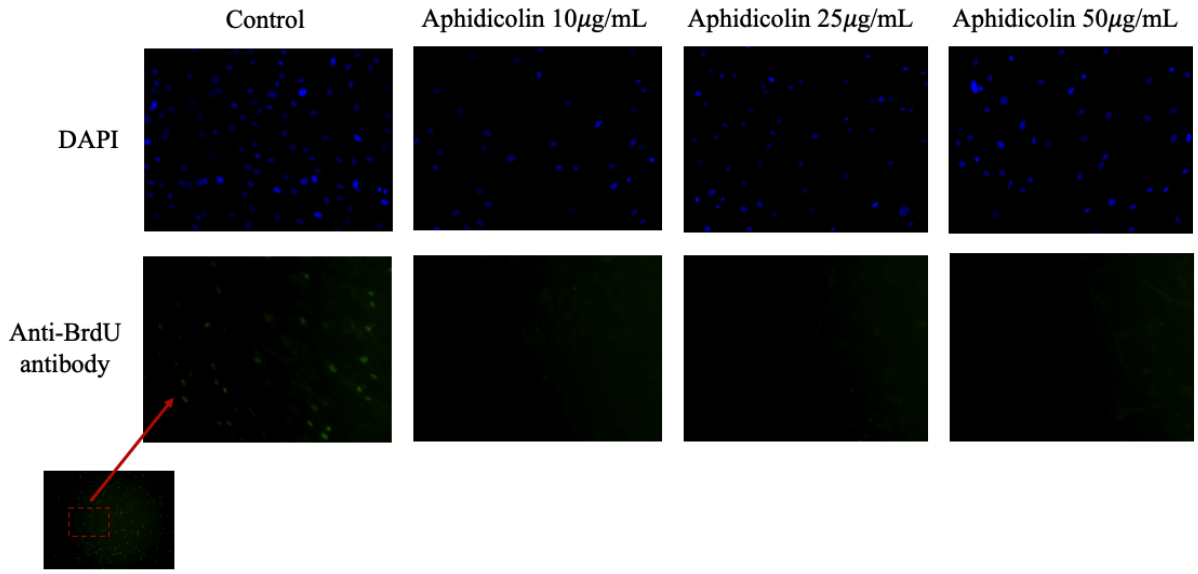

Figure 3.20: Images of non-transfected SMCs after treatment with aphidicolin and control stained with DAPI (top) and Anti-BrdU antibody (bottom). Cells were treated for 24h with aphidicolin or DMSO. For better clarity, only parts of the images are shown. There is BrdU incorporated in the control cells, but not in the cells treated with aphidicolin in all tested concentrations.

Cell Cycle Arrest with Transfected SMCs

The cell cycle arrest should also be confirmed with SMCs, that were transfected with control siRNA or *ZC3HC1* siRNA. The results are shown in figure 3.21. There was no incorporation of BrdU in the transfected cells treated with aphidicolin. As a control, there were non-transfected and transfected cells treated with DMSO. The transfected cells could not be analyzed so only the non-transfected cells are shown here.
For knockdown confirmation, RNA was isolated and a qPCR was run. The cells showed a 97% knockdown of *ZC3HC1*.

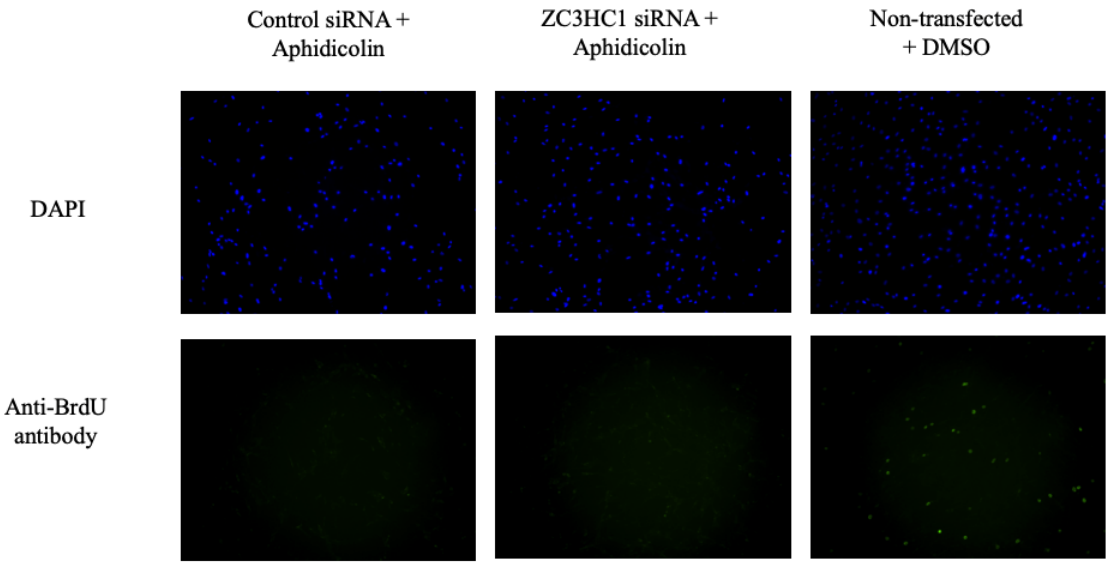

Figure 3.21: Images of SMCs transfected with different siRNAs and treated with aphidicolin 10μg/mL for 24 hours. As a negative control, non-transfected cells treated with DMSO are shown. The cells were stained with DAPI (top) and an anti-BrdU antibody (bottom). You see no signal from the anti-BrdU antibody in the cells treated with aphidicolin.

Analysis of Cell Cycle and Cell Cycle Arrest with Flow Cytometry

The protocol for flow cytometry had to be established with SMCs. Due to the high number of SMCs needed, the immortalized SMCs were used. The staining as described in section 2.1.8 was established in different experiments so it worked well for the cells and experimental setting. It turned out, that it was very important to store the cells overnight after the fixation step. Images of successful and non-successful staining are shown in figure 3.22.

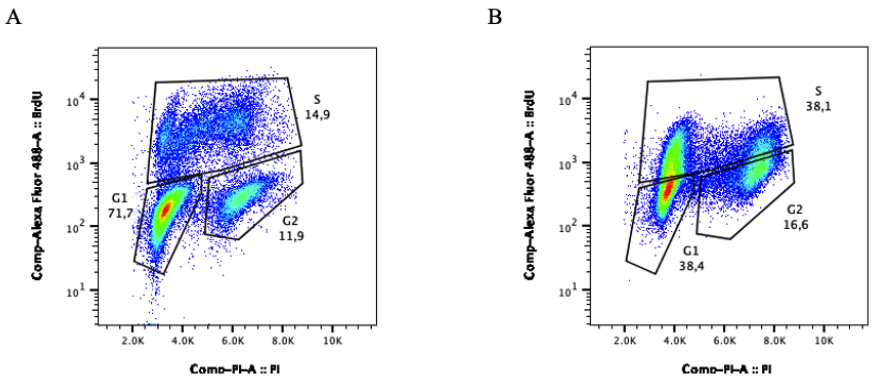

Figure 3.22: Examples of flow cytometry measurements with untreated SMCs with different stainings. A: Staining according to the protocol. The cell cycle distribution is as expected. B: Staining as described in the protocol, but without storage of cells overnight. The distribution of the cells is not as expected. The S-phase is missing and all the cells have a medium BrdU-staining instead of having an upper and a lower group shown in A and the figures below.

Untransfected cells were treated with aphidicolin or DMSO for 24 hours and the cell cycle was analyzed immediately after aphidicolin or DMSO release, 12 hours and 24 hours after. The results are shown in figure 3.23. A successful cell cycle arrest in the cells treated with aphidicolin was seen. Immediately after the release (0h) there are no cells in the S-phase (0.39%) and more cells in the G1-phase (77.1%). After 12 hours it can be seen that the cells have proceeded to the S-phase (40.2% in G1-phase, 41.0% in S-phase). After 48 hours the distribution is almost equal. The cell cycle phases in the control cells are distributed normally without visible cell cycle arrest.

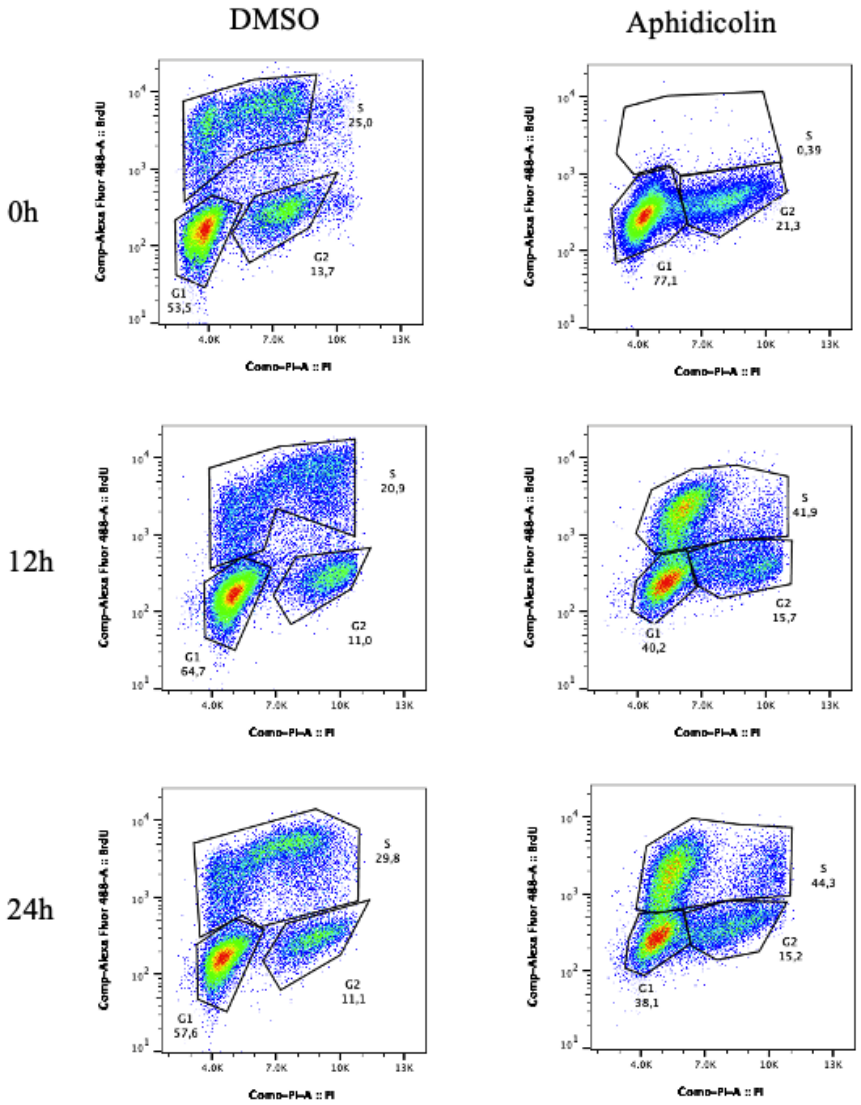

Figure 3.23: Results of flow cytometry with non-transfected immortalized SMCs. Cells were analyzed 0, 12, and 24 hours after the release of aphidicolin/ DMSO after 24 hours of treatment. The cell cycle phases are marked and the percentage of cells in this phase is shown. In the aphidicolin cells, there are almost no cells in the S-phase right after release., which shows a successful cell cycle arrest at this point.

In another experiment, cells were transfected with *ZC3HC1* and control siRNA and treated with aphidicolin or DMSO for 24 hours. As the cells were not stored overnight in PBS after fixation, the BrdU-staining did not work and the results were not evaluable.

4 Discussion

CVDs are the leading cause of death worldwide [WHO, 2020] with hypertension as the leading preventable risk factor for cardiovascular deaths [Murray et al., 2020]. Hypertension is also a very common cardiovascular disease with a complex pathophysiology. Of vital importance is the increased peripheral resistance, which is determined by SMC contractility [Beevers et al., 2001]. On a molecular level, the reason for the modified SMC characteristics is found in the changed phenotype from contractile to synthetic, which increases proliferation and production of extracellular matrix proteins [Fukuda et al., 1999, Owens et al., 2004].

Alongside other risk factors for hypertension (see section 1.1.2), genetics plays an important role in the development of hypertension. GWAS have enabled the discovery of hundreds of loci associated with elevated blood pressure or hypertension [Caulfield et al., 2003, Levy et al., 2009, Kato et al., 2011, Wang et al., 2009, Adeyemo et al., 2009, Consortium et al., 2011, Surendran et al., 2020, Kolifarhood et al., 2019]. Based on the loci the candidate risk genes were identified [Uffelmann et al., 2021].

One of these genes is the candidate gene of this thesis, *ZC3HC1*, on the risk locus 7q32.2, which encodes the protein NIPA. It interacts with cyclin B1 and is in this way involved in cell cycle regulation and mitotic entry [Bassermann et al., 2005b]. This thesis investigated how NIPA influences the phenotype of SMCs and their cell cycle, and how this might contribute to the development of hypertension.

The research question posed above was investigated using primary human aortic SMCs with siRNA knockdown of *ZC3HC1*. It was focused, in particular, on the phenotype characteristics of the *ZC3HC1* knockdown cells and the influence of the knockdown on cyclin B1 and the cell cycle. Experiments were completed by an *ex-vivo* measurement of the contractility of vessels of *zc3hc1* KO-mice.

4.1 Establishing the *ZC3HC1* Knockdown in Human SMCs

As the basis for the experiments of this thesis, a gene knockdown with siRNA had to be established in human aortic SMCs (see section 3.1). All other studies have been conducted with cells with this knockdown.

Transfection with siRNA has become a well-established procedure for mammalian cells [Brummelkamp et al., 2002, Harborth et al., 2001, Morris et al., 2004] and for SMCs [Petersen et al., 2008, Waltregny et al., 2005]. The transfection reagent GenMute provides non-liposomal chemical transfection and shows a higher transfection efficiency compared to other transfection reagents according to the manufacturer (`https://signagen.com/In-Vitro-siRNA-Transfection-Rea SL100568/GenMute-siRNA-Transfection-Reagent`, accessed 24. Feb 2023). This transient RNA transfection was chosen, because it is simple to conduct and shows a very good efficiency.

A knockdown of *ZC3HC1* in HeLa cells was, for example, performed by Bassermann et al. [Bassermann et al., 2005b] or Gunkel and Cordees [Gunkel and Cordes, 2022], but not in human SMCs. Working with SMCs is important, as they are the essential component of the vessel wall and therefore highly involved in the control of blood pressure. Although the cells used in this context are aortic SMCs, they can give an approximation to the behavior of the SMCs of the small resistance vessels. As the results in section 3.1 show, the knockdown was established very successfully on RNA and protein levels. Additionally, it was shown, that the knockdown on RNA level lasts at least 96 hours, which is long enough to be present during all the experiments performed in the other sections. In every experiment, there were some cells put aside to test the knockdown efficiency on RNA levels, which was very good in all experiments. Hence, these results suggest to interpret the findings presented here based on the premise that the knockdown was successful for all cells.

4.2 Phenotype Analysis of SMCs with *ZC3HC1* Knockdown

As described in section 1.3, SMCs can change their phenotype. The usual phenotype for SMCs of the human vessel is the contractile one; in diseases, a switch to the synthetic phenotype occurs [Owens et al., 2004, Fukuda et al., 1999]. The phenotype switch might be an essential aspect in the pathogenesis of hypertension. Investigating the influence of *ZC3HC1* on the phenotype of SMCs may establish a connection between the gene and its association with elevated blood pressure.

The main focus of this thesis is the analysis of the phenotype of SMCs with *ZC3HC1* knockdown compared to cells without the knockdown. For this, the expression of markers for primarily the contractile phenotype was measured and contractility was assessed *in-vitro* and *ex-vivo*. Migration and proliferation were studied, as they are closely linked to the phenotype switch.

Existing knowledge on the phenotype of NIPA-deficient cells is, to date, very limited. In my working group, it was shown that primary SMCs isolated from *zc3hc1* KO-mice had higher migration and proliferation rates, which can be seen the synthetic phenotype [Aherrahrou et al., 2021]. In contrast to this, Linsemann et. al showed a lower proliferation rate for VSMC and HUVEC (human umbilical vein endothelial cells) with *ZC3HC1* suppression [Linseman et al., 2017], which would be a characteristic of the contractile phenotype. Aherrahrou et. al showed also, that the T allele of the SNP rs11556924 is associated with lower *ZC3HC1* expression and higher migration in human SMCs [Aherrahrou et al., 2021]. This finding contradicts the previously held belief that the C allele is the risk allele in hypertension, so that we would expect higher migration (synthetic phenotype) in cells with this genotype.

4.2.1 Gene Expression of Phenotype Markers

There are several markers for SMC phenotypes and for the contractile phenotype in particular. The expression of this markers was studied in *ZC3HC1*- and control-transfected human aortic SMCs stimulated and not stimulated with PDGF, respectively.

Many markers are known for the contractile phenotype of SMCs (for example reviewed in [Owens, 1995]). The expression of two of them, calponin [Duband et al., 1993] and smoothelin [van der Loop et al., 1997], was examined over time in SMCs not stimulated with PDGF. Calponin was downregulated in cells with *ZC3HC1* knockdown; for smoothelin, no difference in expression was shown. In the PDGF-stimulated cells *LMOD1*, *MAP1LC3B*, *TAGLN*, *MGP*, and *ACTG2* were significantly downregulated. The candidate markers for this analysis were identified with RNA sequencing as described by Aherrahrou et al. [Aherrahrou et al., 2021]. As the results indicate a lower expression of contractile proteins, the synthetic phenotype seems to be strengthened by the knockdown.
The genes *EGR1*, *NR4A2*, and *PTGS2* from the cAMP/calcium signaling way are upregu-

lated with *ZC3HC1* knockdown. As the relation was weak, further investigation would be needed to verify this and to connect the genes to the phenotype of the SMCs.

Comparing the PDGF-stimulated cells with the native cells [Aherrahrou et al., 2021], it is seen, that stimulation with PDGF lowers the expression of the contractile markers. This can be explained by the fact that PDGF reduces the synthesis of contractile proteins [Holycross et al., 1992, Corjay et al., 1989] and is an important environmental factor for phenotype modulation of SMCs [Owens et al., 2004].

As a marker for the synthetic phenotype, only osteopontin was studied [Yamamoto et al., 1997] in cells not stimulated with PDGF. It is also associated with arterial SMC proliferation [Gadeau et al., 1993], which also belongs to the synthetic phenotype. At all examined time points after the transfection, *OPN* was downregulated in the *ZC3HC1* knockdown cells with significance. This is a contrast to the results obtained before. Nevertheless, osteopontin is a marker not only for the synthetic phenotype of SMCs but also for example for cancer [Weber et al., 2011] or bone density [Vancea et al., 2021]. So there are many factors that could influence its expression. Investigation of more than one marker for the synthetic phenotype (examples in [Rensen et al., 2007]) would be necessary to make a reliable statement.

4.2.2 Analysis of Contractility

Regarding contractility and phenotypic changes, it is important to distinguish between the contractility of the vessel and the contractile properties of the individual cells. The contractility of the vessel is very important in the pathogenesis of hypertension, where especially the small resistance vessels contribute with increased contractility mainly to the elevation of blood pressure (see also section 1.1.1) [Beevers et al., 2001]. It is important to mention that this increased contractility is mainly caused by the decrease of the lumen diameter of the vessel [Intengan and Schiffrin, 2000, Mulvany et al., 1978], not by increased cell contractility itself. The narrowing of the vessel is a result of proliferation and increased production of extracellular matrix proteins, which can be associated with the synthetic phenotype we know to be predominant in hypertension [Fukuda et al., 1999]. In contrast, an increase in cell contractility with higher production of contractile proteins can be associated with the physiological contractile phenotype. In this thesis, the contractility was studied *in-vitro* with SMCs in a gel contraction assay and *ex-vivo* with myography of aortas from *zc3hc1* knockout mice.

The *in-vitro* experiment shows an increase in synthetic phenotype in cells with *ZC3HC1* knockdown. This could lead to a smaller vessel diameter and could contribute to hypertension.

Contractility was also examined with myography of the aortas of *zc3hc1*-KO mice and wild-type mice. The results showed significantly less contractility in both male and female knock-out mice.
When interpreting these findings, it is important to bear in mind some key aspects of the experimental design used here: First, it assesses the contractility of a vessel and not of cells. Furthermore, it analyses the aorta, which is not comparable to a resistance vessel. Hence, it must be questioned if the decreased contractility is a result of a greater lumen diameter compared to the controls (see above).
Aherrahrou et. al found an increased neointima formation in femoral arteries of *zc3hc1*-KO mice, which results in a decreased lumen diameter [Aherrahrou et al., 2021]. Transferred to the results here, it seems unlikely, that the KO mice have an increased lumen diameter, which would lower their contractility.
In conclusion, it can be assumed that the difference in contractility has a cellular cause. An increase of synthetic phenotype in the SMCs of *zc3hc1*-KO vessels seems likely. Further studies on the cellular level would be necessary to verify this hypothesis.

4.2.3 Migration and Proliferation

Migration and proliferation characteristics of SMCs are closely linked to their phenotype. The synthetic phenotype shows higher migration and proliferation than the contractile phenotype [Owens, 1995]. As mentioned above, there are contrary findings about the influence of *ZC3HC1* on migration and proliferation behavior. While, in my working group, a higher proliferation and migration rate for SMCs isolated out of *zc3hc1*-KO mice was shown [Aherrahrou et al., 2021], Linsemann et al. found a lower proliferation rate for VSMC and HUVEC with *ZC3HC1* suppression [Linseman et al., 2017]. A higher migration rate was shown for SMCs with lower *ZC3HC1* expression due to the T allele of *rs11556924* in human SMCs [Aherrahrou et al., 2021].

Migration

A wound healing assay was established in the working group to study the migration of *ZC3HC1* knockdown cells. No difference in migration could be seen between the knockdown and the control cells (see section 3.3.1), both treated with mitomycin to inhibit proliferation.

The wound healing assay to study migration was developed further in the working group as presented by Aherrahrou et al. [Aherrahrou et al., 2021]. The cells were not treated with mitomycin and migration was examined after 12 hours. A higher migration rate was seen in the SMCs with *ZC3HC1* knockdown. Furthermore, the cells were stimulated with PDGF in another experiment, which showed a higher migration rate in SMCs with *ZC3HC1* knockdown as well. This is consistent with the achieved results so far in the working group with the SMCs from *zc3hc1*-knockout mice, but in contrast to the results of this thesis.

The difference in the results could be traced back to the different treatment of the cells. Mitomycin as a proliferation inhibitor was also shown to decrease migration [Kumar et al., 2015]. Therefore, small differences are not detectable under this treatment. PDGF, which is also increasingly present in hypertension, also increases proliferation and hence the differences between the two groups.

Proliferation

The influence of *ZC3HC1* knockdown on the proliferation rate of SMCs was studied with an ELISA and two cell counting experiments. A high variability was observed over all experiments (see section 3.3.2) and no significant differences in proliferation rate were detected. It has to be emphasized here that proliferation was studied under basal conditions without stimulating the cells with PDGF.

There were other experiments to examine the proliferation of *ZC3HC1* deficient cells in my working group, which came to different results (see also [Aherrahrou et al., 2021]). They found a higher proliferation rate for *zc3hc1* knockout primary mouse SMCs as well as for human SMCs with *ZC3HC1* siRNA knockdown stimulated with PDGF. Out of the measured time points, differences in proliferation only occurred after 24 and 72 hours.

The discrepancy between the results is probably a consequence of the different treatments of the cells. The primary human SMCs with siRNA-mediated knockdown [Aherrahrou et al., 2021] were stimulated with PDGF, which increases proliferation and helps to see small differences. These differences could not be seen in the experiment under basal conditions conducted in this thesis. Moreover, the difference in proliferation occurred late, only after 72 hours, hence a longer observation time could maybe have uncovered proliferation differences. Regarding the experiment with the primary SMCs from KO mice, the complete knockout of *zc3hc1* could be seen to have a stronger effect on migration characteristics than the siRNA knockdown.

Generally speaking, one would expect a higher proliferation rate in cells with *ZC3HC1* knockdown. Because of its function in the cell cycle, it leads to faster accumulation of cyclin B1 with faster cell cycle progression. You can find different results of proliferation assays in the literature: Increased (see [Aherrahrou et al., 2021]), decreased ((see [Linseman et al., 2017]), or no difference found (see [Jones et al., 2016]). These differences could be due to different cell types used and different experimental setups, including an insufficient observation time.

4.2.4 Summary of Phenotype Analysis

Summing up the results of the phenotype analysis, they strengthen the theory, that a deficiency of NIPA leads to a more synthetic phenotype in SMCs. This can be seen in the downregulation of contractile markers, decreased contractility *in-vitro* and *ex-vivo*, and in increased proliferation and migration in further experiments in the working group. This can be explained on a molecular level with an accumulation of cyclin B1 and faster progression of the cell cycle (see section 4.3).

There are some different results from other studies [Linseman et al., 2017, Jones et al., 2016]. An explanation for this discrepancy could be the use of different cells and different experimental setups. It is not clear, why the T allele of *rs11556924* is associated with lower levels of NIPA [Aherrahrou et al., 2021], even though the C allele is the one that is associated with hypertension [Kunnas and Nikkari, 2015]. Further investigations would be needed here.

4.3 Cell Cycle Analysis of SMCs with *ZC3HC1* Knockdown

NIPA is a protein that interacts with cyclin B1 and thereby influences the mitotic entry [Bassermann et al., 2005b]. Analyzing the cell cycle is closely linked to proliferation, which is an important mechanism in hypertension. It is shown that SMCs from SHR have a different cell cycle progression in the G1 and G2 phases [Tanner et al., 2003] and an accelerated entry into the S phase [Hadrava et al., 1992] than those from the normotensive WKY. Connecting the function of NIPA to cell cycle processes assesses NIPA's influence on the phenotype on a molecular level.

As cyclin B1 is the direct interaction partner of NIPA, many studies have investigated the influence of *ZC3HC1* on cyclin B1. The results obtained here are all similar. A lack of NIPA leads to a nuclear accumulation of cyclin B1 ([Bassermann et al., 2005b, Jones et al., 2016, Illert et al., 2012, Aherrahrou et al., 2021]).
To follow-up on the findings reported here, the function of *ZC3HC1* knockdown on G2 progression should be investigated. A cell cycle arrest was established as a first step and confirmed with immunofluorescence staining and flow cytometry.

4.3.1 Cyclin B1 under *ZC3HC1* Knockdown

Regarding the cell cycle proteins which are impacted by NIPA, cyclin B1 plays the most important role. Active NIPA ubiquitinates cyclin B1, which promotes in complex with cdk 1 the mitotic entry [Bassermann et al., 2005a, Johnson and Walker, 1999]. Several studies have shown, that lower expression of *ZC3HC1/zc3hc1* or lower levels of NIPA lead to an accumulation of cyclin B1, for example in HeLa cells [Bassermann et al., 2005b], or in NIPA-deficient mice ([Illert et al., 2012], [Al-Hasani, 2017]). This could be confirmed on the protein level for SMCs in this thesis. The observed downregulation of RNA levels can be interpreted as a compensatory reaction to the increased protein levels.
Jones et al. showed that higher activity of NIPA results in slower nuclear accumulation of cyclin B1 [Jones et al., 2016]. Cyclin B1 is associated with pathophysiological processes. It was shown that increased levels of cyclin B1 lead to higher proliferation rates in SMCs [Braun-Dullaeus et al., 2001] and that cyclin B1 suppression could inhibit neointima formation [Morishita et al., 1994].
Therefore, studying cyclin B1 is still very important to understand the effects of NIPA on the different pathophysiological pathways, for example in hypertension.

4.3.2 Cell Cycle Arrest with Aphidicolin

The cell cycle was arrested with aphidicolin. Analysis of cell cycle proteins could not clearly confirm the arrest. Only cyclin B1 showed a significant decrease, while cyclin E1, cyclin D, and cdk 2 showed no significant difference.
For cyclin D and cyclin B1, this result is as expected (see also figure 2.4) regarding the known levels of their expression during the cell cycle. For the cdks, their level does not alternate as much as the cyclins. Instead, it stays almost constant during the cell cycle [Johnson et al., 2017] such that the expression of cdk 2 fits the theory as well. For cyclin E, an upregulation would be expected, which could not be seen. The data have a high variability, which could explain this result. An analysis of protein levels might be performed to verify the cell cycle arrest by the cell cycle proteins. Because of little material and expected difficulties due to low amounts of protein, this was not done here.

Here, other methods to confirm the cell cycle arrest were chosen. It was confirmed with BrdU immunofluorescence staining and flow cytometry for non-transfected SMCs and with BrdU immunofluorescence staining for SMCs with *ZC3HC1* knockdown. As the flow cytometry was very time-consuming and needed a lot of resources, the failed trial for transfected cells was not repeated. This should be done in further investigations. In addition, the cell cycle progression should be studied with flow cytometry to see the influence of the knockdown on a molecular level. It has been shown that cell cycle progression is different in SHR [Tanner et al., 2003, Hadrava et al., 1992], so a cell culture experiment would be very interesting here to link *ZC3HC1* to hypertension.

4.4 Conclusion and Outlook

In this thesis, the influence of *ZC3HC1* on the phenotype of smooth muscle cells was investigated. The switch to the dedifferentiated synthetic phenotype is an important pathomechanism for the development of hypertension, which the gene *ZC3HC1* could be associated with. Transient transfection with siRNA was established to achieve a knockdown in primary human aortic SMCs to conduct the different experiments.

The immediate influence of *ZC3HC1* on the phenotype was examined with analysis of contractile markers, migration, proliferation, and contractility *in-vitro* and *ex-vivo*. The results showed an increased presence of the synthetic phenotype under *ZC3HC1* knockdown. As NIPA is a cell cycle protein, it is probable, that its deficiency causes cell cycle alterations, which might explain some of the characteristics of the synthetic phenotype, such as proliferation. Cyclin B1 as the main interaction partner of NIPA and responsible for the G2/M phase of the cell cycle, was shown to accumulate under *ZC3HC1* knockdown. This would indicate a faster cell cycle progression, which would result in increased proliferation. The cell cycle of SMCs was arrested successfully in this thesis without studying its progression in *ZC3HC1* knockdown cells.

This thesis provides new insights regarding the role of *ZC3HC1* in hypertension. Some experiments could not be completed due to time constraints. This includes the analysis of cell cycle progression with flow cytometry and immunofluorescence staining for contractile markers under *ZC3HC1* knockdown. This would be interesting to complete in the future. The myography could be conducted with smaller vessels in the future, for example as described by Spiers and Padmanabhan [Spiers and Padmanabhan, 2005] for mesenteric resistance arteries of rats, as they contribute more to the development of hypertension than the big vessels.

A recently published study suggests a completely different function of NIPA [Gunkel and Cordes, 2022]. They found NIPA to be mainly a component of the nuclear basket and doubted its established function as an F-box protein. They found that it is not necessary for maintaining the typical distribution of cyclin B1. However, the influence of NIPA on cyclin B1 was shown before in several different studies [Bassermann et al., 2005b, Jones et al., 2016, Illert et al., 2012, Aherrahrou et al., 2021], hence it is still considered an important aspect in investigating *ZC3HC1* and NIPA. Gunkel and Cordes used HeLa cells [Gunkel and Cordes, 2022], which are oncogene and have several characteristics that could bias the studies regarding cyclin B1, especially compared to SMCs. Further investigations would be needed to reconcile these results.

Clinical medicine improves rapidly. Thereby, also the fiel of genetics develops at a fast pace with path-breaking discoveries like CRISPR/Cas [Jinek et al., 2012] in recent years. Hence, the number of therapies and treatments based on genetics is growing rapidly. For instance, numerous therapies have been developed based on siRNA transfection. In these therapies, it would be also possible to target *ZC3HC1*. Additionally, new research efforts focus increas-

ingly on personalized medicine, which also includes therapies based on the patient's genes. For hypertension most of this is still in the future, but there is already research investigating how certain genes influence the metabolization of certain antihypertensive agents [Hunter et al., 2021]. An example is, how the *UMOD* gene influences the response to loop diuretics (`https://clinicaltrials.gov/ct2/show/NCT03354897`, accessed on 13 March 2023). Another very promising development in this area has been the recent development of a therapeutic approach for hypertension that uses siRNAs to target the Renin-Angiotensin-Aldosteron-System (RAAS) via angiotensinogen [Ranasinghe et al., 2022]. For *ZC3HC1* it could also be a new approach to study its influence on different antihypertensive agents to link the findings from this and similar studies more closely to clinical application.

5 Abstract

Hypertension is an important cardiovascular disease that is known to be the leading preventable risk factor for cardiovascular deaths. Smooth muscle cells play a major role in the pathophysiology of hypertension. They undergo a phenotype switch from contractile to the dedifferentiated synthetic phenotype. The gene *ZC3HC1*, originally identified as a risk gene for CAD, was associated with elevated blood pressure in several studies and encodes for the protein NIPA, which plays a role in the cell cycle in the mitotic entry.

In this thesis, a transient siRNA knockdown of *ZC3HC1* was performed in primary human aortic smooth muscle cells. The knockdown was confirmed on RNA and protein levels. The knockdown cells were studied for the expression of contractile proteins, migration, proliferation, and contractility *in-vitro*. Contractility *ex-vivo* was investigated with *zc3hc1*-KO mice. Additionally, the cell cycle of SMCs was arrested with aphidicolin and this arrest was confirmed with immunofluorescence staining and flow cytometry.

Results showed the downregulation of contractile markers in SMCs with *ZC3HC1* knockdown. Migration and proliferation showed no significant differences, but further experiments in the working group showed an increase in both. Contractility *in-vitro* and *ex-vivo* was decreased for *ZC3HC1* knockdown cells and *zc3hc1*-KO mice, respectively. An accumulation of cyclin B1 under *ZC3HC1* knockdown was shown. The cell cycle was arrested successfully and this was confirmed, but cell cycle progression could not be studied because due to time constraints.

Summing up the results of this thesis, an siRNA-mediated knockdown was used to show the switch to a more synthetic phenotype in SMCs with *ZC3HC1* knockdown compared to control cells. An accumulation of cyclin B1 was shown in SMCs with *ZC3HC1* knockdown, which could cause cell cycle alterations that contribute to the characteristics of the synthetic phenotype.

A Appendix

A.1 Gene Tables for RT^2 Profiler PCR Arrays

A.1.1 Human Cell Motility

Position	UniGene	GenBank	Symbol	Description
A01	Hs.509765	NM_001102	ACTN1	Actinin, alpha 1
A02	Hs.654432	NM_001104	ACTN3	Actinin, alpha 3
A03	Hs.270291	NM_004924	ACTN4	Actinin, alpha 4
A04	Hs.728857	NM_005722	ACTR2	ARP2 actin-related protein 2 homolog (yeast)
A05	Hs.433512	NM_005721	ACTR3	ARP3 actin-related protein 3 homolog (yeast)
A06	Hs.525622	NM_005163	AKT1	V-akt murine thymoma viral oncogene homolog 1
A07	Hs.525330	NM_001663	ARF6	ADP-ribosylation factor 6
A08	Hs.159161	NM_004309	ARHGDIA	Rho GDP dissociation inhibitor (GDI) alpha
A09	Hs.508738	NM_003899	ARHGEF7	Rho guanine nucleotide exchange factor (GEF) 7
A10	Hs.128316	NM_006340	BAIAP2	BAI1-associated protein 2
A11	Hs.479747	NM_014567	BCAR1	Breast cancer anti-estrogen resistance 1
A12	Hs.502842	NM_005186	CAPN1	Calpain 1, (mu/I) large subunit
B01	Hs.350899	NM_001748	CAPN2	Calpain 2, (m/II) large subunit
B02	Hs.74034	NM_001753	CAV1	Caveolin 1, caveolae protein, 22kDa
B03	Hs.690198	NM_001791	CDC42	Cell division cycle 42 (GTP binding protein, 25kDa)
B04	Hs.170622	NM_005507	CFL1	Cofilin 1 (non-muscle)
B05	Hs.638121	NM_016823	CRK	V-crk sarcoma virus CT10 oncogene homolog (avian)
B06	Hs.591402	NM_000757	CSF1	Colony stimulating factor 1 (macrophage)
B07	Hs.596164	NM_005231	CTTN	Cortactin
B08	Hs.529451	NM_005219	DIAPH1	Diaphanous homolog 1 (Drosophila)
B09	Hs.368912	NM_001935	DPP4	Dipeptidyl-peptidase 4
B10	Hs.419815	NM_001963	EGF	Epidermal growth factor
B11	Hs.488293	NM_005228	EGFR	Epidermal growth factor receptor
B12	Hs.497893	NM_001008493	ENAH	Enabled homolog (Drosophila)
C01	Hs.487027	NM_003379	EZR	Ezrin
C02	Hs.654370	NM_004460	FAP	Fibroblast activation protein, alpha
C03	Hs.284244	NM_002006	FGF2	Fibroblast growth factor 2 (basic)
C04	Hs.396530	NM_000601	HGF	Hepatocyte growth factor (hepapoietin A; scatter factor)
C05	Hs.160562	NM_000618	IGF1	Insulin-like growth factor 1 (somatomedin C)
C06	Hs.643120	NM_000875	IGF1R	Insulin-like growth factor 1 receptor
C07	Hs.5158	NM_004517	ILK	Integrin-linked kinase
C08	Hs.694732	NM_000885	ITGA4	Integrin, alpha 4 (antigen CD49D, alpha 4 subunit of VLA-4 receptor)
C09	Hs.643813	NM_002211	ITGB1	Integrin, beta 1 (fibronectin receptor, beta polypeptide, antigen CD29 includes MDF2, MSK12)
C10	Hs.375957	NM_000211	ITGB2	Integrin, beta 2 (complement component 3 receptor 3 and 4 subunit)
C11	Hs.218040	NM_000212	ITGB3	Integrin, beta 3 (platelet glycoprotein IIIa, antigen CD61)
C12	Hs.647035	NM_002314	LIMK1	LIM domain kinase 1
D01	Hs.431850	NM_002745	MAPK1	Mitogen-activated protein kinase 1
D02	Hs.132966	NM_000245	MET	Met proto-oncogene (hepatocyte growth factor receptor)
D03	Hs.2399	NM_004995	MMP14	Matrix metallopeptidase 14 (membrane-inserted)
D04	Hs.513617	NM_004530	MMP2	Matrix metallopeptidase 2 (gelatinase A, 72kDa gelatinase, 72kDa type IV collagenase)
D05	Hs.297413	NM_004994	MMP9	Matrix metallopeptidase 9 (gelatinase B, 92kDa gelatinase, 92kDa type IV collagenase)
D06	Hs.87752	NM_002444	MSN	Moesin

Position	UniGene	GenBank	Symbol	Description
D07	Hs.16355	NM_005964	MYH10	Myosin, heavy chain 10, non-muscle
D08	Hs.474751	NM_002473	MYH9	Myosin, heavy chain 9, non-muscle
D09	Hs.504687	NM_006097	MYL9	Myosin, light chain 9, regulatory
D10	Hs.477375	NM_053025	MYLK	Myosin light chain kinase
D11	Hs.435714	NM_002576	PAK1	P21 protein (Cdc42/Rac)-activated kinase 1
D12	Hs.20447	NM_005884	PAK4	P21 protein (Cdc42/Rac)-activated kinase 4
E01	Hs.494691	NM_005022	PFN1	Profilin 1
E02	Hs.553498	NM_006218	PIK3CA	Phosphoinositide-3-kinase, catalytic, alpha polypeptide
E03	Hs.466871	NM_002659	PLAUR	Plasminogen activator, urokinase receptor
E04	Hs.268177	NM_002660	PLCG1	Phospholipase C, gamma 1
E05	Hs.382865	NM_002662	PLD1	Phospholipase D1, phosphatidylcholine-specific
E06	Hs.531704	NM_002737	PRKCA	Protein kinase C, alpha
E07	Hs.500466	NM_000314	PTEN	Phosphatase and tensin homolog
E08	Hs.395482	NM_005607	PTK2	PTK2 protein tyrosine kinase 2
E09	Hs.491322	NM_004103	PTK2B	PTK2B protein tyrosine kinase 2 beta
E10	Hs.417549	NM_002827	PTPN1	Protein tyrosine phosphatase, non-receptor type 1
E11	Hs.446336	NM_002859	PXN	Paxillin
E12	Hs.413812	NM_006908	RAC1	Ras-related C3 botulinum toxin substrate 1 (rho family, small GTP binding protein Rac1)
F01	Hs.517601	NM_002872	RAC2	Ras-related C3 botulinum toxin substrate 2 (rho family, small GTP binding protein Rac2)
F02	Hs.664080	NM_002890	RASA1	RAS p21 protein activator (GTPase activating protein) 1
F03	Hs.263671	NM_002906	RDX	Radixin
F04	Hs.247565	NM_000539	RHO	Rhodopsin
F05	Hs.247077	NM_001664	RHOA	Ras homolog gene family, member A
F06	Hs.502876	NM_004040	RHOB	Ras homolog gene family, member B
F07	Hs.502659	NM_175744	RHOC	Ras homolog gene family, member C
F08	Hs.6838	NM_005168	RND3	Rho family GTPase 3
F09	Hs.306307	NM_005406	ROCK1	Rho-associated, coiled-coil containing protein kinase 1
F10	Hs.594708	NM_014631	SH3PXD2A	SH3 and PX domains 2A
F11	Hs.195659	NM_005417	SRC	V-src sarcoma (Schmidt-Ruppin A-2) viral oncogene homolog (avian)
F12	Hs.463059	NM_003150	STAT3	Signal transducer and activator of transcription 3 (acute-phase response factor)
G01	Hs.499209	NM_003174	SVIL	Supervillin
G02	Hs.645227	NM_000660	TGFB1	Transforming growth factor, beta 1
G03	Hs.633514	NM_003255	TIMP2	TIMP metallopeptidase inhibitor 2
G04	Hs.471014	NM_006289	TLN1	Talin 1
G05	Hs.515469	NM_003370	VASP	Vasodilator-stimulated phosphoprotein
G06	Hs.643896	NM_003373	VCL	Vinculin
G07	Hs.73793	NM_003376	VEGFA	Vascular endothelial growth factor A
G08	Hs.642813	NM_003380	VIM	Vimentin
G09	Hs.75850	NM_003931	WASF1	WAS protein family, member 1
G10	Hs.590909	NM_006990	WASF2	WAS protein family, member 2
G11	Hs.143728	NM_003941	WASL	Wiskott-Aldrich syndrome-like
G12	Hs.128067	NM_003387	WIPF1	WAS/WASL interacting protein family, member 1
H01	Hs.520640	NM_001101	ACTB	Actin, beta
H02	Hs.534255	NM_004048	B2M	Beta-2-microglobulin
H03	Hs.592355	NM_002046	GAPDH	Glyceraldehyde-3-phosphate dehydrogenase
H04	Hs.412707	NM_000194	HPRT1	Hypoxanthine phosphoribosyltransferase 1
H05	Hs.546285	NM_001002	RPLP0	Ribosomal protein, large, P0
H06	N/A	SA_00105	HGDC	Human Genomic DNA Contamination
H07	N/A	SA_00104	RTC	Reverse Transcription Control
H08	N/A	SA_00104	RTC	Reverse Transcription Control
H09	N/A	SA_00104	RTC	Reverse Transcription Control
H10	N/A	SA_00103	PPC	Positive PCR Control
H11	N/A	SA_00103	PPC	Positive PCR Control
H12	N/A	SA_00103	PPC	Positive PCR Control

Figure A.1: Gene Table for Human Cell Motility qPCR Profiler Array

A.1.2 Human cAMP/Calcium Signalling Pathway Finder

Position	UniGene	GenBank	Symbol	Description
A01	Hs.99913	NM_000684	ADRB1	Adrenergic, beta-1-, receptor
A02	Hs.171189	NM_001621	AHR	Aryl hydrocarbon receptor
A03	Hs.159118	NM_001634	AMD1	Adenosylmethionine decarboxylase 1
A04	Hs.270833	NM_001657	AREG	Amphiregulin
A05	Hs.460	NM_001674	ATF3	Activating transcription factor 3
A06	Hs.150749	NM_000633	BCL2	B-cell CLL/lymphoma 2
A07	Hs.502182	NM_001709	BDNF	Brain-derived neurotrophic factor
A08	Hs.194143	NM_007294	BRCA1	Breast cancer 1, early onset
A09	Hs.65425	NM_004929	CALB1	Calbindin 1, 28kDa
A10	Hs.106857	NM_001740	CALB2	Calbindin 2
A11	Hs.282410	NM_006888	CALM1	Calmodulin 1 (phosphorylase kinase, delta)
A12	Hs.515162	NM_004343	CALR	Calreticulin
B01	Hs.417050	NM_003914	CCNA1	Cyclin A1
B02	Hs.523852	NM_053056	CCND1	Cyclin D1
B03	Hs.647078	NM_004935	CDK5	Cyclin-dependent kinase 5
B04	Hs.72901	NM_004936	CDKN2B	Cyclin-dependent kinase inhibitor 2B (p15, inhibits CDK4)
B05	Hs.119689	NM_000735	CGA	Glycoprotein hormones, alpha polypeptide
B06	Hs.150793	NM_001275	CHGA	Chromogranin A (parathyroid secretory protein 1)
B07	Hs.465929	NM_001299	CNN1	Calponin 1, basic, smooth muscle
B08	Hs.516646	NM_004379	CREB1	CAMP responsive element binding protein 1
B09	Hs.200250	NM_183011	CREM	CAMP responsive element modulator
B10	Hs.483811	NM_001330	CTF1	Cardiotrophin 1
B11	Hs.8867	NM_001554	CYR61	Cysteine-rich, angiogenic inducer, 61
B12	Hs.728989	NM_004083	DDIT3	DNA-damage-inducible transcript 3
C01	Hs.171695	NM_004417	DUSP1	Dual specificity phosphatase 1
C02	Hs.326035	NM_001964	EGR1	Early growth response 1
C03	Hs.1395	NM_000399	EGR2	Early growth response 2
C04	Hs.511915	NM_001975	ENO2	Enolase 2 (gamma, neuronal)
C05	Hs.166015	NM_020996	FGF6	Fibroblast growth factor 6
C06	Hs.728789	NM_005252	FOS	FBJ murine osteosarcoma viral oncogene homolog
C07	Hs.590958	NM_006732	FOSB	FBJ murine osteosarcoma viral oncogene homolog B
C08	Hs.516494	NM_002054	GCG	Glucagon
C09	Hs.654463	NM_005261	GEM	GTP binding protein overexpressed in skeletal muscle
C10	Hs.658534	NM_000164	GIPR	Gastric inhibitory polypeptide receptor
C11	Hs.406266	NM_000189	HK2	Hexokinase 2
C12	Hs.90093	NM_002154	HSPA4	Heat shock 70kDa protein 4
D01	Hs.716396	NM_005347	HSPA5	Heat shock 70kDa protein 5 (glucose-regulated protein, 78kDa)
D02	Hs.89679	NM_000586	IL2	Interleukin 2
D03	Hs.654458	NM_000600	IL6	Interleukin 6 (interferon, beta 2)
D04	Hs.583348	NM_002192	INHBA	Inhibin, beta A
D05	Hs.25292	NM_002229	JUNB	Jun B proto-oncogene
D06	Hs.2780	NM_005354	JUND	Jun D proto-oncogene
D07	Hs.150208	NM_002234	KCNA5	Potassium voltage-gated channel, shaker-related subfamily, member 5
D08	Hs.2795	NM_005566	LDHA	Lactate dehydrogenase A
D09	Hs.134859	NM_005360	MAF	V-maf musculoaponeurotic fibrosarcoma oncogene homolog (avian)

Position	UniGene	GenBank	Symbol	Description
D10	Hs.407995	NM_002415	MIF	Macrophage migration inhibitory factor (glycosylation-inhibiting factor)
D11	Hs.503878	NM_000615	NCAM1	Neural cell adhesion molecule 1
D12	Hs.113577	NM_000267	NF1	Neurofibromin 1
E01	Hs.709191	NM_000625	NOS2	Nitric oxide synthase 2, inducible
E02	Hs.1832	NM_000905	NPY	Neuropeptide Y
E03	Hs.563344	NM_006186	NR4A2	Nuclear receptor subfamily 4, group A, member 2
E04	Hs.75812	NM_004563	PCK2	Phosphoenolpyruvate carboxykinase 2 (mitochondrial)
E05	Hs.728886	NM_182649	PCNA	Proliferating cell nuclear antigen
E06	Hs.339831	NM_006211	PENK	Proenkephalin
E07	Hs.445534	NM_002616	PER1	Period homolog 1 (Drosophila)
E08	Hs.491582	NM_000930	PLAT	Plasminogen activator, tissue
E09	Hs.170839	NM_002667	PLN	Phospholamban
E10	Hs.96	NM_021127	PMAIP1	Phorbol-12-myristate-13-acetate-induced protein 1
E11	Hs.591654	NM_000306	POU1F1	POU class 1 homeobox 1
E12	Hs.654525	NM_006235	POU2AF1	POU class 2 associating factor 1
F01	Hs.631593	NM_014330	PPP1R15A	Protein phosphatase 1, regulatory (inhibitor) subunit 15A
F02	Hs.483408	NM_002715	PPP2CA	Protein phosphatase 2, catalytic subunit, alpha isozyme
F03	Hs.280342	NM_002734	PRKAR1A	Protein kinase, cAMP-dependent, regulatory, type I, alpha (tissue specific extinguisher 1)
F04	Hs.1905	NM_000948	PRL	Prolactin
F05	Hs.196384	NM_000963	PTGS2	Prostaglandin-endoperoxide synthase 2 (prostaglandin G/H synthase and cyclooxygenase)
F06	Hs.408528	NM_000321	RB1	Retinoblastoma 1
F07	Hs.19413	NM_005621	S100A12	S100 calcium binding protein A12
F08	Hs.275243	NM_014624	S100A6	S100 calcium binding protein A6
F09	Hs.639	NM_004057	S100G	S100 calcium binding protein G
F10	Hs.516726	NM_003469	SCG2	Secretogranin II
F11	Hs.510078	NM_005627	SGK1	Serum/glucocorticoid regulated kinase 1
F12	Hs.158322	NM_003053	SLC18A1	Solute carrier family 18 (vesicular monoamine), member 1
G01	Hs.487046	NM_000636	SOD2	Superoxide dismutase 2, mitochondrial
G02	Hs.520140	NM_003131	SRF	Serum response factor (c-fos serum response element-binding transcription factor)
G03	Hs.12409	NM_001048	SST	Somatostatin
G04	Hs.514451	NM_001050	SSTR2	Somatostatin receptor 2
G05	Hs.463059	NM_003150	STAT3	Signal transducer and activator of transcription 3 (acute-phase response factor)
G06	Hs.633301	NM_001058	TACR1	Tachykinin receptor 1
G07	Hs.592317	NM_003239	TGFB3	Transforming growth factor, beta 3
G08	Hs.435609	NM_000360	TH	Tyrosine hydroxylase
G09	Hs.164226	NM_003246	THBS1	Thrombospondin 1
G10	Hs.241570	NM_000594	TNF	Tumor necrosis factor
G11	Hs.643896	NM_003373	VCL	Vinculin
G12	Hs.53973	NM_003381	VIP	Vasoactive intestinal peptide
H01	Hs.520640	NM_001101	ACTB	Actin, beta
H02	Hs.534255	NM_004048	B2M	Beta-2-microglobulin
H03	Hs.592355	NM_002046	GAPDH	Glyceraldehyde-3-phosphate dehydrogenase
H04	Hs.412707	NM_000194	HPRT1	Hypoxanthine phosphoribosyltransferase 1
H05	Hs.546285	NM_001002	RPLP0	Ribosomal protein, large, P0
H06	N/A	SA_00105	HGDC	Human Genomic DNA Contamination
H07	N/A	SA_00104	RTC	Reverse Transcription Control
H08	N/A	SA_00104	RTC	Reverse Transcription Control
H09	N/A	SA_00104	RTC	Reverse Transcription Control
H10	N/A	SA_00103	PPC	Positive PCR Control
H11	N/A	SA_00103	PPC	Positive PCR Control
H12	N/A	SA_00103	PPC	Positive PCR Control

Figure A.2: Gene Table for Human cAMP/Calcium Signalling PathwayFinder qPCR Profiler Array

References

[20 et al., 2007] 20, . B. C. C. J. R. W. . M. W. L. . R. S. M. . S. D. P. . P. M. ., 2, T. . D. C. D. G. . D. D. B. . . N. S. . S. H. E. . W. N. M. . W. B. . . T. J. A., et al. (2007). Genome-wide association study of 14,000 cases of seven common diseases and 3,000 shared controls. *Nature*, 447(7145):661–678.

[Adeyemo et al., 2009] Adeyemo, A., Gerry, N., Chen, G., Herbert, A., Doumatey, A., Huang, H., Zhou, J., Lashley, K., Chen, Y., Christman, M., et al. (2009). A genome-wide association study of hypertension and blood pressure in african americans. *PLoS genetics*, 5(7):e1000564.

[Adua, 2022] Adua, E. (2022). Decoding the mechanism of hypertension through multiomics profiling. *Journal of Human Hypertension*, pages 1–12.

[Aherrahrou et al., 2021] Aherrahrou, R., Reinberger, T., Werner, J., Otto, M., Al-Hasani, J., Munoz-Venegas, M. L., Civelek, M., Schunkert, H., Kessler, T., Erdmann, J., et al. (2021). Deficiency of zc3hc1 increases vascular smooth muscle cell migration, proliferation and neointima formation following injury. *bioRxiv*, pages 2021–09.

[Al-Hasani, 2017] Al-Hasani, J. (2017). *Functional Analysis of the CAD-Risk Gene Zc3hc1.* PhD thesis, University of Luebeck.

[Alexander and Owens, 2012] Alexander, M. R. and Owens, G. K. (2012). Epigenetic control of smooth muscle cell differentiation and phenotypic switching in vascular development and disease. *Annual review of physiology*, 74:13–40.

[Bassermann et al., 2005a] Bassermann, F., Peschel, C., and Duyster, J. (2005a). Mitotic entry: a matter of oscillating destruction. *Cell cycle*, 4(11):1515–1517.

[Bassermann et al., 2007] Bassermann, F., von Klitzing, C., Illert, A. L., Münch, S., Morris, S. W., Pagano, M., Peschel, C., and Duyster, J. (2007). Multisite phosphorylation of nuclear interaction partner of alk (nipa) at g2/m involves cyclin b1/cdk1. *Journal of Biological Chemistry*, 282(22):15965–15972.

[Bassermann et al., 2005b] Bassermann, F., Von Klitzing, C., Münch, S., Bai, R.-Y., Kawaguchi, H., Morris, S. W., Peschel, C., and Duyster, J. (2005b). Nipa defines an scf-type mammalian e3 ligase that regulates mitotic entry. *Cell*, 122(1):45–57.

[Beevers et al., 2001] Beevers, G., Lip, G. Y., and O'Brien, E. (2001). The pathophysiology of hypertension. *Bmj*, 322(7291):912–916.

[Brænne et al., 2015] Brænne, I., Civelek, M., Vilne, B., Di Narzo, A., Johnson, A. D., Zhao, Y., Reiz, B., Codoni, V., Webb, T. R., Foroughi Asl, H., et al. (2015). Prediction of causal candidate genes in coronary artery disease loci. *Arteriosclerosis, thrombosis, and vascular biology*, 35(10):2207–2217.

[Braun-Dullaeus et al., 2001] Braun-Dullaeus, R. C., Mann, M. J., Seay, U., Zhang, L., von der Leyen, H. E., Morris, R. E., and Dzau, V. J. (2001). Cell cycle protein expression in vascular smooth muscle cells in vitro and in vivo is regulated through phosphatidylinositol 3-kinase and mammalian target of rapamycin. *Arteriosclerosis, thrombosis, and vascular biology*, 21(7):1152–1158.

[Brazas and Hagstrom, 2005] Brazas, R. M. and Hagstrom, J. E. (2005). Delivery of small interfering rna to mammalian cells in culture by using cationic lipid polymer-based transfection reagents. In *Methods in enzymology*, volume 392, pages 112–124. Elsevier.

[Brookes, 1999] Brookes, A. J. (1999). The essence of snps. *Gene*, 234(2):177–186.

[Brummelkamp et al., 2002] Brummelkamp, T. R., Bernards, R., and Agami, R. (2002). A system for stable expression of short interfering rnas in mammalian cells. *science*, 296(5567):550–553.

[Cardozo and Pagano, 2004] Cardozo, T. and Pagano, M. (2004). The scf ubiquitin ligase: insights into a molecular machine. *Nature reviews Molecular cell biology*, 5(9):739–751.

[Caulfield et al., 2003] Caulfield, M., Munroe, P., Pembroke, J., Samani, N., Dominiczak, A., Brown, M., Webster, J., Ratcliffe, P., O'Shea, S., Papp, J., et al. (2003). Genome-wide mapping of human loci for essential hypertension. *The Lancet*, 361(9375):2118–2123.

[Cejka et al., 2006] Cejka, D., Losert, D., and Wacheck, V. (2006). Short interfering rna (sirna): tool or therapeutic? *Clinical science*, 110(1):47–58.

[Chobanian et al., 1987] Chobanian, A. V., Haudenschild, C. C., et al. (1987). Smooth muscle cell migration and proliferation: atherogenic mechanisms in hypertension. *Atherosclerosis*, 67(2-3):215–221.

[Consortium et al., 2011] Consortium, C., Consortium, K., consortium, E., consortium, C.-H., Aspelund, T., Garcia, M., Chang, Y.-P. C., O'Connell, J. R., Steinle, N. I., et al. (2011). Genetic variants in novel pathways influence blood pressure and cardiovascular disease risk. *Nature*, 478(7367):103–109.

[Consortium et al., 2013] Consortium, C., Deloukas, P., Kanoni, S., Willenborg, C., Farrall, M., Assimes, T. L., Thompson, J. R., Ingelsson, E., Saleheen, D., Erdmann, J., et al. (2013). Large-scale association analysis identifies new risk loci for coronary artery disease. *Nature genetics*, 45(1):25–33.

[Corjay et al., 1989] Corjay, M. H., Thompson, M., Lynch, K., and Owens, G. (1989). Differential effect of platelet-derived growth factor-versus serum-induced growth on smooth muscle α-actin and nonmuscle β-actin mrna expression in cultured rat aortic smooth muscle cells. *Journal of Biological Chemistry*, 264(18):10501–10506.

[Davis-Dusenbery et al., 2011] Davis-Dusenbery, B. N., Wu, C., and Hata, A. (2011). Micromanaging vascular smooth muscle cell differentiation and phenotypic modulation. *Arteriosclerosis, thrombosis, and vascular biology*, 31(11):2370–2377.

[de Las Fuentes et al., 2021] de Las Fuentes, L., Sung, Y. J., Noordam, R., Winkler, T., Feitosa, M. F., Schwander, K., Bentley, A. R., Brown, M. R., Guo, X., Manning, A., et al. (2021). Gene-educational attainment interactions in a multi-ancestry genome-wide meta-analysis identify novel blood pressure loci. *Molecular psychiatry*, 26(6):2111–2125.

[Di et al., 2015] Di, J., Huang, H., Qu, D., Tang, J., Cao, W., Lu, Z., Cheng, Q., Yang, J., Bai, J., Zhang, Y., et al. (2015). Rap2b promotes proliferation, migration and invasion of human breast cancer through calcium-related erk1/2 signaling pathway. *Scientific reports*, 5(1):1–11.

[Duband et al., 1993] Duband, J.-L., Gimona, M., Scatena, M., Sartore, S., and Small, J. V. (1993). Calponin and sm22 as differentiation markers of smooth muscle: spatiotemporal distribution during avian embryonic development. *Differentiation*, 55(1):1–11.

[Edwards et al., 2005] Edwards, A. O., Ritter III, R., Abel, K. J., Manning, A., Panhuysen, C., and Farrer, L. A. (2005). Complement factor h polymorphism and age-related macular degeneration. *Science*, 308(5720):421–424.

[Erbilgin et al., 2013] Erbilgin, A., Civelek, M., Romanoski, C. E., Pan, C., Hagopian, R., Berliner, J. A., and Lusis, A. J. (2013). Identification of cad candidate genes in gwas loci and their expression in vascular cells [s]. *Journal of lipid research*, 54(7):1894–1905.

[Folkow, 1982] Folkow, B. (1982). Physiological aspects of primary hypertension. *Physiological reviews*, 62(2):347–504.

[Fukuda et al., 1999] Fukuda, N., Hu, W.-Y., Satoh, C., Nakayama, M., Kishioka, H., Kubo, A., and Kanmatsuse, K. (1999). Contribution of synthetic phenotype on the enhanced angiotensin ii-generating system in vascular smooth muscle cells from spontaneously hypertensive rats. *Journal of hypertension*, 17(8):1099–1107.

[Gachkar, 2018] Gachkar, S. (2018). *Role of Thyroid Hormones in Body Temperature Regulation*. PhD thesis, University of Luebeck.

[Gachkar et al., 2017] Gachkar, S., Oelkrug, R., Martinez-Sanchez, N., Rial-Pensado, E., Warner, A., Hoefig, C. S., López, M., and Mittag, J. (2017). 3-iodothyronamine induces tail vasodilation through central action in male mice. *Endocrinology*, 158(6):1977–1984.

[Gadeau et al., 1993] Gadeau, A.-P., Campan, M., Millet, D., Candresse, T., and Desgranges, C. (1993). Osteopontin overexpression is associated with arterial smooth muscle cell proliferation in vitro. *Arteriosclerosis and Thrombosis: A Journal of Vascular Biology*, 13(1):120–125.

[Gaziano et al., 2006] Gaziano, T., Reddy, K. S., Paccaud, F., Horton, S., and Chaturvedi, V. (2006). Cardiovascular disease. *Disease Control Priorities in Developing Countries. 2nd edition*.

[Gibbs et al., 2003] Gibbs, R. A., Belmont, J. W., Hardenbol, P., Willis, T. D., Yu, F., Yang, H., Ch'ang, L.-Y., Huang, W., Liu, B., Shen, Y., et al. (2003). The international hapmap project.

[Gunkel and Cordes, 2022] Gunkel, P. and Cordes, V. C. (2022). Zc3hc1 is a structural element of the nuclear basket effecting interlinkage of tpr polypeptides. *Molecular Biology of the Cell*, 33(9):ar82.

[Hadrava et al., 1992] Hadrava, V., Tremblay, J., Sekaly, R.-P., and Hamet, P. (1992). Accelerated entry of aortic smooth muscle cells from spontaneously hypertensive rats into the s phase of the cell cycle. *Biochemistry and Cell Biology*, 70(7):599–604.

[Harborth et al., 2001] Harborth, J., Elbashir, S. M., Bechert, K., Tuschl, T., and Weber, K. (2001). Identification of essential genes in cultured mammalian cells using small interfering rnas. *Journal of cell science*, 114(24):4557–4565.

[Harrison et al., 2021] Harrison, D. G., Coffman, T. M., and Wilcox, C. S. (2021). Pathophysiology of hypertension: the mosaic theory and beyond. *Circulation research*, 128(7):847–863.

[Herold, 2019] Herold, G. e. a. (2019). *Innere Medizin*. Gerd Herold, Köln.

[Hirschhorn and Daly, 2005] Hirschhorn, J. N. and Daly, M. J. (2005). Genome-wide association studies for common diseases and complex traits. *Nature reviews genetics*, 6(2):95–108.

[Hochstrasser, 1996] Hochstrasser, M. (1996). Ubiquitin-dependent protein degradation. *Annual review of genetics*, 30(1):405–439.

[Holycross et al., 1992] Holycross, B., Blank, R., Thompson, M., Peach, M., and Owens, G. (1992). Platelet-derived growth factor-bb-induced suppression of smooth muscle cell differentiation. *Circulation research*, 71(6):1525–1532.

[Hunter et al., 2021] Hunter, P. G., Chapman, F. A., and Dhaun, N. (2021). Hypertension: Current trends and future perspectives. *British Journal of Clinical Pharmacology*, 87(10):3721–3736.

[Hwang et al., 1995] Hwang, A., Maity, A., McKenna, W. G., and Muschel, R. J. (1995). Cell cycle-dependent regulation of the cyclin b1 promoter. *Journal of Biological Chemistry*, 270(47):28419–28424.

[Ikegami et al., 1978] Ikegami, S., TAGUCHI, T., OHASHI, M., OGURO, M., NAGANO, H., and MANO, Y. (1978). Aphidicolin prevents mitotic cell division by interfering with the activity of dna polymerase-α. *Nature*, 275(5679):458–460.

[Illert et al., 2012] Illert, A. L., Kawaguchi, H., Antinozzi, C., Bassermann, F., Quintanilla-Martinez, L., von Klitzing, C., Hiwatari, M., Peschel, C., de Rooij, D. G., Morris, S. W., et al. (2012). Targeted inactivation of nuclear interaction partner of alk disrupts meiotic prophase. *Development*, 139(14):2523–2534.

[Intengan and Schiffrin, 2000] Intengan, H. D. and Schiffrin, E. L. (2000). Structure and mechanical properties of resistance arteries in hypertension: role of adhesion molecules and extracellular matrix determinants. *Hypertension*, 36(3):312–318.

[Jackman and O'Connor, 1998] Jackman, J. and O'Connor, P. M. (1998). Methods for synchronizing cells at specific stages of the cell cycle. *Current protocols in cell biology*, (1):8–3.

[Jackson and Eldridge, 2002] Jackson, P. K. and Eldridge, A. G. (2002). The scf ubiquitin ligase: an extended look. *Molecular cell*, 9(5):923–925.

[Jinek et al., 2012] Jinek, M., Chylinski, K., Fonfara, I., Hauer, M., Doudna, J. A., and Charpentier, E. (2012). A programmable dual-rna–guided dna endonuclease in adaptive bacterial immunity. *science*, 337(6096):816–821.

[Johnson et al., 2017] Johnson, A. D., Alberts, B., Lewis, J., Morgan, D., Raff, M., Roberts, K., and Walter, P. (2017). *Molekularbiologie der Zelle*. John Wiley & Sons.

[Johnson and Walker, 1999] Johnson, D. G. and Walker, C. L. (1999). Cyclins and cell cycle checkpoints. *Annual review of pharmacology and toxicology*, 39.

[Jones et al., 2016] Jones, P. D., Kaiser, M. A., Najafabadi, M. G., McVey, D. G., Beveridge, A. J., Schofield, C. L., Samani, N. J., and Webb, T. R. (2016). The coronary artery disease-associated coding variant in zinc finger c3hc-type containing 1 (zc3hc1) affects cell cycle regulation. *Journal of Biological Chemistry*, 291(31):16318–16327.

[Kannel, 1989] Kannel, W. B. (1989). Risk factors in hypertension. *Journal of cardiovascular pharmacology*, 13:S4–10.

[Kato et al., 2008] Kato, N., Miyata, T., Tabara, Y., Katsuya, T., Yanai, K., Hanada, H., Kamide, K., Nakura, J., Kohara, K., Takeuchi, F., et al. (2008). High-density association study and nomination of susceptibility genes for hypertension in the japanese national project. *Human molecular genetics*, 17(4):617–627.

[Kato et al., 2011] Kato, N., Takeuchi, F., Tabara, Y., Kelly, T. N., Go, M. J., Sim, X., Tay, W. T., Chen, C.-H., Zhang, Y., Yamamoto, K., et al. (2011). Meta-analysis of genome-wide association studies identifies common variants associated with blood pressure variation in east asians. *Nature genetics*, 43(6):531–538.

[Kim et al., 2019] Kim, B., Park, J.-H., and Sailor, M. J. (2019). Rekindling rnai therapy: materials design requirements for in vivo sirna delivery. *Advanced materials*, 31(49):1903637.

[Kim and Eberwine, 2010] Kim, T. K. and Eberwine, J. H. (2010). Mammalian cell transfection: the present and the future. *Analytical and bioanalytical chemistry*, 397:3173–3178.

[Kolifarhood et al., 2019] Kolifarhood, G., Daneshpour, M. S., Khayat, B. S., Saadati, H. M., Guity, K., Khosravi, N., Akbarzadeh, M., and Sabour, S. (2019). Generality of genomic findings on blood pressure traits and its usefulness in precision medicine in diverse populations: A systematic review. *Clinical Genetics*, 96(1):17–27.

[Kumar et al., 2015] Kumar, V., Ali, M. J., and Ramachandran, C. (2015). Effect of mitomycin-c on contraction and migration of human nasal mucosa fibroblasts: implications in dacryocystorhinostomy. *British Journal of Ophthalmology*, 99(9):1295–1300.

[Kunnas and Nikkari, 2015] Kunnas, T. and Nikkari, S. T. (2015). Association of zinc finger, c3hc-type containing 1 (zc3hc1) rs11556924 genetic variant with hypertension in a finnish population, the tamrisk study. *Medicine*, 94(32).

[Levy et al., 2009] Levy, D., Ehret, G. B., Rice, K., Verwoert, G. C., Launer, L. J., Dehghan, A., Glazer, N. L., Morrison, A. C., Johnson, A. D., Aspelund, T., et al. (2009). Genome-wide association study of blood pressure and hypertension. *Nature genetics*, 41(6):677–687.

[Levy et al., 2007] Levy, D., Larson, M. G., Benjamin, E. J., Newton-Cheh, C., Wang, T. J., Hwang, S.-J., Vasan, R. S., and Mitchell, G. F. (2007). Framingham heart study 100k project: genome-wide associations for blood pressure and arterial stiffness. *BMC medical genetics*, 8(1):1–11.

[Lifton et al., 2001] Lifton, R. P., Gharavi, A. G., and Geller, D. S. (2001). Molecular mechanisms of human hypertension. *Cell*, 104(4):545–556.

[Lim and Kaldis, 2013] Lim, S. and Kaldis, P. (2013). Cdks, cyclins and ckis: roles beyond cell cycle regulation. *Development*, 140(15):3079–3093.

[Linseman et al., 2017] Linseman, T., Soubeyrand, S., Martinuk, A., Nikpay, M., Lau, P., and McPherson, R. (2017). Functional validation of a common nonsynonymous coding variant in zc3hc1 associated with protection from coronary artery disease. *Circulation: Cardiovascular Genetics*, 10(1):e001498.

[Livak and Schmittgen, 2001] Livak, K. J. and Schmittgen, T. D. (2001). Analysis of relative gene expression data using real-time quantitative pcr and the 2- $\delta\delta$ct method. *methods*, 25(4):402–408.

[López-Mejías et al., 2013] López-Mejías, R., Genre, F., García-Bermúdez, M., Corrales, A., González-Juanatey, C., Llorca, J., Miranda-Filloy, J. A., Rueda-Gotor, J., Blanco, R., Castañeda, S., et al. (2013). The zc3hc1 rs11556924 polymorphism is associated with increased carotid intima-media thickness in patients with rheumatoid arthritis. *Arthritis research & therapy*, 15(5):1–5.

[Ma et al., 2019] Ma, H., He, Y., Bai, M., Zhu, L., He, X., Wang, L., and Jin, T. (2019). The genetic polymorphisms of zc3hc1 and smarca4 are associated with hypertension risk. *Molecular Genetics & Genomic Medicine*, 7(11):e942.

[Mills et al., 2016] Mills, K. T., Bundy, J. D., Kelly, T. N., Reed, J. E., Kearney, P. M., Reynolds, K., Chen, J., and He, J. (2016). Global disparities of hypertension prevalence and control: a systematic analysis of population-based studies from 90 countries. *Circulation*, 134(6):441–450.

[Mills et al., 2020] Mills, K. T., Stefanescu, A., and He, J. (2020). The global epidemiology of hypertension. *Nature Reviews Nephrology*, 16(4):223–237.

[Morishita et al., 1994] Morishita, R., Gibbons, G. H., Kaneda, Y., Ogihara, T., and Dzau, V. J. (1994). Pharmacokinetics of antisense oligodeoxyribonucleotides (cyclin b1 and cdc 2

kinase) in the vessel wall in vivo: enhanced therapeutic utility for restenosis by hvj-liposome delivery. *Gene*, 149(1):13–19.

[Morris et al., 2004] Morris, K. V., Chan, S. W.-L., Jacobsen, S. E., and Looney, D. J. (2004). Small interfering rna-induced transcriptional gene silencing in human cells. *Science*, 305(5688):1289–1292.

[Mulvany et al., 1978] Mulvany, M., Hansen, O., and Aalkjaer, C. (1978). Direct evidence that the greater contractility of resistance vessels in spontaneously hypertensive rats is associated with a narrowed lumen, a thickened media, and an increased number of smooth muscle cell layers. *Circulation research*, 43(6):854–864.

[Murray et al., 2020] Murray, C. J., Aravkin, A. Y., Zheng, P., Abbafati, C., Abbas, K. M., Abbasi-Kangevari, M., Abd-Allah, F., Abdelalim, A., Abdollahi, M., Abdollahpour, I., et al. (2020). Global burden of 87 risk factors in 204 countries and territories, 1990–2019: a systematic analysis for the global burden of disease study 2019. *The Lancet*, 396(10258):1223–1249.

[Newton-Cheh et al., 2009] Newton-Cheh, C., Johnson, T., Gateva, V., Tobin, M. D., Bochud, M., Coin, L., Najjar, S. S., Zhao, J. H., Heath, S. C., Eyheramendy, S., et al. (2009). Genome-wide association study identifies eight loci associated with blood pressure. *Nature genetics*, 41(6):666–676.

[Oparil et al., 2003] Oparil, S., Zaman, M. A., and Calhoun, D. A. (2003). Pathogenesis of hypertension. *Annals of internal medicine*, 139(9):761–776.

[Ouyang et al., 2003] Ouyang, T., Bai, R.-Y., Bassermann, F., Von Klitzing, C., Klumpen, S., Miething, C., Morris, S. W., Peschel, C., and Duyster, J. (2003). Identification and characterization of a nuclear interacting partner of anaplastic lymphoma kinase (nipa). *Journal of Biological Chemistry*, 278(32):30028–30036.

[Owens, 1995] Owens, G. K. (1995). Regulation of differentiation of vascular smooth muscle cells. *Physiological reviews*, 75(3):487–517.

[Owens et al., 2004] Owens, G. K., Kumar, M. S., and Wamhoff, B. R. (2004). Molecular regulation of vascular smooth muscle cell differentiation in development and disease. *Physiological reviews*, 84(3):767–801.

[Padmanabhan and Dominiczak, 2021] Padmanabhan, S. and Dominiczak, A. F. (2021). Genomics of hypertension: the road to precision medicine. *Nature Reviews Cardiology*, 18(4):235–250.

[Petersen et al., 2008] Petersen, E. J., Miyoshi, T., Yuan, Z., Hirohata, S., Li, J. Z., Shi, W., and Angle, J. F. (2008). sirna silencing reveals role of vascular cell adhesion molecule-1 in vascular smooth muscle cell migration. *Atherosclerosis*, 198(2):301–306.

[Pidkovka et al., 2007] Pidkovka, N. A., Cherepanova, O. A., Yoshida, T., Alexander, M. R., Deaton, R. A., Thomas, J. A., Leitinger, N., and Owens, G. K. (2007). Oxidized phospholipids induce phenotypic switching of vascular smooth muscle cells in vivo and in vitro. *Circulation research*, 101(8):792–801.

[Ranasinghe et al., 2022] Ranasinghe, P., Addison, M. L., and Webb, D. J. (2022). Small interfering rna therapeutics in hypertension: A viewpoint on vasopressor and vasopressor-sparing strategies for counteracting blood pressure lowering by angiotensinogen–targeting small interfering rna.

[Recillas-Targa, 2006] Recillas-Targa, F. (2006). Multiple strategies for gene transfer, expression, knockdown, and chromatin influence in mammalian cell lines and transgenic animals. *Molecular biotechnology*, 34:337–354.

[Rensen et al., 2007] Rensen, S., Doevendans, P., and Van Eys, G. (2007). Regulation and characteristics of vascular smooth muscle cell phenotypic diversity. *Netherlands Heart Journal*, 15:100–108.

[Rhodes et al., 2019] Rhodes, C. J., Batai, K., Bleda, M., Haimel, M., Southgate, L., Germain, M., Pauciulo, M. W., Hadinnapola, C., Aman, J., Girerd, B., et al. (2019). Genetic determinants of risk in pulmonary arterial hypertension: international genome-wide association studies and meta-analysis. *The Lancet Respiratory Medicine*, 7(3):227–238.

[Risch and Merikangas, 1996] Risch, N. and Merikangas, K. (1996). The future of genetic studies of complex human diseases. *Science*, 273(5281):1516–1517.

[Sakota et al., 2014] Sakota, Y., Ozawa, Y., Yamashita, H., Tanaka, H., and Inagaki, N. (2014). Collagen gel contraction assay using human bronchial smooth muscle cells and its application for evaluation of inhibitory effect of formoterol. *Biological and Pharmaceutical Bulletin*, 37(6):1014–1020.

[Saxena et al., 2007] Saxena, R., Voight, B. F., Lyssenko, V., Burtt, N. P., de Bakker, P. I., Chen, H., Roix, J. J., Kathiresan, S., Hirschhorn, J. N., Daly, M. J., et al. (2007). Genome-wide association analysis identifies loci for type 2 diabetes and triglyceride levels. *Science*, 316(5829):1331–1336.

[Saxena et al., 2018] Saxena, T., Ali, A. O., and Saxena, M. (2018). Pathophysiology of essential hypertension: an update. *Expert review of cardiovascular therapy*, 16(12):879–887.

[Schunkert et al., 2011] Schunkert, H., König, I. R., Kathiresan, S., Reilly, M. P., Assimes, T. L., Holm, H., Preuss, M., Stewart, A. F., Barbalic, M., Gieger, C., et al. (2011). Large-scale association analysis identifies 13 new susceptibility loci for coronary artery disease. *Nature genetics*, 43(4):333–338.

[Sherry et al., 2001] Sherry, S. T., Ward, M.-H., Kholodov, M., Baker, J., Phan, L., Smigielski, E. M., and Sirotkin, K. (2001). dbsnp: the ncbi database of genetic variation. *Nucleic acids research*, 29(1):308–311.

[Shi and Chen, 2014] Shi, N. and Chen, S.-Y. (2014). Mechanisms simultaneously regulate smooth muscle proliferation and differentiation. *Journal of biomedical research*, 28(1):40.

[Singh et al., 2023] Singh, S., Choudhury, A., Hazelhurst, S., Crowther, N., Boua, P., Sorgho, H., Agongo, G., Nonterah, E., Micklesfield, L., Norris, S., et al. (2023). Genome-wide association study meta-analysis of blood pressure traits and hypertension in sub-saharan african populations: An awi-gen study.

[Singh et al., 2017] Singh, S., Shankar, R., and Singh, G. P. (2017). Prevalence and associated risk factors of hypertension: a cross-sectional study in urban varanasi. *International journal of hypertension*, 2017.

[Spiers and Padmanabhan, 2005] Spiers, A. and Padmanabhan, N. (2005). A guide to wire myography: Angela spiers and neal padmanabhan. *Hypertension: methods and protocols*, pages 91–104.

[Staessen et al., 2003] Staessen, J. A., Wang, J., Bianchi, G., and Birkenhäger, W. H. (2003). Essential hypertension. *The Lancet*, 361(9369):1629–1641.

[Sun et al., 2017] Sun, H.-J., Ren, X.-S., Xiong, X.-Q., Chen, Y.-Z., Zhao, M.-X., Wang, J.-J., Zhou, Y.-B., Han, Y., Chen, Q., Li, Y.-H., et al. (2017). Nlrp3 inflammasome activation contributes to vsmc phenotypic transformation and proliferation in hypertension. *Cell death & disease*, 8(10):e3074–e3074.

[Surendran et al., 2020] Surendran, P., Feofanova, E. V., Lahrouchi, N., Ntalla, I., Karthikeyan, S., Cook, J., Chen, L., Mifsud, B., Yao, C., Kraja, A. T., et al. (2020). Discovery of rare variants associated with blood pressure regulation through meta-analysis of 1.3 million individuals. *Nature genetics*, 52(12):1314–1332.

[Tanner et al., 2003] Tanner, F. C., Greutert, H., Barandier, C., Frischknecht, K., and Luescher, T. F. (2003). Different cell cycle regulation of vascular smooth muscle in genetic hypertension. *Hypertension*, 42(2):184–188.

[Uffelmann et al., 2021] Uffelmann, E., Huang, Q. Q., Munung, N. S., De Vries, J., Okada, Y., Martin, A. R., Martin, H. C., Lappalainen, T., and Posthuma, D. (2021). Genome-wide association studies. *Nature Reviews Methods Primers*, 1(1):1–21.

[Untergasser et al., 2012] Untergasser, A., Cutcutache, I., Koressaar, T., Ye, J., Faircloth, B. C., Remm, M., and Rozen, S. G. (2012). Primer3—new capabilities and interfaces. *Nucleic acids research*, 40(15):e115–e115.

[van der Loop et al., 1997] van der Loop, F. T., Gabbiani, G., Kohnen, G., Ramaekers, F. C., and van Eys, G. J. (1997). Differentiation of smooth muscle cells in human blood vessels as defined by smoothelin, a novel marker for the contractile phenotype. *Arteriosclerosis, thrombosis, and vascular biology*, 17(4):665–671.

[Vancea et al., 2021] Vancea, A., Serban, O., and Fodor, D. (2021). Relationship between osteopontin and bone mineral density. *Acta Endocrinologica (Bucharest)*, 17(4):509.

[Visscher et al., 2017] Visscher, P. M., Wray, N. R., Zhang, Q., Sklar, P., McCarthy, M. I., Brown, M. A., and Yang, J. (2017). 10 years of gwas discovery: biology, function, and translation. *The American Journal of Human Genetics*, 101(1):5–22.

[Waltregny et al., 2005] Waltregny, D., Glénisson, W., Tran, S. L., North, B. J., Verdin, E., Colige, A., and Castronovo, V. (2005). Histone deacetylase hdac8 associates with smooth muscle α-actin and is essential for smooth muscle cell contractility. *The FASEB journal*, 19(8):966–968.

[Wang et al., 2015] Wang, M., Kim, S. H., Monticone, R. E., and Lakatta, E. G. (2015). Matrix metalloproteinases promote arterial remodeling in aging, hypertension, and atherosclerosis. *Hypertension*, 65(4):698–703.

[Wang et al., 2006] Wang, W., Lee, E. T., Fabsitz, R. R., Devereux, R., Best, L., Welty, T. K., and Howard, B. V. (2006). A longitudinal study of hypertension risk factors and their relation to cardiovascular disease: the strong heart study. *Hypertension*, 47(3):403–409.

[Wang et al., 2009] Wang, Y., O'Connell, J. R., McArdle, P. F., Wade, J. B., Dorff, S. E., Shah, S. J., Shi, X., Pan, L., Rampersaud, E., Shen, H., et al. (2009). Whole-genome association study identifies stk39 as a hypertension susceptibility gene. *Proceedings of the National Academy of Sciences*, 106(1):226–231.

[Warren et al., 2017] Warren, H. R., Evangelou, E., Cabrera, C. P., Gao, H., Ren, M., Mifsud, B., Ntalla, I., Surendran, P., Liu, C., Cook, J. P., et al. (2017). Genome-wide association analysis identifies novel blood pressure loci and offers biological insights into cardiovascular risk. *Nature genetics*, 49(3):403–415.

[Watanabe et al., 2019] Watanabe, K., Stringer, S., Frei, O., Umićević Mirkov, M., de Leeuw, C., Polderman, T. J., van der Sluis, S., Andreassen, O. A., Neale, B. M., and Posthuma, D. (2019). A global overview of pleiotropy and genetic architecture in complex traits. *Nature genetics*, 51(9):1339–1348.

[Weber et al., 2011] Weber, G. F., Lett, G. S., and Haubein, N. C. (2011). Categorical meta-analysis of osteopontin as a clinical cancer marker. *Oncology reports*, 25(2):433–441.

[Wellman et al., 2001] Wellman, G., Cartin, L., Eckman, D., Stevenson, A., Saundry, C., Lederer, W., and Nelson, M. (2001). Membrane depolarization, elevated ca2+ entry, and gene expression in cerebral arteries of hypertensive rats. *American Journal of Physiology-Heart and Circulatory Physiology*, 281(6):H2559–H2567.

[WHO, 2014] WHO (2014). Global status report on noncomminicalble diseases 2014. Website. Online available `https://apps.who.int/iris/bitstream/handle/10665/148114/9789241564854_eng.pdf`; accessed 16 Jan 2023.

[WHO, 2020] WHO (2020). The top 10 causes of death. Website. Online available `https://www.who.int/news-room/fact-sheets/detail/the-top-10-causes-of-death`; accessed 03 Jan 2023.

[Williams et al., 2018] Williams, B., Mancia, G., Spiering, W., Agabiti Rosei, E., Azizi, M., Burnier, M., Clement, D. L., Coca, A., De Simone, G., Dominiczak, A., et al. (2018). 2018 esc/esh guidelines for the management of arterial hypertension: The task force for the management of arterial hypertension of the european society of cardiology (esc) and the european society of hypertension (esh). *European heart journal*, 39(33):3021–3104.

[Wright et al., 1999] Wright, J. H., Munar, E., Jameson, D. R., Andreassen, P. R., Margolis, R. L., Seger, R., and Krebs, E. G. (1999). Mitogen-activated protein kinase kinase activity is required for the g2/m transition of the cell cycle in mammalian fibroblasts. *Proceedings of the National Academy of Sciences*, 96(20):11335–11340.

[Yamamoto et al., 1997] Yamamoto, M., Aoyagi, M., Azuma, H., and Yamamoto, K. (1997). Changes in osteopontin mrna expression during phenotypic transition of rabbit arterial smooth muscle cells. *Histochemistry and cell biology*, 107:279–287.

[Yamase et al., 2016] Yamase, Y., Kato, K., Horibe, H., Ueyama, C., Fujimaki, T., Oguri, M., Arai, M., Watanabe, S., Murohara, T., and Yamada, Y. (2016). Association of genetic variants with atrial fibrillation. *Biomedical reports*, 4(2):178–182.

Acknowledgements

I would particularly like to thank my supervisor Zouhair Aherrahrou for his great support and advice. Additionally, I would like to thank my doctoral supervisor and former director of the institute, Jeanette Erdmann, for the working space and material, the topic of this thesis, and the support. Special thanks go to Sandra Wrobel and Annett Liebers for the great technical support. Thanks to all members of the Institute for Cardiogenetics for their great helpfulness.

I would also like to thank the cooperating working groups, which enabled some of the experiments, the Institute for Endocrinology and Diabetes of the University of Lübeck with its director Prof. Dr. Jens Mittag, and the Clinic for Rheumatology and Clinical Immunology UKSH Lübeck with the director Prof. Dr. Gabriela Riemekasten.